8-2019

Debris-Slide Susceptibility Modelling Using GIS Technology in the Great Smoky Mountains National Park

Raja Das
East Tennessee State University

Debris-slide Susceptibility Modelling Using GIS Technology in the Great Smoky Mountains National Park

---

A thesis

presented to

the faculty of the Department of Geosciences

East Tennessee State University

In partial fulfillment

of the requirements for the degree

Master of Science in Geosciences

---

by

Raja Das

July 2019

Dr. Arpita Nandi, Chair

Dr. Andrew Joyner

Dr. Ingrid Luffman

Keywords: Debris-slide Susceptibility, GIS, Great Smoky Mountains National Park, Knowledge-driven, Data-driven

ABSTRACT

Debris-slide Susceptibility Modelling Using GIS Technology in the Great Smoky Mountains National Park

by

Raja Das

Debris-slides are one of the most frequently occurring geological hazards in metasedimentary rocks of the Anakeesta ridge in Great Smoky Mountains National Park (GRSM), which often depends on the influence of multiple causing factors or geo-factors such as geological structures, slope, topographic elevation, land use, soil type etc. or a combination of these factors. The main objective of the study was to understand the control of geo-factors in initiating debris-slides using different knowledge and data-driven methods in GIS platform. The study was performed in three steps: (1) Evaluation of geometrical relationship between geological discontinuity and topographic orientation in initiation of debris-slides, (2) Preparation of knowledge-driven debris-slide susceptibility model, and (3) Preparation of data-driven debris-slide susceptibility models and compare their efficacy. Performance of the models were evaluated mostly using area under Receiver Operating Characteristic (ROC) curve, which revealed that the models were statistically significant.

ACKNOWLEDGEMENTS

I would like to express my sincere gratitude to my supervisor Dr. Arpita Nandi for her constant guidance and motivation during the completion of this work and beyond. Without her expert knowledge and persistent supervision completing the proposed work would not have been possible.

I also extend my humble gratitude to my thesis committee members, Dr. Andrew Joyner and Dr. Ingrid Luffman for their unconditional efforts in helping me with my thesis work, and even otherwise.

I also lovingly acknowledge all my friends at ETSU, especially Reagan Cornett for assisting me in the field.

I sincerely acknowledge the United States National Park Service for sharing data and granting permission to carry out field surveys in the Great Smoky Mountains National Park.

Last but not the least, I am also indebted to my family members, my wife and my parents for their persistent encouragement and reassurance in the days of need.

TABLE OF CONTENTS

CHAPTER 1

INTRODUCTION

Debris-slides are a type of mass wasting event, where unconsolidated rock fragments mixed with soil and other plant debris become saturated with water and move downslope, under the force of gravity. In presence of favorable causative factors such as slope angle, geology, soil type, land use etc. and triggering factors such as rainfall and earthquakes, most of the mountainous region in the world have undergone slope modification process (Van Western 1996). Debris-slides are a common phenomenon in the Appalachian region, where so far, more than 3000 debris-slides have been identified. Most of these slides were triggered by torrential rainfall associated with hurricanes and storms (Wieczorek et al. 2000). The Great Smoky Mountain National Park (GRSM) in the Appalachian Mountains is the most visited national park in the United States with over 11.3 million visitors per year. Therefore, debris-slide not only possess a serious threat to the millions of visitors in the park but these events can cause serious damage to the roads, federal properties, and lands.

Adverse orientations of geological discontinuities and topographic slopes can play a crucial role in controlling the initiation mechanism of the debris-slide. Depending upon the mutual geometric orientation of the topographic slope and aspect relative to geological discontinuities, three different modes of slope failure are possible, namely: (i) Planar (ii) Wedge and (iii) Topple (Godman and Bray 1976; Hoek and Bray 1981). Movement of the bedrock along the geological discontinuity planes is known as rock kinematics and slope instability analysis based on kinematic properties is called kinematic analysis. The kinematic analysis is often performed for site-specific slope instability analysis by plotting orientations of geological discontinuities and topographic slopes using the stereographic projection or stereonet (Markland

1972; Hoek and Bray 1981; Yoon et al. 2002). However, for a regional scale study, where orientation of discontinuities may vary significantly, the traditional stereonet-based kinematic analysis is an unrealistic approach. Therefore, to overcome such a geotechnical obstacle, GIS technology can be an effective solution. Very few studies have employed GIS based kinematic analysis for large study areas (Ghosh et al. 2010). Ganther (2003) and Ghosh et al. (2010) adapted an unique technique to develop a Digital Structural Model in a GIS platform based on the orientation of the geological discontinuities by interpolating them to perform the kinematic analysis. However, the accuracy of such model a greatly depends on factors like quality of data, accuracy in data measurement, density of point data, distribution of exposures etc. (Ghosh et al. 2010). One of the previous studies conducted by Ryan (1989) in the Anakeesta ridge of GRSM found that the chute of the debris-slide were mostly formed due to the intersection of different discontinuity planes, which lead to abundant wedge failures. Hence, performing a GIS based kinematic analysis will be an effective analytical approach to understand the role of geological discontinuities in influencing the initiation of debris-slides.

To understand the spatial probability of debris-slide in the future, one of the primary steps is to develop the debris-slide susceptibility map with the assumption that the factors, which were responsible for slope failure in the past, most likely will again contribute to slope failure in the future (Varnes 1978; Carrara et al. 1995; Guzzetti et al. 1999). Generation of debris-slides highly depends on the influence of causative factors or geo-factors such as slope angle, lithology, elevation, drainage, rainfall, land use etc. in different proportions. Several methods for regional scale debris-slide susceptibility modelling are available, which are mainly of two categories: heuristic or data-driven and empirical or knowledge-driven. Physically based models are third option for debris-slide susceptibility analysis. These model employs simulation techniques using different geotechnical data, however, development of this model is beyond the scope of the

present study. Heuristic or knowledge-driven methods can be either direct, where detailed geomorphological and geological mapping is required to model the debris-slide (Brabb 1984) or indirect, where numerical weights are assigned to the geo-factors by the expert (Hansen 1984; Varnes 1984). The subjectivity of selecting geo-factors and assigning weights is at the sole discretion of the investigator and is often done by applying his/her knowledge gained from dealing with similar kinds of situation in the past. However, this kind of approach can be proven effective if the correct sets of geo-factors are selected for the analysis as the role of geo-factors varies with changes in the physical environment of the terrain (Ghosh et al. 2013).

Empirical or data-driven methods apply statistical or mathematical approaches to calculate the relationship between the geo-factors and debris-slides. A Geographic Information System (GIS) provides a powerful analytical platform to execute advanced statistical equations for slope instability analysis in larger spatial extents. Data-driven methods are broadly divided into two groups, namely, bivariate and multivariate. Bivariate process deals with the individual classes of a geo-factor to calculate weights of geo-factors based on the one to one relationship with the geo-factors and debris-slide. Most multivariate models work like a black box that process multiple geo-factors at a time against the debris-slide occurrence data using statistical software like SAS, SPSS etc.

Different debris-slide studies have been conducted in the Anakeesta Ridge of GRSM between 1970's to 2017. However, no attempt has been made to understand the role of geological discontinuities in controlling debris-slide initiation. Henderson (1996), and Nandi et al. (2016) modelled debris-slide susceptibility of the area using different statistical approaches. Again, the role of geological discontinuity was not included in their study. This study aims to evaluate the role of geological discontinuity and include the information in susceptibility models

by using a novel approach to develop comprehensive knowledge of debris-slide phenomenon in the Anakeesta Ridge of GRSM. Following are the specific objectives of the study:

(i) Develop a GIS-based kinematic model for predicting the debris-slide initiation zones using the geometrical relationship between geological discontinuities and topographical orientation.

(ii) Develop a GIS-based knowledge-driven debris-slide susceptibility model using the Weighted Overlay method.

(iii) Develop four data-driven debris-slide susceptibility models and compare their ficacy in a GIS platform.

The above mentioned objectives form the driving questions for three separate studies, which are presented in the three consecutive chapters (Chapter 2, 3 and 4). The all-inclusive flow chart in the next page shows the preparation of debris-slide susceptibility models.

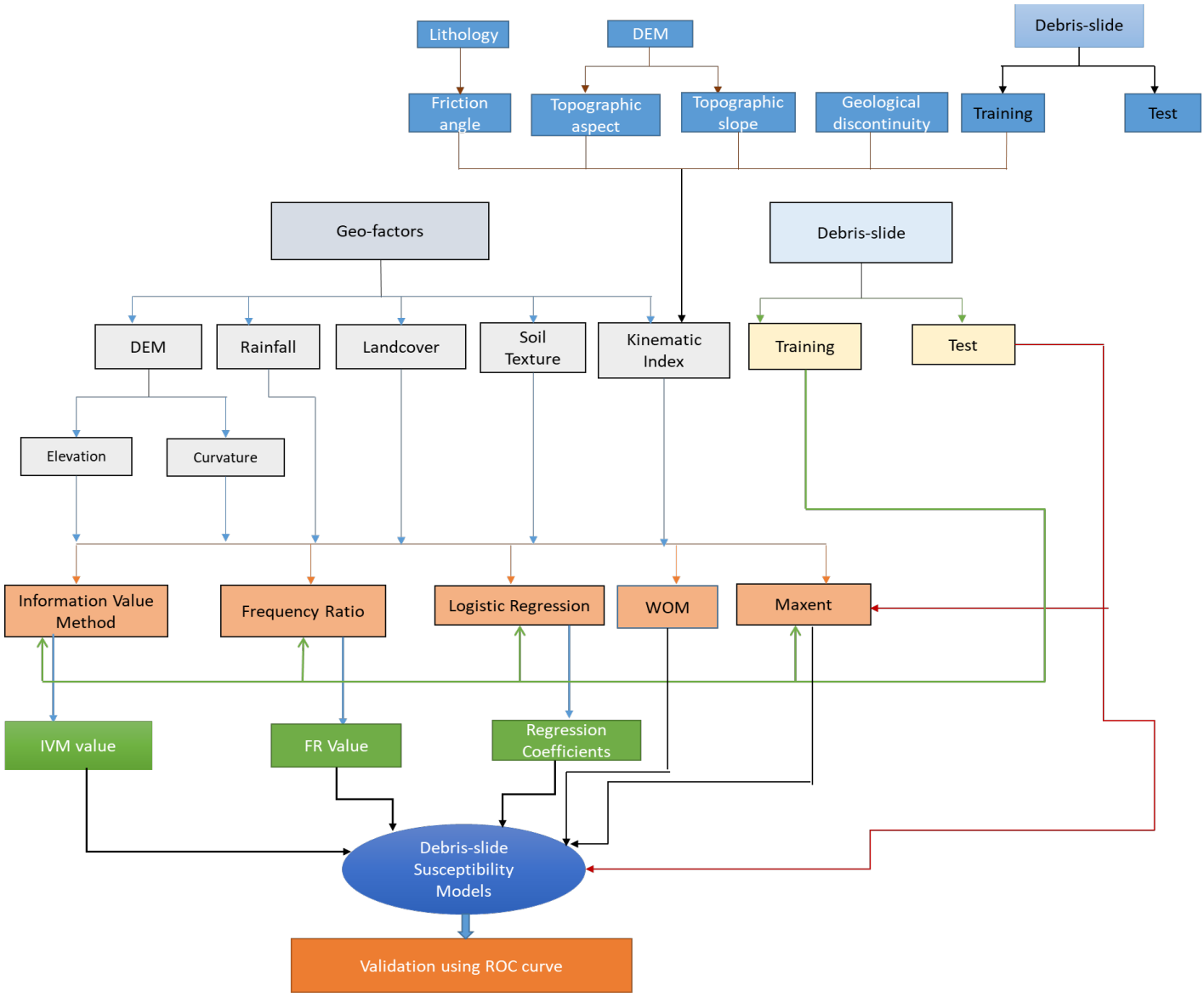

Flow chart of the study

CHAPTER 2

Debris-slide Assessment Using Spatial Distribution of Structural Orientation Data and Kinematic Properties of Rock, Great Smoky Mountains National Park, TN

Abstract

Geological discontinuities, and their geometrical relationship with orientation of topographical slope, known as bedrock kinematics, play a crucial role in controlling slope stability within a rock mass. This study aims to develop a GIS based kinematic model based on the mutual relationship between topographic slope and geological discontinuities to predict debris-slide initiation zones in the Anakeesta rock formation of Great Smoky Mountain National Park, Tennessee. Debris-slide locations were mapped from aerial photographs, satellite imagery, and directly from field surveys. Topographical information such as slope angle and direction for the entire study area were extracted from high resolution Light Detection and Ranging (LiDAR) digital elevation model using ArcGIS 10.5.1. Orientation of geological discontinuities were measured during field surveys. The kinematic model was developed using the orientation of topographical slope and geological discontinuities and 75 percent of the debris-slide locations (192 slides) were used to build the kinematic model. Results showed the presence of four distinct sets of discontinuities, resulted in eleven possible combinations of slope failure. Wedge failure was found to be the dominant mechanism of failure followed by planar failure, and 67% of existing debris-slide pixels were represented by the two failure modes. Based on mechanism of failure and combination of responsible discontinuities, percent weightage was calculated and Weighted Sum analysis was performed to estimate the debris-slide susceptibility of the study area on a scale of 0 to 1. The susceptibility model was validated using 64 known debris-slides, and area under Receiver Operating Characteristic (ROC) value of 0.67 indicated that the susceptibility model is valid. It was concluded that kinematics of bedrock discontinuities with respect to topographical slope are an important contributing factor in controlling the slope stability in the Anakeesta Formation.

Keywords: *Debris-slide, Kinematic analysis, Great Smoky Mountains National Park, GIS.*

1. Introduction

A debris-slide initiates when unbroken rock characterized by displacement of one or multiple failure surfaces is disrupted into several units, often becomes saturated with water, and starts moving downslope. The mechanism of debris-slide type failures can initiate from adverse orientation of bedrock discontinuities that might lead to planar, wedge, or topple failures or any combination of the three. The mobility of a slope caused by movement along bedrock discontinuities is known as kinematics. Several researchers have studied the spatial distribution and geometrical relationships of geological discontinuities in rock formations and combined them with topographic slopes to contribute to different modes of rock slope failure including debris-slides (Godman and Bray, 1976; Hoek and Bray, 1981; Matheson, 1983; Cruden, 1989; Gokceoglu et al., 2000; Roy and Mandal, 2009). Reduction of rock shear strength parameters like internal friction and cohesion against the sliding movement of a rock block plays an important role in slope instability (Ghosh et al., 2010). Weathering is common along planes of discontinuities and could affect rock shear strength. The rock mass and associated discontinuities could be weakened by the presence of partly infilled clay, gypsum, calcite, or water through in freeze thaw activities (Aydin, 2006). Therefore, to evaluate the reason for debris-slide in an area, it is important to analyze geological discontinuities and rock shear strength, and recognize their mutual relationship with topographic slope and aspect.

Several debris-slide predictive models are found in the literature. Some models predict debris-slide source or initiation areas, whereas others focus on the pathway and runout of the phenomenon. Statistical based susceptibility models like logistic regression, artificial neural network, frequency ratio etc. exist in the literature where the contribution of different causative factors for debris-slides initiation such as slope, aspect, lithology, rock

discontinuities, soil texture, curvature etc. are used to predict spatial probability of future debris-slide occurrences (Henderson, 1997; Nandi and Shakoor, 2010; Ghosh et al., 2013). These geo-environmental factors are cost-effectively acquired at a regional scale, except acquisition of site specific field data for geological discontinuities. The kinematical approach to evaluate site-specific geological discontinuities for slope instability analysis is well documented in the literature and is commonly performed by an engineering geologist during any road, tunnel, or dam site geotechnical evaluation. In kinematic analysis orientation of field measured geological discontinuity and slope are plotted using stereographic projections to evaluate potential initiation zones for rock slope failure (Markland 1972; Hoek and Bray, 1981; Yoon et al. 2002). While kinematic analysis is common during site specific analysis, the approach is rarely used in regional scale studies. In tectonically affected mountainous terrain, often orientation of discontinuities is widely spread within the same set of data, which makes a conventional stereonet-based approach problematic in selecting appropriate representative discontinuity values for the analysis (Park et al., 2015). Data collection is time consuming, unreachable in treacherous terrain, and hard to execute in larger study areas. Park et al. 2015, used traditional kinematic analysis and grid-based probabilistic analysis for rock slope stability along a 2.6-km-long stretch of Baehuryeong Road, Korea where the researchers studied 23 rock slopes along the road corridor. For probabilistic analysis, a 1m DEM was used to calculate the topographic slope aspect in ArcGIS and discontinuity orientations were mapped in the field. The analysis calculated the percentage of unstable area susceptible to planar and wedge failures. Gunther (2003) and Ghosh et al. (2010) made unique attempts to create a Digital Structural Model (DSM) based on orientation of geological discontinuities by applying an interpolation technique in GIS to perform the kinematical analysis for a large

study area. Gunther (2003) used SLOPEMAP which is a suite of QUICKBASIC programs to map the geometric and kinematic properties of bedrock in Oker Water Reservoir, Lower Saxony, Germany. He constructed a continuous DSM from point data of discontinuity orientations of bedding and joint planes using Inverse Distance Weighting interpolation of structural discontinuities. Ghosh et al. 2010, used a similar approach in Darjeeling Himalaya, India where they divided the study area into small structural domains based on the major trend of discontinuity orientations. They dissolved the azimuth, dip angle of discontinuities into linear cosine components, and interpolated a continuous DSM using Inverse Distance Weighting interpolation in ArcGIS. The slope angle and aspect of the terrain was derived from 10 m × 10 m 'CartoDEM', prepared from 2.5 m resolution stereo-images of IRS P5 Cartosat-1 satellite. Their study showed the kinematic analysis prediction map could estimate up to 46% of the existing slope failure locations. The accuracy of spatial interpolation highly depends on the accuracy of data collection, collection point density, distribution of good exposure etc. and does not always completely represent the local structural variation (Ghosh et al., 2010).

Debris-slides are persistent phenomena in the Appalachian region (Henderson, 1997) and triggered by high rainfall associated with hurricanes and storms (Wieczorek, et al., 2000). Debris-slides in the Appalachian mountain are caused by excessive rainfall that increases pore water pressure in thin soil cover and rock discontinuities (Eshner and Patric 1982; Hupp, 1983). The Great Smoky Mountains National Park (GRSM) has experienced heavy rainfall and associated damaging debris-slide events. Several studies have been conducted on debris-slides in Anakeesta Ridge and Mt. Leconte, of GRSM from 1970's to till date. Bogucki (1970) studied debris-slides and flood damage resulting from a cloudburst on September 1951 over the Mt. Leconte Sugarland Mountain, in Alum Cave Creek

watershed. He found the slope angle for most of the debris-slide scars varied from 35° to 44° with a mean of 40° and any slope angle below 20° was considered safe. Clark (1987) studied rainfall associated with debris-slides in Anakeesta Ridge and emphasized the importance of precipitation thresholds and movement mechanism of failure to understand the probability of debris-slide initiation zones. Ryan (1989) examined the change in debris scar morphology in Anakeesta Ridge by using aerial photographs from 1953 to 1987 and performed wedge failure analysis. He found abundant release surfaces in the Anakeesta phyllite formation and the chute of the slides was formed due to wedge failure caused by the intersection of different discontinuities. Henderson (1997) performed debris-slide susceptibility analysis in the Mount Leconte-Newfound Gap area in the Great Smoky Mountain, TN and NC using GIS. He employed logistic regression and failure rate analysis using six geo-factors: slope angle, slope aspect, slope form (plan and profile), geology, distance to the ridge crests, and precipitation, to map debris-slide susceptibility. Nandi and Shakoor (2017) also used a logistic regression model in the Upper West Prong Little Pigeon River watershed containing Anakeesta Formation using 3 m LiDAR data and more recent slide surfaces. They concluded that a combination of steep and concave slopes, weathered and jointed phyllitic bedrock, surficial deposit, and infiltration from spring and summer thunderstorm events were responsible for debris-slides initiation. Mandal and Nandi (2017) used HEC-HMS hydrological model to estimate rainfall-runoff-infiltration relationships of phyllitic bedrock and surficial deposits in debris-slide initiation. Results indicated a high rate of infiltration in debris-slide scar areas compared to non-debris scar areas, where infiltration values reached maximum rates immediately following peak rainfall, and were followed by increased surface runoff.

All previous debris-slide research in the study area were conducted either to understand the influence of precipitation on slides or to map susceptibility of debris initiation zones. While rainfall is the main triggering factor for debris-slides in the area (Bogucki, 1970; Clark, 1987; Ryan, 1989), all slopes are not vulnerable to mass wasting. The stability of a slope is highly controlled by the orientation of geological discontinuities, internal friction angle (ϕ) of the rock along with slope and aspect of the topography. Therefore, the kinematic relationship between topography with structural orientation must be understood in order to identify the spatial probability of debris-slides initiation zones. Except Ryan's (1989) and Nandi and Shakoor's (2017) site-specific wedge failure analysis on selected slopes in the Anakeesta Formation using stereographic projections, no detailed work has been performed at a regional scale using GIS to map rock discontinuity kinematics and establish a relationship with topography that initiates debris-slide formation. Therefore, the objectives of this study are to, (i) evaluate the role of major geological discontinuities in debris-slide initiation, (ii) develop a kinematic model and implement it at a regional scale using ArcGIS, and (iii) validate the accuracy of the model in the Upper West Prong Little Pigeon River watershed's Anakeesta Formation.

2. Background

2.1. Study area

The study was conducted in the Upper West Prong Little Pigeon River watershed (31.90 sq. miles/82.63 sq. km.), in Great Smoky Mountain National Park that includes Mt. LeConte, Newfound Gap, and Route 441, which winds through it. The elevation of the study area ranges from 402 m (1313 ft) to 2010 m (6094 ft). Temperature varies from -2.2˚C (28 ˚F) to 31.1˚C (88˚F) at the base and -7.2˚C (19 ˚F) to 18.3˚C (65˚F) at the tops of the ridges. Average annual rainfall increases with elevation and is 140 cm (55 inches) at the base and 216 cm (85 inches) at the highest ridge in the park (National Park Service). The area receives snow around 2.45 cm (1 inch) or more, over 1-5 events per year at lower elevation and up to 61 cm (2 feet) at higher elevation.

Most of the debris-slide patches are mainly concentrated around the southeastern part of the watershed especially in the Anakeesta rock formation. Therefore, rock slope instability analysis was confined within the Anakeesta Formation.

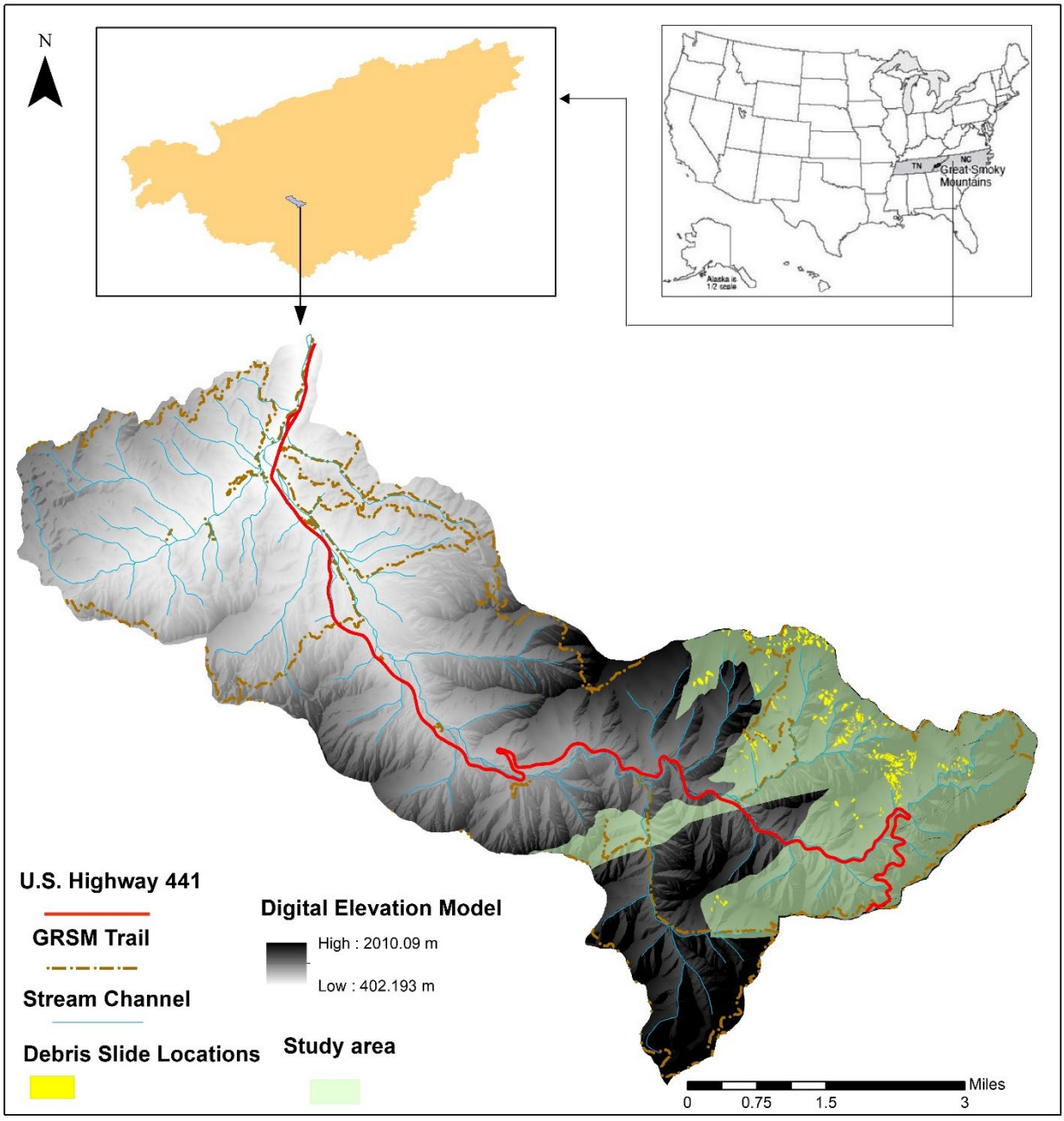

Figure 1: Digital Elevation Model of study area within the Great Smoky Mountain National Park, TN with debris flow locations (yellow dots).

2.2. *Geological setting*

The study area rocks are part of the Ocoee Series of late Precambrian age, characterized by a thick mass of clastic metasedimentary rock, which includes sandstone and interbedded slate, phyllite, and schist (Figure 2). The Ocoee Series rests on a basement complex of granite and metasedimentary gneiss of earlier Precambrian age (Moore, 1988). The formation shows the signature of folding and faulting with varying degrees of metamorphism and has a spatial extent from Ashville, North Carolina to Cartersville, Georgia, covering a distance of more than 225 km (175 miles) (King et al., 1968). The overlying Ocoee Series is divided into three groups: Snowbird, Great Smoky, and Walden Creek Groups (Figure 3), each separated by thrust faults (King et al., 1958). A large part of the watershed falls under the Great Smoky Group which is separated from Snowbird group by a low angle thrust fault called the Greenbrier Fault. The Mingus Fault, located in the north of the study area, is a high angle reverse fault trending east-west and exposed within the Anakeesta Formation. The Oconaluftee Fault that trends NW-SE and dips towards the south, is a right lateral fault located in the western part of the study area that separates the Anakeesta Formation from Copperhill Formation (Bogucki, 1970). Thunderhead Sandstones named after Thunderhead Mountain consist of thickly bedded, fine-grained arkosic conglomerate and coarse-grained metasandstone interbedded with graphitic metasiltstone and slate.

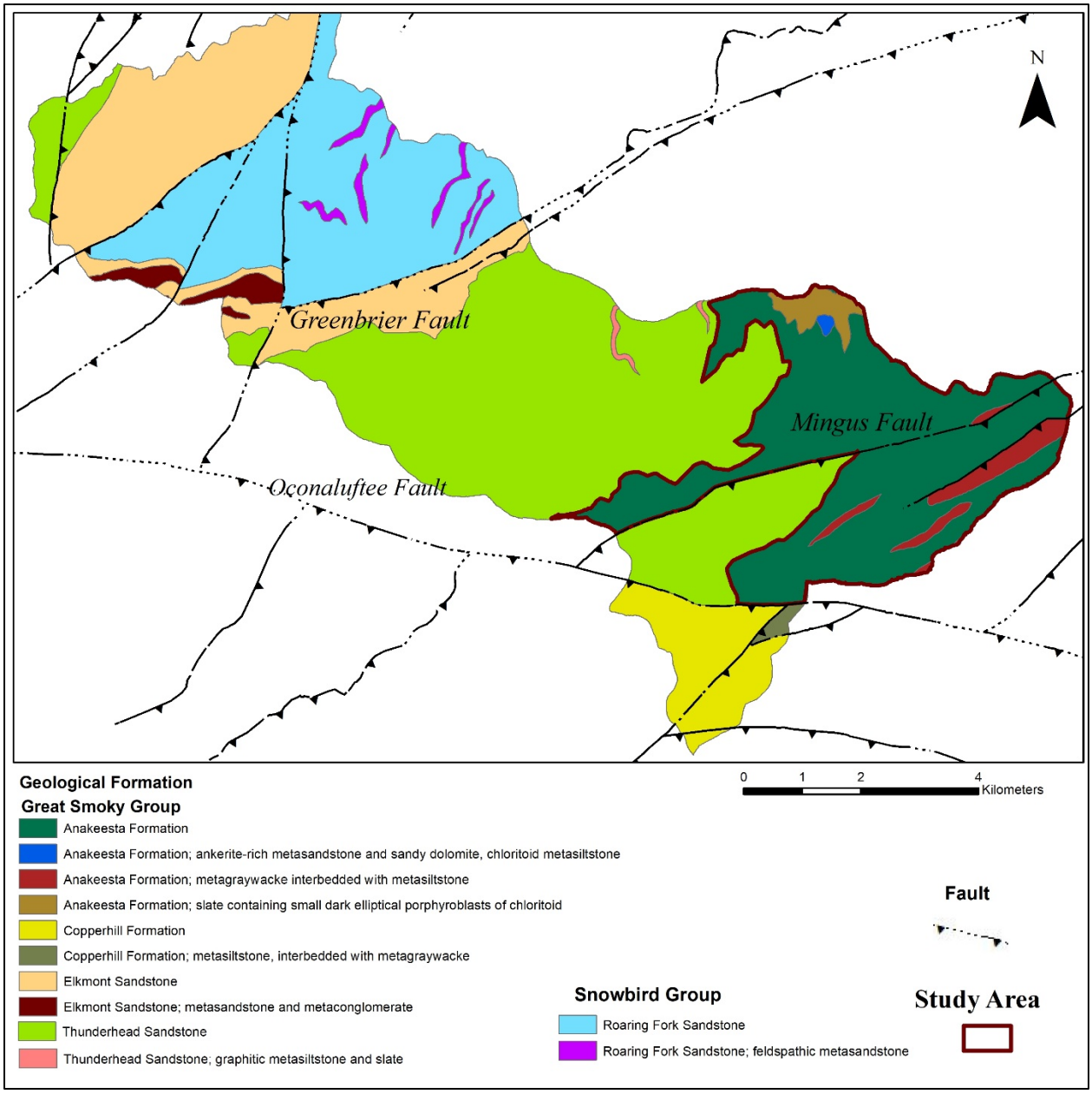

Figure 2: Geological Map of the Study Area (Source: King, Neuman, and Hadley, 1968).

<table>
<tr><td rowspan="6">Lower Cambrian</td><td colspan="2" rowspan="2">Chilhowee Group</td><td>Helenmode Formation
Hesse Quartzite
Murray Shale
Nebo Quartzite
Nicholas Shale
Cochran Formation</td></tr>
<tr><td rowspan="5">Later Precambrian</td><td rowspan="4">Ocoee Series</td><td>Walden Creek Group</td><td>Sandsuck Formation
Wilhite Formation
Shields Formation
Licklog Formation</td></tr>
<tr><td>Great Smoky Group</td><td>Unnamed Sandstone (Copperhill Sandstone)
Anakeesta Formation
Great Smoky Group, undivided
Thunderhead Sandstone
Elkmont Sandstone</td></tr>
<tr><td colspan="2">Formations of the Ocoee Series not assigned to groups - Cades Cove Sandstone, rocks of Webb Mountain and Big Ridge, and Rich Butt Sandstone</td></tr>
<tr><td>Snowbird group</td><td>Pigeon Siltstone
Metcalf Phyllite
Roaring Fork Sandstone
Longarm Quartzite
Wading Branch Formation</td></tr>
<tr><td>Earlier Pre-Cambrian</td><td colspan="3">Basement Complex</td></tr>
</table>

Figure 3: Stratigraphy of Great Smoky Mountain National Park and Vicinity (Source: Philip B. King et al., 1968).

The Anakeesta Formation conformably lies on the Thunderhead Formation and contains a great variety of rock, varying in color from dark gray (due to presence of graphite) to rusty orange (due to sulfide minerals). The main rock types include phyllite, chloritoidal slate, graphitic and sulfidic slate, feldspathic sandstone, laminated metasiltstone, and coarse-grained metagraywacke (Southworth et al., 2005). The thickness of the formation varies from 610 m (2000 ft) to 1524 m (5000 ft). The

formation poses abundant discontinuities in terms of bedding, joint, and cleavage that form numerous planes for slope failure (Clark et al., 1987).

2.3. Debris-slide history

The study area does not have a consistent documentation of debris-slide information. However, previous studies suggest that over time the frequency of debris-slides has increased (Clark, 1987 ; Ryan, 1989) and the scars have increased in volume and extent moving towards the crest of the ridge (Ryan, 1989). Most of the slides in the study area were caused by severe storm events and are listed below in Table 1. Six more landslides took place due to extreme rainfall in the vicinity of Anakeesta Ridge, however, those were not included in this study because they fell outside the study area.

Table 1: Past debris flow events in the Upper West Prong River Watershed.

Date	Type of Storm	Area
10 July 1942	Thunderstorm	Newfound Gap
1 September 1951	Cloudburst	Mt. Leconte
15 June 1971		Mt. Leconte
March 1975 – through 1983	Multiple Storm	Anakeesta Ridge
August 3,1978	Thunderstorm	Mt. Leconte
Mar / Sep 1985	Thunderstorm	Anakeesta Ridge
July 1984	Thunderstorm	Anakeesta Ridge
10 August 1984	Thunderstorm	Anakeesta Ridge
28 June , 1993	Cloudburst	Mt. Leconte
October 4-6, 1995	Hurricane Opal	Mt. Leconte / Anakeesta Ridge
16-17 September, 2004	Hurricane Ivan	Mt. Leconte / Anakeesta Ridge
August 5-6, 2012	Thunderstorm	Anakeesta Ridge
Sept. 10-14, 2017	Hurrican Irma	Anakeesta Ridge

(Source: Clark, 1987; Nandi and Shakoor, 2017)

3. Methodology

The study consisted of five distinct parts. First, the debris-slide initiation zones were mapped. Second, field data were collected from bedrock exposures and debris-slide initiation zones. Third, field data were analyzed to prepare kinematic models based on the rock discontinuities. Fourth, ArcGIS 10.5 software was used to build the regional kinematic model at the watershed scale. Finally, the kinematic model was validated using the ROC curve method.

3.1. Data collection

All debris-slide patches or initiation zones were directly digitized as polygons from satellite imagery, and aerial photographs from 2004 to 2018 and verified during field surveys. Polygons were converted to shapefile format and projected to North America Albers Equal Area Conic projection. The debris-slide location database was split into training (75%) and testing (25%) groups.

Field data collection included site description, GPS location, bedrock type, structural discontinuity measurement including dip and dip direction of discontinuity planes, topographic slope angle, and direction. Structural discontinuity data were also collected from previous literature (Ryan, 1989). Additional rock mass property data were collected according to Rock Mass Rating (RMR) System guidelines proposed by Bieniawski (1989). A Schmidt hammer was used to measure the uniaxial compressive strength of the rock exposure in each field location. Rock Quality Designation (RQD) was calculated using the following relation (Palmstrøm, 1982):

$$\textit{If } J_v < 4.5, \textit{ then RQD of the rock is 100\%.}$$

$$\textit{If } J_V \geq 4.5, \textit{ then } RQD = (115 - 3.3 * J_V) \quad \ldots\ldots \quad \textit{Equation 1}$$

where J_v = number of discontinuities present per m^3 volume of rock outcrop.

Joint spacing was computed by summing the total number of discontinuities per meter length of all discontinuity sets (Palmstrøm, 1982).

Condition of discontinuities and groundwater conditions were estimated qualitatively by evaluating the physical condition of the slope and subsequently, a rating was assigned to the slope. To estimate the internal rock friction angle (ϕ), direct shear test results from previous studies in the area (Ryan,1989), standard value for rock type (West and Shakoor, 2018), RMR rating, and empirical method by Aydan et al. (1993) were compared. A conservative value was adopted based on observed field condition.

LiDAR Digital Elevation Model (DEM) with spatial resolution of 0.76 m was downloaded from State of Tennessee GIS Clearinghouse (http://www.tngis.org/). ArcGIS 10.5 was used to derive raster maps of slope angle and aspect from the LiDAR DEM.

3.2. Kinematical analysis of debris-slides

The analysis was performed in two steps. In the first step, the orientations of geological structures were plotted in the Stereonet 10.2.0 (Allmendinger et al., 2012) to estimate the pole clusters and average trend of different sets of discontinuity planes and the plunge of intersection caused by different discontinuity planes. The following conditions should be fulfilled for planar and wedge failure (Hoek and Bray, 1981): (1) the potential failure plane must have dip/plunge direction similar to the rock face's dip direction, i.e. the potential discontinuity plane must lie at minimum of ± 20° to the dip direction of the topographic slope angle, (2) dip/plunge amount of the potential failure plane should be greater than the friction angle (ϕ) of the rock but less than the topographic slope angle. According to Goodman (1989), pre-condition for topple failure, (i) the friction angle (ϕ) of the rock must be less than the dip/plunge of the

discontinuity, (ii) both discontinuity and topographic slope should be steep, where the discontinuity dips opposite to the topographic slope. The above-mentioned conditions are expressed in terms of equations 2 & 3 (Ghosh et al. 2010):

$\phi \leq \beta \leq \theta$ *(for Plane and Wedge Failure)……Equation 2*

$\theta \geq [\phi + (90° - \beta)]$ *(for Topple Failure)…… Equation 3*

where θ is the slope angle of the topography with slope aspect ±30° to the dip/plunge direction of the discontinuities, β is the dip/plunge amount of the discontinuity and ϕ is the friction angle of the rock. After extracting the average orientation of different discontinuity planes in the study area, different kinematically possible failure modes associated with discontinuities were plotted in Stereonet 10.2.0.

In the second stage, slopes greater than the dip/plunge of the discontinuity were extracted from LiDAR derived slope angle map using ArcGIS (10.5.1). Topographic slope aspect equal to ± 30° in the dip/plunge direction of the discontinuity were extracted from the aspect map. Slope direction range was set to ±30° instead of ±20° to capture variation along the dip/plunge direction of discontinuity in meta-sedimentary rocks of the Great Smoky Group. Next, the slope and aspect output maps were overlaid using Mask tool for the two raster data layers and the common area of both maps was identified as spatial locations for kinematically possible slope failures. This process was repeated for each discontinuity that satisfied Equation 2. The overlapping area between the slope and aspect maps represented places where either planar or wedge failure was possible depending upon the nature of the discontinuity. A threshold value of 70° was set for the dip/plunge of the discontinuity planes as the pre-condition for topple failure, as applied by Ghosh et al. (2010). Dip angles below 70° were not further considered for topple analysis. Next, dip or plunge amount and

friction angle (ϕ) values were applied in Equation 3 and subsequently potential slope gradient was extracted. Topographic slope direction for toppling was extracted at 180° to the dip direction with addition of ±30° to determine the topographic slope for topple failure.

Subsequently, using the training data of the debris-slide initiation zone, the percentage of actual debris-slides matched with the kinematically possible potential spatial location maps created from equation 2 and 3, were calculated. The percent match of individual discontinuities were summed and scaled to 100%. The newly re-calculated percentage values were assigned as the weightage of individual discontinuity layer. A Weighted Sum Analysis was performed to compute a kinematical susceptibility map in a 0-1 scale, based on the influence of the different sets of discontinuities. Values close to 1 indicated high probability of debris-slide and vice-versa. The test data (25% of actual debris-slide areas) were used to validate the effectiveness of the susceptibility model. To validate the model, a Receiver Operating Characteristic (ROC) curve was generated to calculate the Area Under the Curve (AUC) using SPSS software.

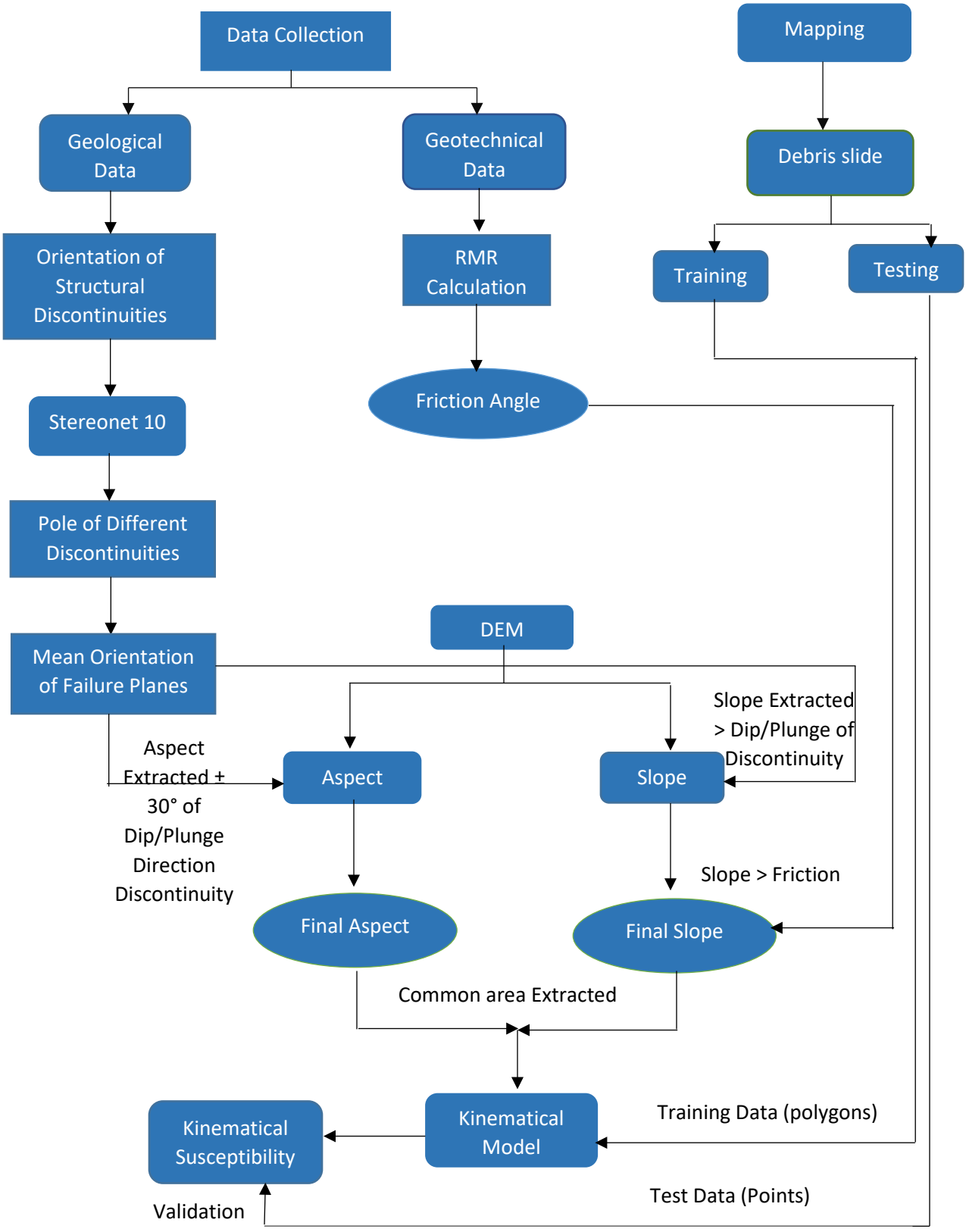

Figure 4: Flow Chart of the Methodology

4. Results

4.1. Evaluation of rock slope instability in Anakeesta Formation

The proposed methodology for rock slope instability analysis followed a deterministic approach on a GIS platform to model the debris-slide susceptibility of the study area solely based on the geometrical relationships between topographical slope and aspect, and orientations of the discontinuities. In total, 256 debris-slide polygons were mapped, of which 185 polygons were used for model training purposes and the rest were used for validation. The majority of the debris-slide areas were concentrated in the northeastern part of the study area close to Mt. Leconte peak and surrounding ridges (Figure 1). All slide initiation zones were concentrated in the Anakeesta Formation, were within close vicinity of a drainage channel, and commonly occurred in concave topographic slopes, which might have initiated by bedrock structural discontinuities. The current study did not focus of genesis of concave slopes and drainage channels.

In the field, 243 discontinuity orientations were measured and an additional 179 discontinuity orientation data points were used from Ryan (1989) in the same study area in the Anakeesta Formation. The pole plot of all discontinuity orientation planes is represented in Figure 5. Additionally, RMR rating of the rock mass in Anakeesta Formation was calculated for fourteen field sites along hiking trails using the parameters UCS, RQD, discontinuity spacing, condition, and groundwater condition (Table 2). The RMR rating of the Anakeesta Formation ranged from 55 to 29, which belongs to Class III and VI, classified as ‘fair rock’ to ‘poor rock’ after Bieniawski (1989).

Table 2: RMR (Bieniawski, 1989) information of the Anakeesta Formation.

Parameters	Range	RMR rating Range
Uniaxial Compressive Strength (UCS)	10 to 48 (MPa)	4
RQD	8% to 40 %	8 - 3
Joint spacing	20 mm to 200 mm	8
Joint Condition	Slightly rough surfaces, separation <1 mm, highly weathered to slickenside surface, separation <1 mm	20 to 10
Ground Water Condition	Dripping - Dry	15 – 4
Rock Mass Class		55 – 29 Class III to VI
Rock Friction Angle for class III and 1V rock		25 to 35 and 15 to 25 degrees
Average rock friction angle		25 degrees

Friction angle values were also estimated using other methods summarized in Table 3. However, rock friction angle value produced by the RMR method was reasonable considering the weathering pattern and low RMR in the rock types.

Table 3: Comparison of friction angle (ϕ) obtained from different sources.

	Ryan,1989	Barton and Chaubey (1977)	RMR Table (Bieniaswki 1989)	Empirical Method (Aydan et al., 1993)	West and Shakoor, 2017
Anakeesta Slate/Phyllite	58.2	25-30	25	35.5 to 47.5	35-50

The stereographic projection plots and field investigation showed the presence of four dominant planar features (Figure 5). One of the planar features was identified as Bedding Plane (52° 151) and the rest were identified as joint sets during field

investigation. These four sets of discontinuities could result in 11 possible failure modes (Figure 6). Wedges formed due to intersections of Joint1_ Joint2 and Joint2_Joint3 had a plunge amount less than friction angle (ϕ) which automatically ruled out the possibility of failure from those two combinations of discontinuities based on Equation 2. The remaining nine modes of failure could kinematically take place in the study area and are summarized in Table 4. Of the nine sets, four sets of possible planar failure maps were presented in Figure 8, and four set of wedge failure maps were presented in Figure 7 based on Equation 2. The topple failure map was produced based on equation 3, but not presented here due to its very small area of coverage.

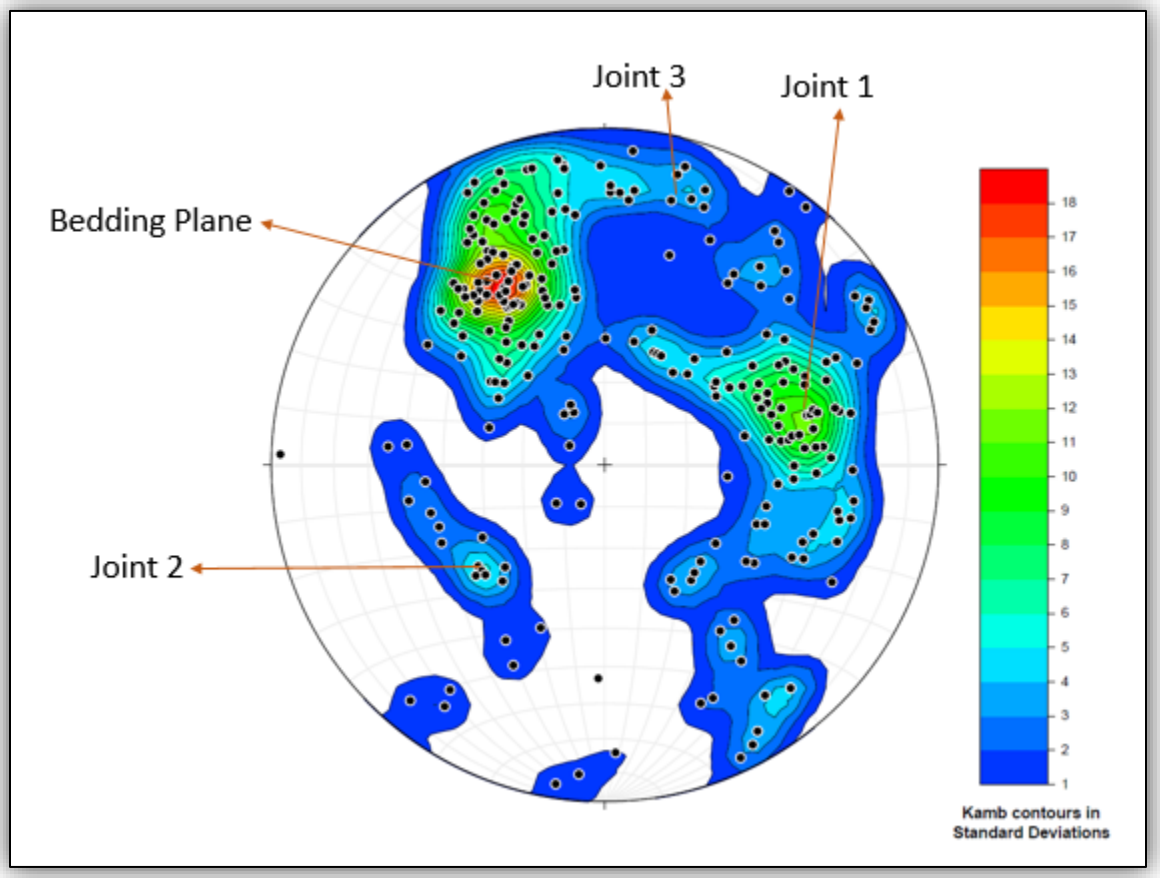

Figure 5: Pole contours of different discontinuity planes in Anakeesta Formation.

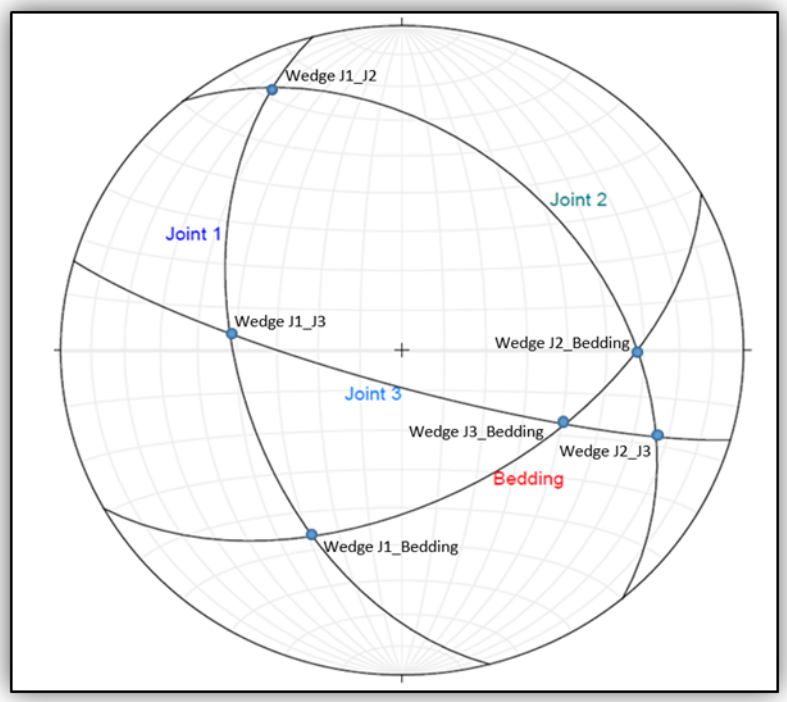

Figure 6: Average orientation of different discontinuity planes extracted from pole clusters in Anakeesta Formation.

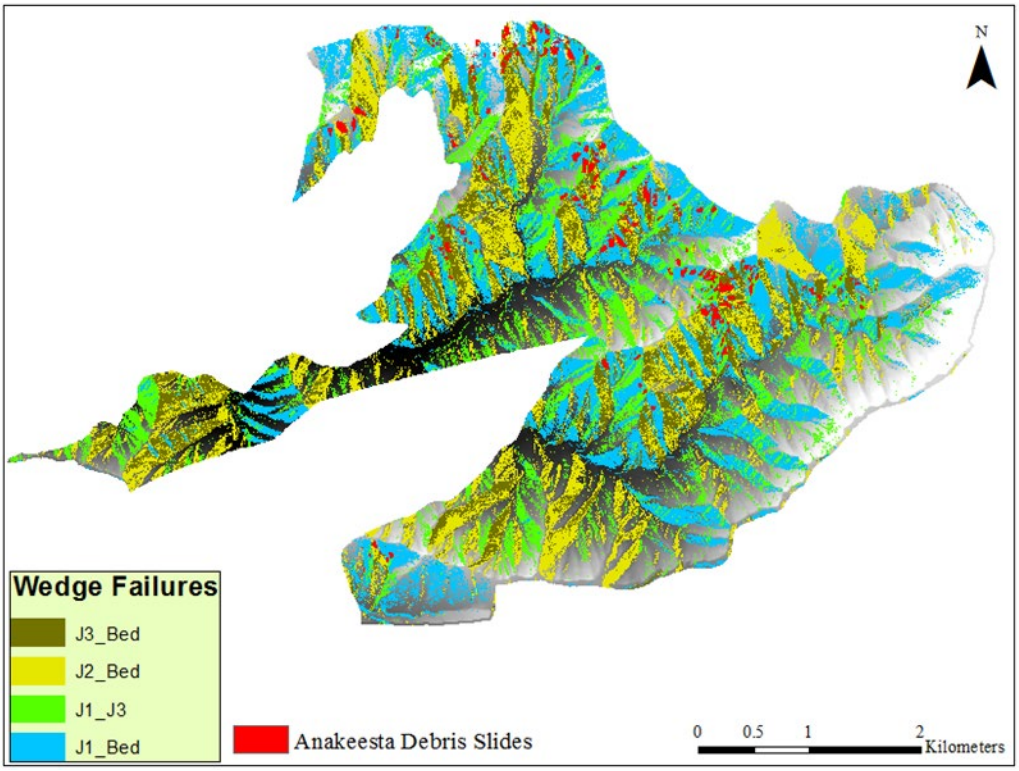

Figure 7: Probable locations where wedge failure is kinematically possible.

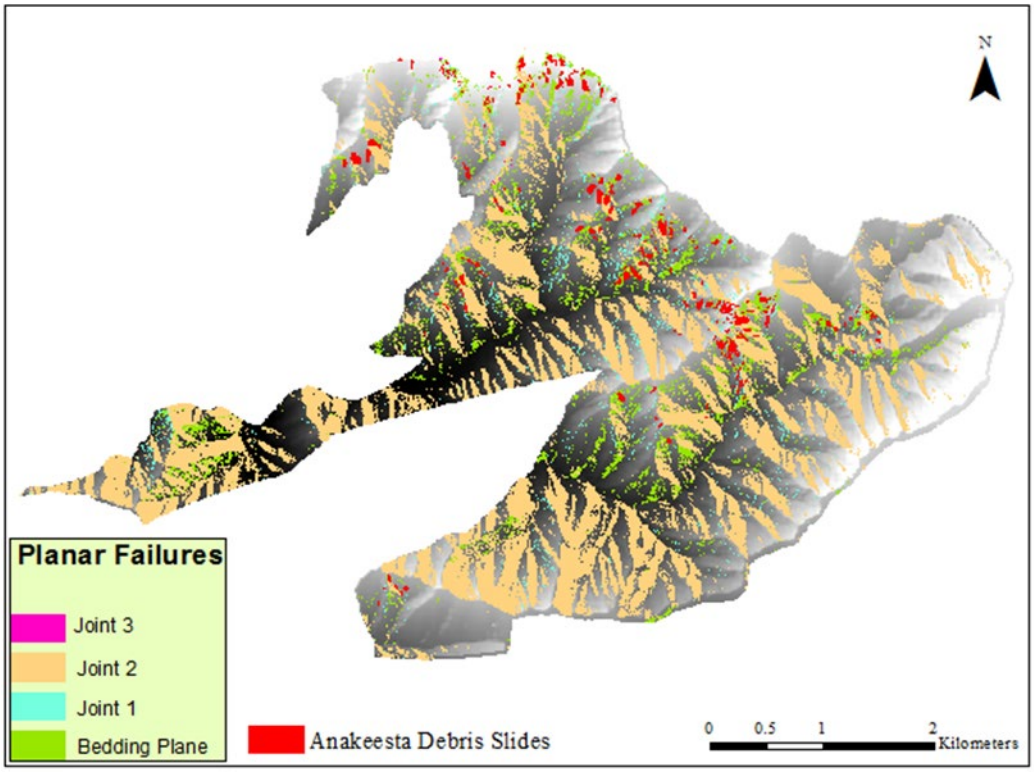

Figure 8: Probable locations where planar failure is kinematically possible.

The number of pixels covering each of nine possible modes of failure due to presence of discontinuities were calculated (Table 4). Then debris-slide training data was overlaid to compute the number of pixels associated with individual failure mode present within each slide areas. Failure mode density was then calculated using the Equation 4.

$$Failure\ mode\ density\ (\%) = \frac{Failure\ mode\ in\ Debris-slide}{Total\ Debris-slide} \quad \ldots\ldots\ Equation\ 4$$

where, total numbers of debris-slide pixel (Training data) = 413,406

Discontinuity plane Joint2 showed the maximum number of pixels (1,428,953) where planar failure mode was kinematically possible (Figure 8), although, the failure mode density was 1.03%. Joint1 was the greatest contributor to planar failure, with a failure mode density of 5.53%, followed by the sliding along Bedding Plane (1.75%). A higher failure mode density implied greater influence on slope instability by the set of discontinuities. Joint3 was the least important in terms of planar failure as it suggested only 209 pixels had the capability to cause planar failure and represented only 99 existing debris-slide pixels.

Wedge combination between Bedding and Joint1 contributed highest to the debris-slide with failure mode density of 27.04% (Table 4). This was followed by the Bedding-Joint2 and Bedding-Joint3 failure mode density of 12% and 4.87% respectively. Joint 1-Joint 3 combination had the least influence total failure (4.22%). The numbers suggest that combinations of different joint planes with Bedding Plane contributed significantly to slope instability in the study area.

Topple failure was very rare in the Anakeesta Formation and could not be found during field investigation. The results also support the observation, only Joint 3 in the study area qualified for the topple analysis as the minimum slope angle for the discontinuity

has been set to 70° and most of the discontinuities were too shallow to fulfill the criteria. However, the result revealed that Joint3 predicted only 1202 pixels of debris-slide.

The summation of all failure mode density was 56.753%. Further, this percentage was recalculated to 100%, where discontinuity set Bedding – Joint 1 forming wedge had the highest weightage (47.645%) and topple failure due to Joint 3 had the lowest value (0.510 %) (Table 4). Subsequently, the kinematical susceptibility map was generated, and debris-slides polygons were overlaid for visual comparison (Figure 9).

Table 4: Details of different kinematically possible failure modes associated with discontinuities and their prediction rate.

Discontinuity	Dip/Plunge Direction	Dip/Plunge	Failure Mechanism	Possible failure mode due to discontinuity (pixels)	Failure mode in Debris-slide (pixels)	Failure mode density (%) = $\frac{\text{Failure mode in Debris-slide}}{\text{Total Debris-slide}}$	Weightage for Overlay Analysis (Failure mode density recalculated in 100%)
Bedding	151	52	Planar	89468	7222	1.75	3.08
Joint 1	255	50	Planar	558955	22874	5.53	9.74
Joint 2	50	39	Planar	1428953	4295	1.03	1.81
Joint 3	196	81	Planar	209	99	0.023	0.040
Bedding – Joint 1	204	37	Wedge	2471782	111769	27.04	47.645
Bedding – Joint 2	89	32	Wedge	2854179	49646	12.00	21.144
Bedding – Joint 3	115	47	Wedge	452446	20136	4.87	8.581
Joint 1 – Joint 2	335	12	Wedge	Not applicable	Not applicable	Not applicable	0
Joint 1 – Joint 3	276	48	Wedge	740664	17456	4.22	7.435
Joint 2 – Joint 3	110	23	Wedge	Not applicable	Not Applicable	Not applicable	0
Joint 3	196	81	Topple	2595893	1202	0.29	0.510

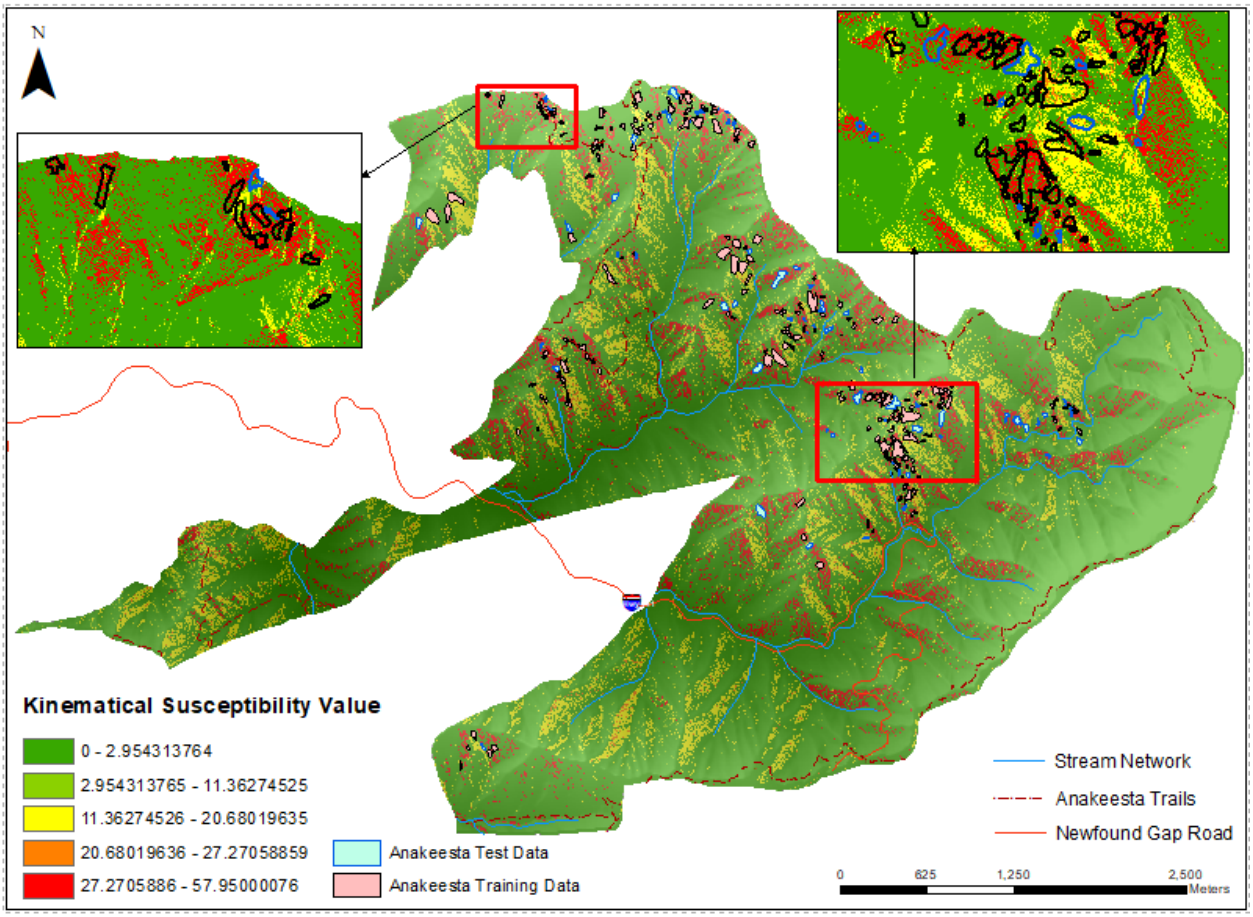

Figure 9: Kinematical susceptibility map of the study area.

4.2. Validation

To validate the model, 1000 points were used, of which 500 points were debris-slide data (from the 25% testing dataset) and 500 were non-debris-slide (pseudo point) locations. The debris-slide points were classified as 1, and non-debris-slide points were classified as 0. Subsequently, the data were exported to SPSS statistical software (SPSS 24) to generate the Receiver Operating Characteristic (ROC) curve and to calculate the Area Under the Curve (AUC) for the susceptibility model. The higher the AUC, the better the model is at predicting the presence (1) and absence (0) data realistically. The validation of kinematical susceptibility model yielded AUC value of 0.67 for the test data (Figure 10).

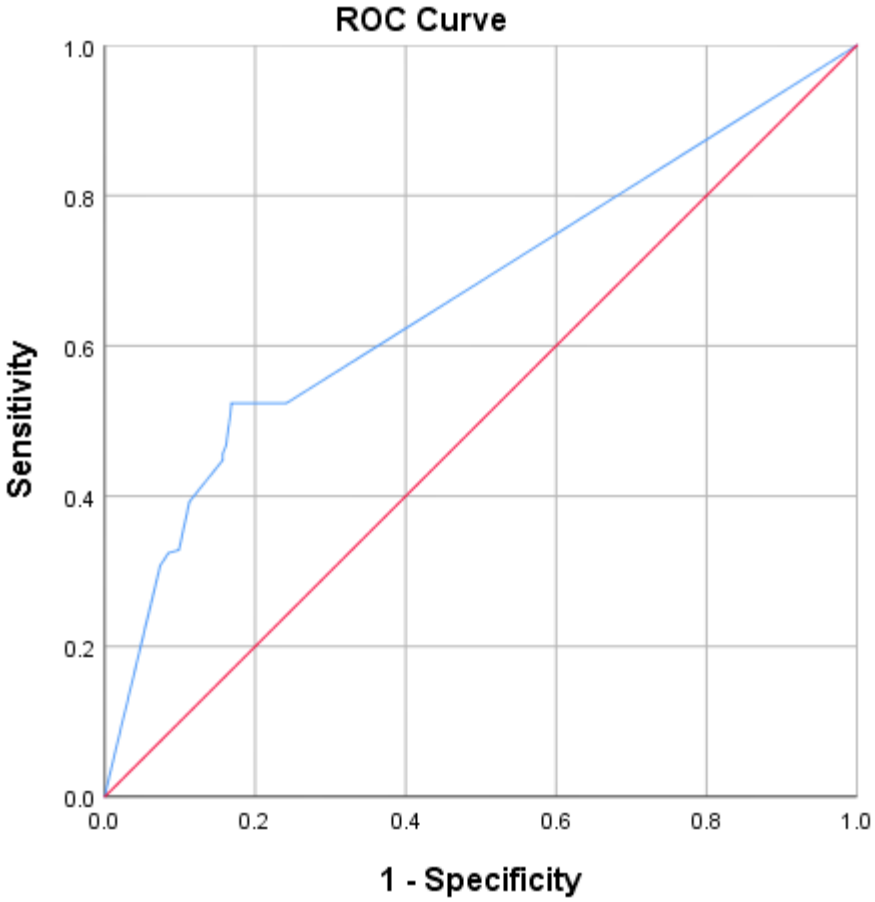

Figure 10: ROC curve for the Test Data.

5. Discussion

The Kinematical model was developed based on the orientation of mapped discontinuities with the assumption that the discontinuities responsible for slope failures in the past, will also be responsible for slope failure in the future and are ubiquitously distributed throughout the study area showing some variation in orientation. Variation in orientation of the discontinuities was confirmed during field study and while plotting the data in the Stereonet 10. To accommodate the variability in the discontinuity orientations, slope aspect limit was subsequently increased from ±20° to ±30°, which represented the inherent inhomogeneity in structural orientations. The majority of the study area was inaccessible and covered by heavy vegetation, and lack of good exposures throughout the study area made fieldwork somewhat limited. Therefore, discontinuity orientations were mostly measured along roadside cut slopes and hiking trails.

The internal friction angle (ϕ) of the rock was calculated considering the high weathering pattern of the rocks to represent the actual field situation. Lower internal friction angle (ϕ) of rocks accounted for highly weathered schist/slate, generally made of low grade metamorphic rocks with slaty or crenulation cleavage. The choice of friction angle value was comparable with the values mentioned by other researches, except from Ryan's study (1989), where his hand specimen laboratory test results yielded higher fiction angle values. It may be possible that the hand specimens were collected from competent sections of the formation, rich in secondary quartz mineralization.

For the Anakeesta Formation, wedge failure was found to be the predominant mode of failure followed by planar failure, which supported field observation and was also verified from previous studies (Ryan 1989, Bogucki 1970). For wedge failure mechanism, the intersection of Bedding Plane and Joint Plane 1 (Bedding_J1) was the most prominent one,

which predicted 27% of debris-slide locations in the training data. The intersections of these structural discontinuities had shallow plunge angles that were steeper (greater) than the internal friction angle (ϕ) of the rock, making these combinations more vulnerable towards kinematical slope failure. On the other hand, most wedge combinations between the different joint planes except J1_J1 and J2_J3 had plunge angles less than the internal friction angle (ϕ) and were eliminated from the possibility of any kind of kinematic failure. Planar failure alone does not seem to have a significant influence on debris-slides. However, it is important to note that debris-slides generated during heavy rainfall, can increase hydrostatic pressure along these weak discontinuity planes and may eventually result in multimode slope failure. Except J3, all other discontinuities in this formation had shallow to moderate dip angles, therefore, J3 was the only structural discontinuity that caused possible topple failure, as topple is only possible in steeply dipping discontinuities. In the study, only 1202 pixels (0.29%) of the study area were mapped for topple failure, and confirmed qualitatively during field investigation. Hence, it was concluded, toppling was inconsequential at least in the Anakeesta Formation.

The accuracy of the kinematic susceptibility model was evaluated by calculating Receiver Operating Characteristics (ROC) (Lee, 2005; Fawcett, 2006) and the percentage of known debris-slides in various susceptibility categories. In the ROC method, the area under the ROC curve (AUC) (values ranging from 0.5 to 1.0), were used to evaluate the accuracy of the model. The AUC value for the test data was 0.67. The model showed a moderately high prediction rate, which is consistent with other findings, as debris-slides are complicated phenomena that often depend on many additional geo-factors like landcover, rainfall, soil type, and hydrological condition etc. Therefore, it will be unrealistic to expect a very high prediction rate based solely on the kinematical model. However, this study effectively

demonstrates the importance of kinematical analysis and the credibility of the kinematical susceptibility model to act as an independent variable along with other geo-factors to create a robust debris-slide susceptibility map of an area.

This paper demonstrated a methodology for kinematical model of slope failure where knowledge of both engineering geology and GIS technology are required to successfully produce realistic results. Absence of debris-slide inventory data from the Great Smoky Mountain National Park was one of the main challenges in the study. Developing a debris-slide inventory database was a difficult task and time consuming. Hence, study of more satellite imagery and field investigations are required to enhance the present inventory database and incorporate the slides within other related formations, especially the Thunderhead formation. Field studies indicated smaller scale slope instability in the adjacent Thunderhead formation is also controlled by geologic discontinuities. In the study LiDAR DEM was the best available digital terrain model for topographical mapping especially considering spatial resolution and the amount of detail preserved. Slope faces were classified for each 0.76×0.76 m^2 pixel, therefore, one could easily understand the amount of topographical details that have been analyzed and used in this study. However, derivatives of the DEM i.e., slope, aspect maps, in some places showed small linear strips, which are often associated with LiDAR DEM. The prediction rate of the model might have been improved if the linear stripes were not present in the LiDAR data, which broke the continuity of the predictive pixels in some part of the susceptibility map. However, considering the objective of the study and information sought, usage of the high resolution DEM has provided us a satisfactory result for the study area.

6. Conclusion

This paper successfully demonstrates an effective methodology to perform rock kinematical analysis in a GIS platform. Traditional stereonet-based kinematical analysis is appropriate for detailed site-specific slope stability analysis, however, for a large and partially inaccessible area, adopting a GIS-based kinematic model can save considerable time and effort. Success of such a kinematical model relies heavily on the accuracy in measuring the orientation of geological discontinuities and collection of other auxiliary data. Hence, adapting a systematic approach to identifying the correct sets of discontinuities and calculating the mean orientation is key to developing a good kinematical model.

In this study, four sets of bedrock discontinuities were identified in low-grade metasedimentary Anakeesta Formation, which included one bedding plane and three joint planes. Wedges formed due to the intersections of the bedding plane with other joint planes were found to be the most crucial mechanisms for slope instability in the study area. A moderate prediction rate of the kinematical model suggested the influence of additional factors in controlling debris-slide initiation. Pragmatically, orientation of geological structures single handedly cannot control slope stability or initiate a debris-slide in an area. Rather, unfavorable structural orientations combined with adverse spatial distribution of other factors like rainfall intensity, drainage pattern, landcover etc. as a whole controls the distribution of debris-slides.

The final kinematical susceptibility model was developed using a two stage approach. In the first stage, deterministic models were developed by executing the kinematic equation in a GIS platform based on the mean orientation of the discontinuities and topographic slope angle and aspect. In the second stage, a weighted sum analysis was performed to

refine the models based on known debris-slide initiation areas. The final kinematical susceptibility map was produced that numerically predicted the probability of geological discontinuity-controlled failures in the area, which is also a function of topographical slope angle, aspect, and lithology. Therefore, the kinematical susceptibility map can replace all the above mentioned geo-factors in order to run multi-criteria analysis for debris or other landslide susceptibility models and act as an independent geo-factor. The study concluded that the kinematical susceptibility maps can serve as the base maps to identify target areas for detailed geotechnical surveys, which will save considerable amount of time and money.

References

Allmendinger, R. W., Cardozo, N., and Fisher, D., 2012, Structural geology algorithms: Vectors and tensors in structural geology: Cambridge University Press (book to be published in early 2012).

Aydan, Ö., Akagi, T., Kawamoto, T.,1993, "The squeezing potential of rocks around tunnels; theory and prediction". Rock Mechanics and Rock Engineering. 26 (2), pp. 137–163. 1993. DOI: 10.1007/BF01023620

Aydin, A., Basu, A., 2006, The use of Brazilian test as a quantitative measure of rock weathering. Rock Mechanics and Rock Engineering 39(1): 77–85, doi : 10.1007/s00603-005-0069-0.

Barton, N.R., Choubey, V., 1977, The shear strength of rock joints in theory and practice. Rock Mech. 10(1-2), 1-54.

Bogucki, D.J., 1976, Debris slides in the Mt. Le Conte area, Great Smoky Mountains National Park, U.S.A.: Geografiska Annaler, Vol 58(3), pp. 179–191.

Clark, G. Michael., 1987, " Debris slides and Debris Flow Historical Events in the Appalachians South of the Glacial Border ." Reviews in Engineering Geology 7: 125-138.

Cruden, D.M., 1989, Limits to common toppling. Canadian Geotechnical Journal, 26: 737–742.

Eschner, A.R., and Patric, J.H., 1982, Debris Avalanches in Eastern Upland Forests. Journal of Forestry 80:343-347

Fawcett, T., 2006, An introduction to ROC analysis. Pattern Recognition Letters, 27, 861-874.

Ghosh, S., Günther, A., Carranza, E.J.M., van Westen, CJ., Jetten, VG., 2010, Rock slope instability assessment using spatially distributed structural orientation data in Darjeeling Himalaya (India). Earth Surf Proc Land 35(15):1773–1792

Ghosh,S., Das,R., Goswami,B., 2013, Developing GIS-based techniques for application of knowledge and data-driven methods of landslide susceptibility mapping. Indian Journal of Geosciences 67 (3-4), 249-272.

Gokceoglu, C., Sonmez, H., Ercanoglu, M., 2000, Discontinuity controlled probabilistic slope failure risk maps of the Altindag (settlement) region in Turkey. Eng Geol 55(4):277–296

Goodman, R. E., 1989, Introduction to RockMechanics,-2nd Edn, John Wiley and Sons, Inc., New York.

Goodman, R.E., Bray, J.W., 1976, Toppling of rock slopes. In Rock Engineering: American Society of Civil Engineers, Geotechnical Engineering Division Conference, Boulder, Colorado, Vol. II, pp. 201–234.

Günther A. 2003, SLOPEMAP: programs for automated mapping of geometrical and kinematical properties of hard rock hill slopes. Computers & Geosciences 29(7): 865–875.

Henderson, J. P., 1997, Debris slide Susceptibility Analysis in the Mt. LeConte-Newfound Gap Area of the Great Smoky Mountains, Tennessee and North Carolina. Unpublished Masters Thesis, The University of Tennessee, Knoxville.

Hoek E, Bray, J.W., 1981, Rock slope engineering. Institution of Mining and Metallurgy, London.

Hupp, C. R., 1983, Seedling establishment on a landslide site. Castanea. 48: 89-98.

King, P.B., Neuman, R.B., Hadley, J.B., 1968, Geology of the Great Smoky Mountains National Park, Tennessee and North Carolina.. U. S. Geol. Surv. Prof. Pap. 587.

King, Phillip B., Jarvis, B. Hadley., Robert, B., Neuman, Warren Hamilton, 1958 . " Stratigraphy of the Ocoee Series , Great Smoky Mountains , Tennessee and North Carolina . " Geological Society of America Bulletin 69 : 947-966 .

Lee, S., 2005., Application of logistic regression model and its validation for landslide susceptibility mapping using GIS and remote sensing data. Int J Remote Sens 26(7):1477–1491

Mandal, A., Nandi, A., 2017, Hydrological Modeling to Estimate Runoff and Infiltration in Southeastern Appalachian Debris Flow Complex, 3rd North American Symposium on Landslides, Roanoke, Virginia, USA.

Markland, J.T., 1972, A useful technique for estimating the stability of rock slopes when the rigid wedge sliding type of failure is expected. Imperial College Rock Mechanics, Reserach Report, no.19, Imperial College Press, London.

Matheson, GD., 1983, Rock Stability Assessment in Preliminary Site Investigations – Graphical Methods, Report 1039. Transport and Road Research Laboratory: Crownthorne.

Moore, H.L.A., 1988, A Roadside Guide to the Geology of the Great Smoky Mountains National Park. University of Tennessee Press, Knoxville, TN. 178 pp.

Nandi, A., Shakoor, A., 2010, A GIS-based landslide susceptibility evaluation using bivariate and multivariate statistical analyses. Engineering Geology - ENG GEOL. 110. 11-20. 10.1016/j.enggeo.2009.10.001.

Nandi, A., Shakoor, A., 2017, Predicting debris flow initiation zone using statistical and rock kinematic analysis, a case study from West Prong Little Pigeon River, TN, NASL Proceedings, 2017.

Palmstrom A., 1982, The volumetric joint count - A useful and simple measure of the degree of rock mass jointing. IAEG Congress, New Delhi, 1982. pp. V.221 – V.228.

Park, H.J., Lee, J.H., Kim, K.M., Um, J.G., 2016, Assessment of rock slope stability using GIS-based probabilistic kinematic analysis. Eng Geol 203:56–69.

Philip B. King, Robert B. Neuman, Jarvis B. Hadley, Geology of the Great Smoky Mountains National

Park, Tennessee and North Carolina, Geological Survey Professional Paper 587 (Washington: Government Printing Office, 1968).

Roy, S., Mandal, N., 2009. Modes of hill-slope failure under overburden loads: insights from physical and numerical models. Tectonophysics 473: 324–340

Ryan, P. T., 1989, Debris slides and Flows on Anakeesta Ridge Within the Great Smoky Mountains National Park Tennessee, U.S.A. Unpublished Master's Thesis, The University of Tennessee, Knoxville

Serafim, J.L., Pereira, J.P., 1983, Considerations of the geomechanical classification of Bieniawski. Proceeding on International Symposium on Engineering Geology in Underground Construction. A.A. Balkema, Boston, 33-43.

Southworth, S., Schultz,A., Denenny,D,. 2005, Geologic Map of the Great Smoky Mountains National Park Region, Tennessee and North Carolina. U.S. Geological Survey Open File Report 2005-1225, scale 1:100,000.

West, T.R., Shakkor, A.,2018, *GEOLOGY APPLIED To ENGINEERING.* Long Grove, Illinois: Waveland Press, Inc.

Wieczorek, G.F, Morgan, B.A., Campbell, R. H., 2000, Debris-flow hazards in the Blue Ridge of central Virginia: Environmental and Engineering Geoscience, 6 (1), pp. 3- 23.

Yoon, W.S., Jeong, U.J., Kim, J.H., 2002, Kinematic analysis for sliding failure of multi-faced rock slopes. Eng Geol 67:51–61

CHAPTER 3

Application of Knowledge-driven Method for Debris-Slide Susceptibility Mapping in Regional Scale

Abstract

Debris-slides are a frequent hazard in fragile decomposed metasedimentary rocks in the Anakeesta rock formation in Great Smoky Mountain National Park. The spatial distribution of existing debris-slide areas could be used to prepare susceptibility maps for future debris-slide initiation zones. This work aims to create a debris-slide susceptibility map using a knowledge-driven method in a GIS platform in Anakeesta Formation of Great Smoky Mountains National Park. Six geofactors, namely, elevation, annual rainfall, slope curvature, land cover, soil texture and various slope failure modes were used to create the susceptibility map. Debris-slide locations were mapped from satellite imagery, previous studies, and field visits. A Weighted Overlay Analysis was performed to generate the final susceptibility map, where individual classes of geofactors were ranked and were assigned weights based on their influence on debris-slides. The final susceptibility map was classified into five categories: very low, low, moderate, high and very high susceptibility zones. Validation of the result shows very high category predicted ~10%, high and moderate categories predicted 75.5% and ~14.5% of the existing debris-slide pixels respectively. This study successfully depicts the advantage and usefulness of the knowledge-driven method, which can save a considerable amount of time and reduce complicated data analysis unlike statistical or physically based methods. However, the accuracy of the model highly depends on the researcher's experience of the area and selection of appropriate geofactors.

Keywords: Debris-slide Susceptibility; Heuristic; Weighted Overlay Analysis; Great Smoky Mountains National Park.

---

1. Introduction

Debris-slides are fast movements of earth materials, which occur mid-latitudes including subarctic regions (Rapp and Stromquist, 1976) and humid tropics (Simonett, 1970). Debris-slides are common in the Appalachian Valley and Ridge, and Blue Ridge physiographic provinces of the United States (Bogucki, 1976). Van Westen (1993) discussed that under the presence of favorable causal and triggering factors, such as earthquakes and extreme rainfall, most of the mountainous terrains are susceptible to slope failure. The same was pointed out by Bogucki (1976), who found that a combination of Appalachian slope and rainfall has eroded the mountains by several thousand noticeable debris-slides. About 2000

slides have formed in Georgia, North Carolina, Tennessee, Kentucky, West Virginia, and Virginia and as many as 200 deaths that may have been caused directly by slide activity from 1940 to recent (Scott 1972, Wooten, et al., 2016). Additionally, these events have caused damage to homes, property and road networks, and have had major impacts on federal lands.

It is important to develop a detailed understanding of the causes and mechanisms of debris-slide events for better prediction and risk assessment. One of the preliminary steps to evaluate events and predict future slide related hazards is to develop debris-slide susceptibility maps (Pradhan, 2011). These maps are used to identify zones that are prone to mass failures depending on geofactors that have caused slides in past. Presumably, the same factors would cause the slides in future (Varnes, 1978; Carrara et al., 1995; Guzzetti et al., 1999). Geographic Information Systems (GIS) provides a powerful tool to analyze spatial hazard related data, and hence, it has become an indispensable tool for regional slope failure hazard and risk analysis. Several authors have applied different methods to map slope failure susceptibility and hazard (e.g., Nandi and Shakoor, 2010; Pradhan, 2011; Lee and Pradhan, 2007). Regional slope failure mapping is generally grouped into three categories: (i) heuristic or knowledge-driven methods (ii) data-driven methods and (iii) physically-based models. The heuristic methods are again divided into direct or indirect methods. A direct heuristic method deals with detailed field investigation of area's geomorphology, geology, and hydrology (Brabb, 1984). The accuracy of the method is highly dependent on the experience of the investigator and the precision level of the work (Ghosh et al., 2013). On the other hand, indirect heuristic methods are based on assigning weights or rating to individual geofactors according to their importance, which is solely

decided by the investigator, based on similar existing research (Hansen, 1984; Varnes, 1984).

Data-driven methods are mostly statistical, which include bivariate and multivariate analysis and are primarily based on observed data of landslide occurrences and relevant spatial geofactors (Nandi and Shakoor, 2010; Ghosh et al., 2013). In these methods, several causative factors for debris-slides are integrated with the slide inventory to statistically model the relationship between the geofactors and slope failure.(Van Westen, 1993). Nandi and Shakoor (2017) used the same approach to study debris-slide susceptibility in Upper West Prong Little Pigeon River (WPLPR) watershed in the southern Appalachian Mountains, where debris-slide locations were identified from aerial photographs and satellite images. Topographical, bedrock geology, and hydrological data were collected, processed, and constructed into a spatial database using GIS. A Logistic regression model was used to evaluate the role of these factors in controlling debris-slide susceptibility. While the method was rigorous and powerful, the limitations of the method were (i) time consuming and not recommended for urgent projects, and (ii) rock discontinuity data were not used as an input variable. Therefore, the objective of this research is to include bedrock discontinuity data that play crucial role in controlling the debris-slide events in the form of rock kinematical index, and create a knowledge-driven susceptibility model for predicting the spatial probability of debris-slide initiation zones.

2. Study area

The study was conducted in the Anakeesta rock formation in the Upper West Prong Little Pigeon River watershed (WPLPR), Great Smoky Mountain National Park, TN. The elevation of the study area ranges from 1105 m to 2010 m. Temperature in Great Smoky

Mountains varies from -2.2˚C (28 ˚F) to 31.1˚C (88˚F) at the base and -7.2˚C (19 ˚F) to 18.3˚C (65˚F) at the ridges. The area receives annual rainfall of 1397 mm (55 inches) at the base and 2159 mm (85 inches) at the highest point of the park. The rainfall increases with increase in elevation and is highest at the Anakeesta Formation. Torrential rainfall associated with severe thunderstorms and hurricanes are the main triggering factors for debris-slides in the study area (Bogucki, 1976; Clark, 1987).

Geologically, the Anakeesta Formation is characterized by fine grained dark colored sedimentary and metasedimentary rock having craggy pinnacle structure i.e., needle-shaped rock faces and steep slopes. The dark color of the rocks is mainly due to the presence of graphite and some part of the formation exhibit a rusty orange color due to the presence of iron sulfide minerals, mainly pyrite. The main rock types include phyllite, chloritoid slate, graphitic and sulfidic slate, feldspathic sandstone, laminated metasiltstone and coarse grained metagraywacke (Southworth et al., 2012). Different sets of discontinuities exist in the form of joints, fractures and to some extent as cleavage, which enhances weathering along these discontinuity planes.

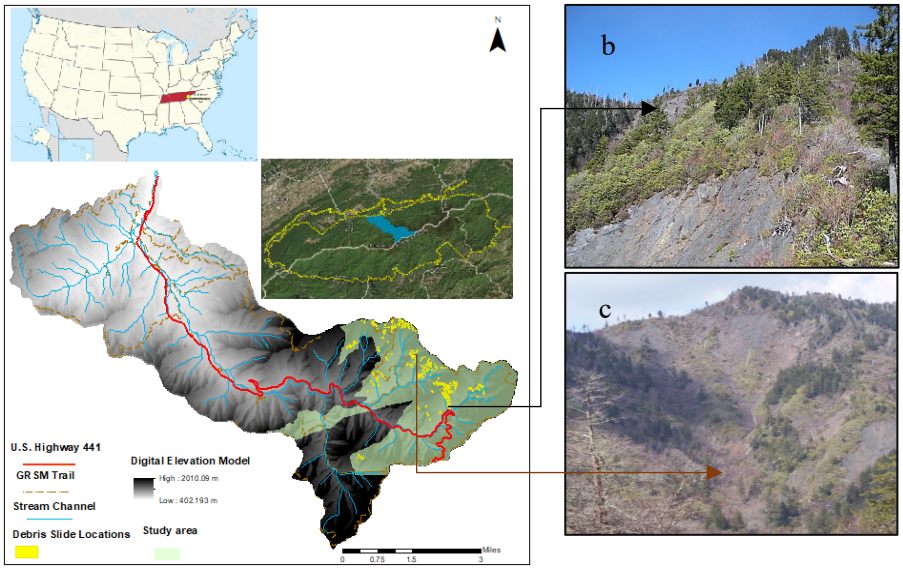

Fig. 1. Study area (a), Debris-slide initiation zones photos in Anakeesta Formation (b, c). [Photo courtesy: Greg Hoover (b) gosmokies.knoxnews.com (c)]

3. Methodology

The present study used both digital data and field investigation, which are described in the following sections.

3.1. Digital Data

To create the debris-slide susceptibility map, six geofactors, namely, elevation, rainfall accumulation, soil texture, land cover, slope curvature, and various bedrock discontinuity layers responsible for slope failures were used. Elevation and slope curvature maps were derived from LiDAR Digital Elevation Model (DEM) of 0.76 m spatial resolution. The LiDAR DEM for Tennessee is available at TNGIS website (http://www.tngis.org/). Soil texture, land cover and rainfall accumulation maps were collected from the National Park Service's database (https://irma.nps.gov/DataStore/Search/Quick) (Fig.2.a-e). Debris-slide initiation locations were digitized from historical to recent aerial photos and satellite imageries, and about 30% of the locations were confirmed during field studies. The debris-slide initiation locations were used to evaluate the suitability of susceptibility analysis.

3.2. *Field investigation and Kinematical index*

Geometrical relationship between orientations of the topographic slope and geological discontinuities play an important role in controlling slope instability in an area; this is known as rock kinematics. Slope instability analysis based on this mutual relationship is known as rock kinematic analysis. Factors like topographic slope angle and aspect, internal friction angle of the rock, and orientation of geological discontinuities relative to each other control slope stability within a rock mass. Depending upon the number of geological discontinuities and their orientations with the topography, three different

modes of rock failure can occur (i) Planar (ii) Wedge (iii) Topple (Eq. 1 and 2) (Ghosh et al., 2010).

$$\phi \leqslant \beta \leqslant \theta \text{ (for Plane and Wedge Failure)} \quad (1)$$

$$\theta \geqslant [\phi + (90° - \beta)] \text{ (for Topple Failure)} \quad (2)$$

The kinematical index layer was prepared using the geometric relationship between geological discontinuities and the topographic slope angle and direction (Fig. 2f). From field mapping and previous work, structural orientations (dip angle and dip direction) of a total of 313 discontinuities were used in the study. The internal friction angle (ϕ) of the bedrock was estimated from Rock Mass Rating system data collected in the field (Bieniawski, 1989). Topographic slope angle (θ) was obtained from the LiDAR DEM, dip/plunge angle (β) and direction of discontinuities were obtained by plotting the structural data in Stereonet 10 software (Allmendinger et al., 2012). Subsequently, equations 1 & 2 were used in ArcGIS to spatially detect the areas where slope failures were kinematically possible (Ghosh et al. 2010):

Eleven combinations of planar, wedge, and topple failures were possible in the study area that produced 11 different kinematic layers susceptible to failure. Wedge type failures were dominant in the study area, and were more prevalent in bedding (52° ⟶ 151°) and one of the joint plane (50°⟶ 255°) governed discontinuities. All layers were ranked based on presence of actual debris-slide initiation locations, and the ranked layers were combined into one kinematic index layer. A detailed description of the preparation of composite kinematic index layer is presented in a forthcoming paper (Das, et al., in preparation).

A Weighted Overlay Analysis was performed to generate the debris-slide susceptibility map, using a heuristic approach. Weighted Overlay Analysis tool is available in the Spatial Analyst extension in ArcGIS 10.5. All geofactor layers were converted into raster format and rescaled to a 0.76 m grid size. Based on field studies and prior knowledge of the study area, individual classes of the geofactors were ranked and relative weights were assigned to each individual geofactor. The weights represented the degree of influence of individual geofactors in producing debris-slides in the region on a scale of 0 to 100 that added up to 100%. Table 1 summarizes the different geofactors and their corresponding weighting that were used in the susceptibility analysis. A flow chart provides a step by step process of the methodology (Figure 3).

Table 1. Summary table of the geofactors.

Geofactor	**Source**	**Average (Range)**	**Weight**
Elevation	Digital Elevation Model	1526 m (1105m – 2010m)	30
Rainfall	National Park Services	2051mm (1854mm– 2159mm)	25
Soil	National Park Services	Channery loam, Channery silt loam, Loam, Slide area, Peat, Very Channery loam	15
Kinematical Index	Digital elevation model and Lithological map (National Park Service)	5.68 (0 - 57.95)	15
Land cover	National Park Services	Barren land, Deciduous forest, Developed Open space, Developed low intensity, Developed medium intensity, Evergreen Forest, Mixed Forest, Shrub	10
Curvature	Digital Elevation Model	-6.62 (-6839 to + 11380)	5

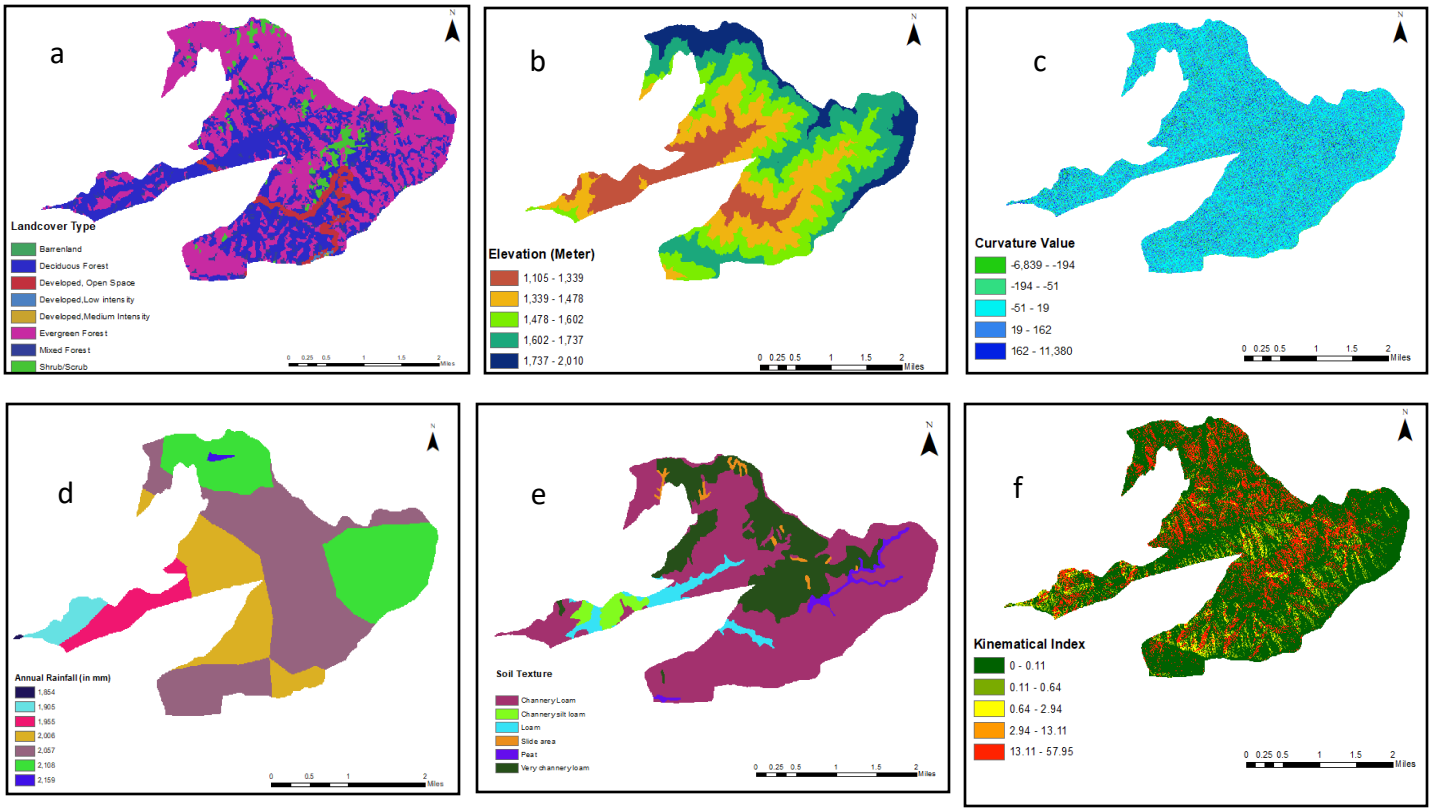

Fig. 2. Geofactors used in generation of susceptibility model : (a) Land cover (b) Elevation (c) Curvature (d) Annual Rainfall (e) Soil Texture (f) Kinematical Index.

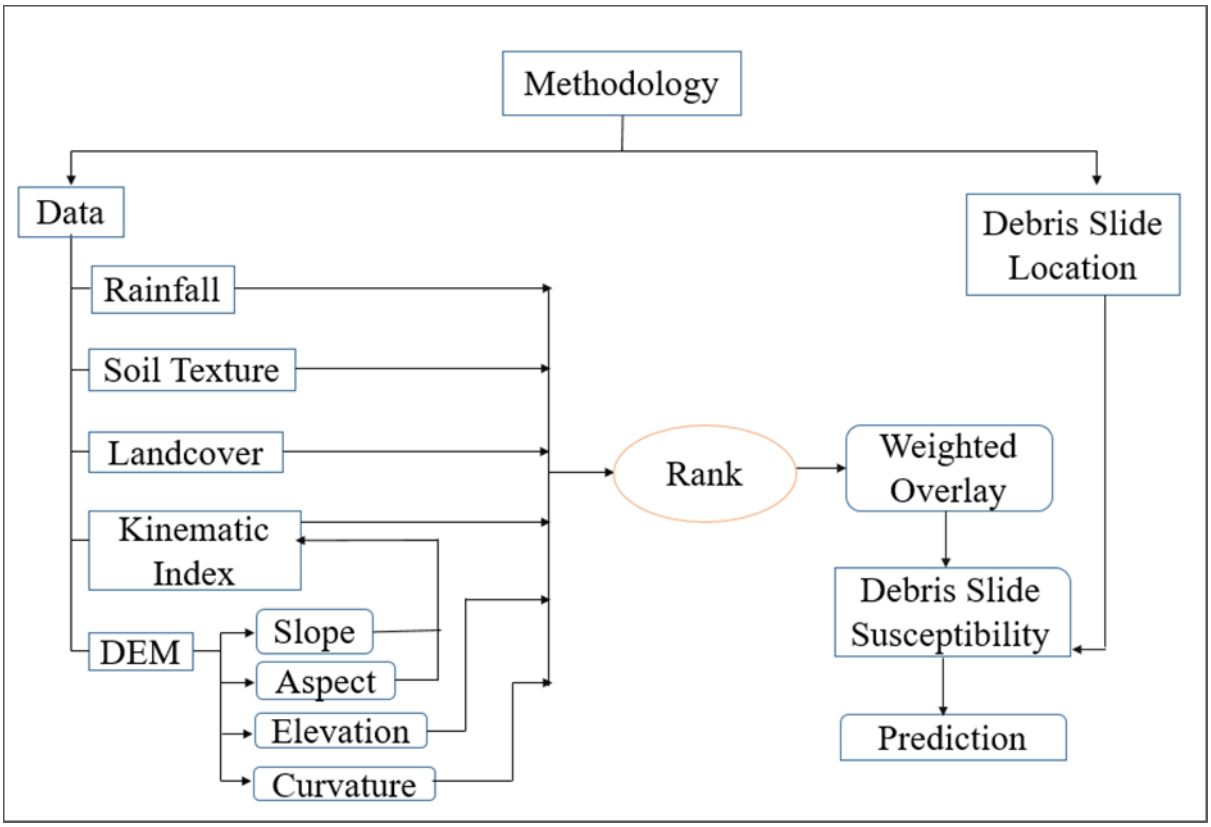

Fig. 3. Flow chart of the methodology

4. Result

In the study area, 256 debris-slide initiation zones were identified (Fig. 1a). Majority of debris-slides were present in the Newfound Gap and Mt. LeConte areas in the northeastern corner. The elevation of the area ranges from 1105 m to 2010 m with a mean of 1526.64 m (Fig. 2b), rainfall varied from 1854.2 mm to 2159 mm (Fig. 2d) and curvature ranged from -6839.87 to +11380 with a mean of -6.62 (Fig. 2c) (Table 1). A negative curvature value stands for upwardly convex surface and positive value indicates concave surface at that cell.

The debris-slide initiation zone susceptibility map from the Weighted Overlay Analysis was classified into: very low, low, medium, high, and very high susceptibility categories (Fig. 4). Only 0.03 % and 9% of the total map area was located under very low and low susceptibility zones, respectively. When the map was compared with actual debris-slide initiation zones, these low and very low susceptibility areas exhibited no trace of past or recent slide activity. Medium susceptibility zones occupied 43.43% of the study area and predicted 14.44 % of actual debris-slide occurrence zones. High susceptibility zones represented the largest area in the map (45.43%) and accounted for 75.53 % of slides in the study area. Very high susceptibility covered only 2% of the total study area; however, nearly 10% of the known slide locations were in this zone (Fig. 5).

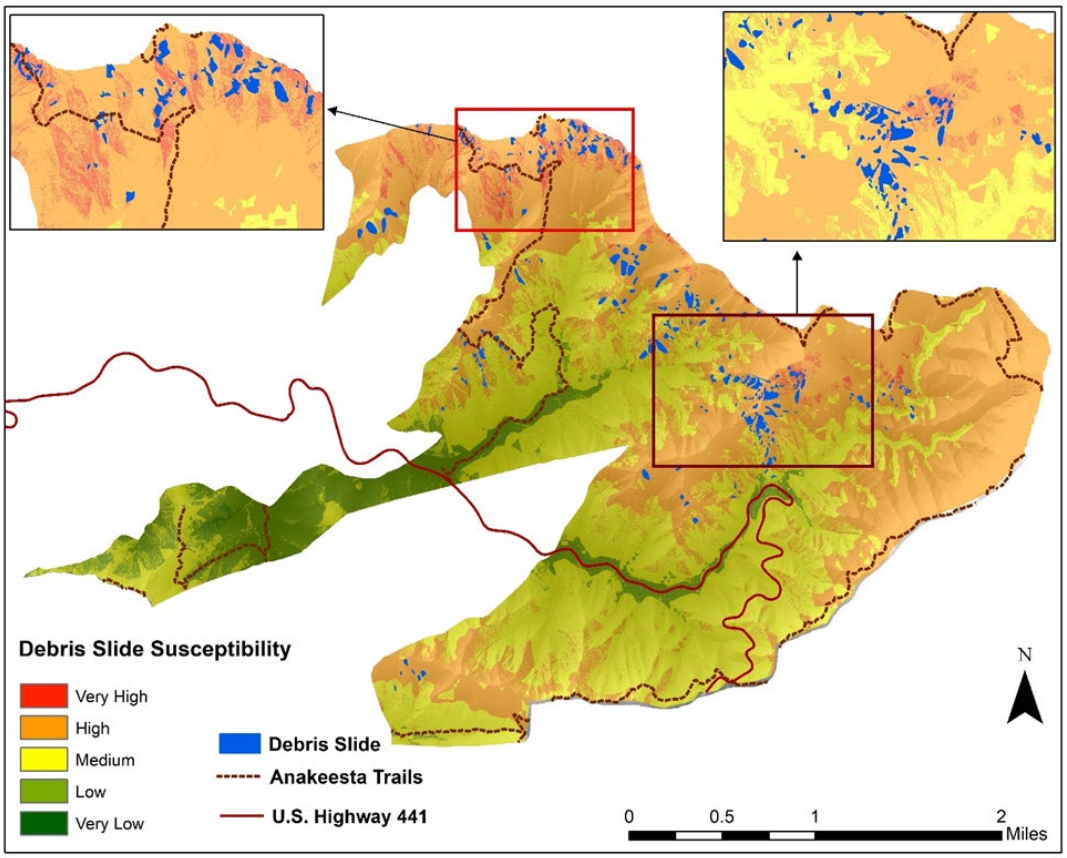

Fig. 4. Debris-slide susceptibility map.

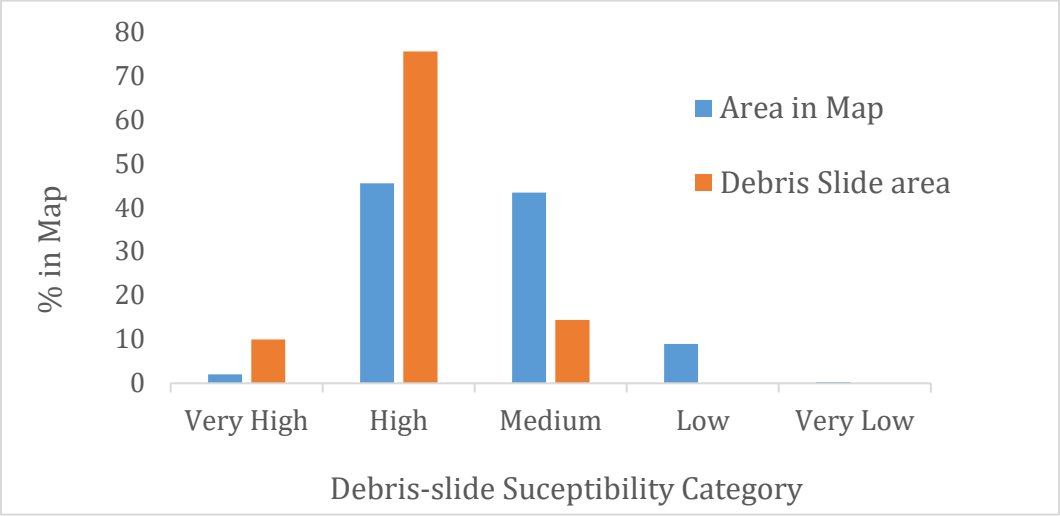

Fig. 5. Debris-slide susceptibility zones compared to the known slide initiation areas.

5. Discussion

Anakeesta Ridge in the northeastern part of the study area has experienced failures in the past and is expected to experience failures under the present climatic, geological, and

hydrological conditions. Failures in high elevation, and high rainfalls area support the finding. Additionally, the very channery loam soil texture seems to have a positive correlation with debris-slide initiation zones. These soils are subangular, blocky, and friable earth materials derived from weathering of the phyllitic Anakeesta Formation. Evergreen forest and shrub are the dominant vegetation in the area and show strong spatial relation with debris-slides. Curvature does not reveal any trend with the initiation of slides, debris-slides could be found in both concave and convex surfaces. The field study and spatial analysis suggested the presence of kinematically triggered failures due to movement of geological discontinuities within bedrock. The investigation also suggested that initial wedge failures dominated the slides on steeper slopes and these slides were eventually converted into debris flows with increasing water content, and soil/decomposed plant/broken rock debris as they moved along existing drainage channels. The present drainage channels were probably paleo debris flow channels, but they were not studied during this research.

The model predicted the existing debris-slides with high accuracy, where 86% of the known slides were situated in high and very high susceptibility categories. However, this study focused on rapid analysis using a heuristic approach. Success of a heuristic model relies on the expert's opinion and selecting incorrect geofactors and assigning inappropriate weighting can lead to erroneous results. Future work will apply data-driven statistical-based approaches like logistic regression or artificial neural networks to model the debris-slide susceptibility and compare the results with the heuristic approach used in the existing study.

The study used 256 debris-slide initiation zones; however the dates of failure were unknown, therefore, several thunderstorms and hurricanes induced debris-slides could not

be studied. That hindered the spatio-temporal probability analysis of debris-slides in the area. In the future, a time-stamped debris-slide inventory should be generated in order to provide a complete spatio-temporal hazard analysis of the area.

6. Conclusion

This paper successfully demonstrated the usefulness of the heuristic model or knowledge-driven method to rapidly generate a debris-slide susceptibility map. This study also introduced a kinematical index layer, which is a new addition, and could be included as one of the structural geology based geofactors for debris-slide susceptibility modelling. A satisfactory result was achieved by using this new variable. Validation of the model shows most of the debris-slides (86%) were located in very high and high susceptible zones. Therefore, it can be concluded that the geofactors used in this study were appropriate for the region's conditions and most likely are important inpredicting debris-slides in the study area.

References

Allmendinger, R. W., Cardozo, N. C., and Fisher, D., 2012, Structural Geology Algorithms: Vectors & Tensors: Cambridge, England, Cambridge University Press, 289 pp.

Bogucki, D.J., 1976, Debris slides in the Mt. Le Conte Area, Great Smoky Mountains National Park, U.S.A., Geografiska Annaler: Series A, Physical Geography, 58:3, 179-191, doi:10.1080/04353676.1976.11879937.

Brabb, E.E., 1984, Innovative approaches to landslide hazard mapping. 4th International Symposium on Landslides, Toronto 1,307-324.

Carrara A., Cardinali M., Guzzetti F., Reichenbach P. (1995) Gis Technology in Mapping Landslide Hazard. In: Carrara A., Guzzetti F. (eds) Geographical Information Systems in Assessing Natural Hazards. Advances in Natural and Technological Hazards Research, vol 5. Springer, Dordrecht.

Clark, G.M., 1987, Debris slide and debris flow historical events in the Appalachians south of the glacial border: Geological Society of America, Reviews in Engineering Geology, Volume VII, p. 125-137.

Ghosh, S., Das, R., Goswami, B., 2013, Developing GIS-based techniques for application of knowledge and data-driven methods of landslide susceptibility mapping. Indian Journal of Geosciences 67 (3-4), 249-272.

Ghosh, S., Günther, A., Carranza, E. J., Westen, C.J. & Jetten, V.G., 2010, Rock slope instability assessment using spatially distributed structural orientation data in Darjeeling Himalaya (India). Earth Surface Processes and Landforms. 35. 1773 – 1792, doi:10.1002/esp.2017.

Guzzetti, F., Carrara, A., Cardinali, M., Reichenbach, P., 1999, Landslide hazard evaluation: a review of current techniques and their application in a multi-scale study, Central Italy. Geomorphology 31, 181–216.

Hansen A., 1984, Landslide hazard analysis. In: Brunsden, D. & Prior, D.B. (Eds.), Slope Instability, John Wiley and Sons, New York, pp. 523-602.

Nandi, A., Shakoor, A., 2010, A GIS-based landslide susceptibility evaluation using bivariate and multivariate statistical analyses. Engineering Geology 110, 11–20, doi:10.1016/j.enggeo.2009.10.001.

Nandi, A., Shakoor, A., 2017, Predicting Debris Flow Initiation Zone Using Statistical And Rock Kinematic Analyses, A Case Study From West Prong Little Pigeon River, TN, 3rd North American Symposium on Landslides, p. 912-922.

Pradhan, B., 2011, Use of GIS-based fuzzy logic relations and its cross application to produce landslide susceptibility maps in three test areas in Malaysia. Environmental Earth Sciences, 63(2), 329–349.

Rapp, A., Stromquist, L., 1976, Slope Erosion Due to Extreme Rainfall in the Scandinavian Mountains, Geografiska Annaler: Series A, Physical Geography, 58:3, 193-200, doi:10.1080/04353676.1976.11879938.

Scott, R.C., 1972, The geomorphic significance of debris avalanching in the Appalachian Blue Ridge Mountains [Ph.D. thesis]: Athens, University of Georgia, 185 p.

Simonett, D. S., 1970, The role of landslides in slope development in the high rainfall tropics: Final report, Office of Naval Research, Geography Branch, 583(11), NR 389–133, 24 p.

Southworth, Scott, Schultz, Art, Aleinikoff, J.N., and Merschat, A.J., 2012, Geologic map of the Great Smoky Mountains National Park region, Tennessee and North Carolina: U.S. Geological Survey Scientific Investigations Map 2997, one sheet, scale 1:100,000, and 54-p. pamphlet. (Supersedes USGS Open-File Reports 03–381, 2004–1410, and 2005–1225.)

Lee, S., Pradhan, B., 2007, Landslide hazard mapping at Selangor, Malaysia using frequency ratio and logistic regression models. Landslides 4, 33–41, doi:10.1007/s10346-006-0047-y.

Varnes, D.J., 1978, Slope movements types and processes. *In*: Landslides: Analysis and Control, R.L. Schuster and R.L. Krizek (eds.), Special Report 176. Transportation Research Board, National Academy of Sciences, Washington, D.C., 11-33 p.

Varnes, D.J., 1984, IAEG Commission on Landslides and other Mass-Movements, Landslide Hazard Zonation: a review of principles and practice. UNESCO Press, Darantiere, Paris, 61 p.

Van Westen, CJ., 1993, Application of Geographical Information System to landslide hazard zonation. ITC Publication no. 15, lTC, Enschede, The Netherlands, 245 pp.

Wooten, Richard M.; Witt, Anne C.; Miniat, Chelcy F.; Hales, Tristram C.; Aldred, Jennifer L., 2016, Frequency and magnitude of selected historical landslide events in the southern Appalachian Highlands of North Carolina and Virginia: relationships to rainfall, geological and ecohydrological controls, and effects. In: Greenberg, Cathryn H.; Collins, Beverly S. editors. Natural Disturbances and Historic Range of Variation. Springer International Publishing, p. 203-262, doi:10.1007/978-3-319-21527-3_9.

CHAPTER 4

Debris-slide Susceptibility Mapping Using Logistic Regression, Maxent, Information Value Method and Frequency Ratio in The Great Smoky Mountains National Park, TN

Abstract

Debris-slide is one of the main forms of slope failures that has been causing slope instability for the past couple of decades in the Anakeesta ridge of Great Smoky Mountains National Park (GRSM). Creating a debris-slide susceptibility map is one of the most effective ways to understand the spatial probability of any future debris-slide event. Methods for developing debris-slide susceptibility map can be broadly classified into two groups: data-driven and knowledge-driven. The objective of the study was to create four data-driven debris-slide susceptibility maps using two multivariate models (logistic regression and Maxent) and two bi-variate models (Information Value Method and frequency ratio) in the Anakeesta rock formation of GRSM and compare the efficacy of the models. In order to develop the models, six debris-slide causing factors or geo-factors, including elevation, curvature, soil texture, land use, annual rainfall and geological discontinuity data (kinematic index) were used in the study. Debris-slide locations were mapped using satellite imagery and aerial photographs from 2004 to 2018, which were further verified during field surveys. Subsequently, the debris-slide data set was randomly divided into 75:25 ratio for training and testing purpose.

Information Value Method and frequency ratio models were developed using ArcGIS 10.6.0. Both models calculate density of debris-slides within the individual classes of geo-factors, however, each uses a different statistical formula. Logistic regression model was developed in ArcGIS 10.6.0 and SPSS, using dichotomous debris-slide data, where the regression coefficients were calculated in SPSS software and the logistic regression equation was executed in ArcGIS. Maxent model was generated in the standalone version of Maxent software using presence only debris-slide data. The efficacy of the models was tested using area under the Receiver Operating Characteristic (ROC) curve, which yielded 0.855, 0.863, 0.856 and 0.853 for IVM, frequency ratio, logistic regression and Maxent respectively. Considering pros and cons of the models and the closeness of the ROC value, it was difficult to select the best model. However, frequency ratio performed slightly better than other models in terms of ROC curve value. These debris-slide maps contain important pieces of geo-technical information that might be helpful to administrators and planners to select places for further infrastructure development as well as to carry out detailed geo-technical investigation in selected locations.

Keywords: *Debris-slide Susceptibility, Great Smoky Mountains, Information Value method, Frequency Ratio, Logistic regression, Maxent.*

1. Introduction

Throughout the history of the earth, mountainous terrains have been subjected to various large and small-scale mass movements, resulting in degradation of slopes and shaping of the landscape. Under the presence of favorable causal and triggering factors, such as earthquakes and extreme rainfall, most mountainous terrain has undergone at least one type of slope failure (Van Western, 1993). Mass movements in terms of rockslide, debris-slide, mudflow, avalanche etc. are one of the major natural disasters, which cause significant infrastructural damage, and loss of life and properties. Therefore, it is important to develop a detailed understanding of the causes and mechanisms of such events for better prediction and prevention planning. The terminology "landslide" includes a wide range of mass movement processes that cause slope instability due to downward movement of slope material such as rock, soil, secondary weathered material, or combination of these. Debris-slide is one category of landslides that involves chaotic movement of rock fragments and debris within coarser soil type (Varnes, 1978). Debris-slides generate when unconsolidated rock fragments mixed with sand or soil become saturated with water and roll rapidly downslope from the steeper slopes. With increase in water content, a debris-slide can gain more speed and transform into a debris flow or debris avalanche.

All 50 states in United States are prone to landslides, however, physiographic provinces like the Rocky Mountains, Appalachian Mountains, and Pacific Coastal Ranges are marked as zones of "severe landslide problems" by USGS (www.usgs.gov). On average, landslides cause 25-50 casualties each year in the United States (USGS). Direct effects of landslides includes loss of human life, damage of properties and natural resources, interruption in communication etc. (Gupta and Joshi, 1990). Because landslides occur at a local scale, and

therefore, despite their magnitude and effect, they may remain unrecognized so that people often don't consider landslides as a major hazard (Henderson, 1997).

While addressing the debris-slide or other slope failure phenomena, it is important to develop a detailed understanding of the factors causing failure and their relationship with different types of slope failure. Debris-slide causative factors includes local geology, slope angle, relief, lithology, soil type, land use, drainage pattern etc. (Nandi and Shakoor, 2010; Ghosh et al., 2013). The primary causative factors for a landslide can be determined by examining the landslide patch that has experienced repeated sliding over a long period of time and hence, this makes landslide a predictable geological hazard (Jones, 1992). One of the primary steps to predict the zones for future landslide is to develop a landslide susceptibility map based on these landslide causative factors often known as geo-factors. Therefore, accuracy of a landslide susceptibility map heavily relies on the identification of the correct sets of geo-factors and importance of these geo-factors considerably varies in different physical environment (Ghosh et al., 2013). Landslide susceptibility maps aim to demarcate future landslide zones with the assumption that the factors responsible for past landslide, most likely will cause sliding again in the future (Varnes, 1978; Carrara et al., 1995; Guzzetti et al., 1999).

To develop the landslide susceptibility map, varieties of methods are available, which are broadly classified into three groups (i) knowledge driven or heuristic, (ii) data driven or empirical, and (iii) deterministic. Heuristic approaches are entirely based on the judgement of the expert/scientist, who collects data and conducts the survey. The main advantage of this method is that it is independent of historic landslide data. However, the validation of the model becomes difficult in this situation (Ghosh et al., 2013). The heuristic approach

can also be termed as 'Expert Evaluation Approaches' (Lerio, 1996) are further divided into two types, (i) direct method and (ii) indirect method. In the direct heuristic method, the scientist directly carries out a detailed landslide assessment based on his/her experience of dealing with similar kind of situations in other areas and performs a slope instability analysis directly from geomorphological mapping (Aleotti and Chowdhury, 1999). However, absence of explicit rules for the assessment and subjectivity in selection of causative factors and techniques for the evaluation are some disadvantages of this method, which creates difficulties for other investigators to update the landslide susceptibility maps and compare their results (Leroi, 1996; Van Westen et al., 2003). While applying the indirect heuristic approach, the expert selects the geo-factors responsible for landslides based on his/her personal experience and assign weighted values to the factors depending upon the contribution of factors in causing the slope instability (Soeters and Van Westen, 1996). Further, numerical rating of indirect method can be either predefined e.g., Bureau of Indian Standard (BIS) method in India or expert driven such as Multi-class overlay, Fuzzy-logic etc. (van Western, 1996). Again, in the case of indirect methods, the subjectivity of assigning weights to the individual classes of the factors is at the sole discretion of the experts; therefore, assignment of weights to the geo-factor will significantly vary among the investigators. However, heuristic methods allow more flexibility to understand the role of different geo-factors in causing slope instability in a specific geo-environment, as the role of these geo-factors might changes with changes in geo-environmental condition (Ghosh et al., 2013).

Data driven or empirical methods apply the statistical and mathematical relationship between the landslide causing factors and occurrence of landslides. Statistical methods use a data driven approach for landslide susceptibility analysis for the historical landslide data

and associated causing factors to determine their relative importance and inter relationships (van Westen, 1993; Guzzetti et al., 1999; Ghosh et al., 2013). With emergence of GIS technology, application of statistical approaches became popular in landslide susceptibility analysis (Aleotti and Chowdhury, 1999), as they enable susceptibility analysis at a greater spatial extent. Currently, upgraded versions of GIS softwares provide advanced tools to perform complex statistical analysis and have become indispensable for landslide susceptibility analysis. Statistical approaches can be either bivariate or multivariate. In bivariate analyses different landslide causing geo-factors such as terrain slope angle, lithology, land use, elevation etc. are evaluated individually against occurrence of the landslide. Information Value Method (IVM), Frequency ratio, Weight of Evidence (WofE) are some of the bivariate models, which calculate the density of landslides in different classes geo-factors using different statistical equations. A multivariate statistical approach involves simultaneous processing of multiple geo-factors against the landslide data. Logistic regression and discriminant analysis are two of the frequently used multivariate statistical approaches in landslide study (Ayalew and Yamagishi, 2005). Discriminant analysis works well with continuous variables (Clerici and Dall'Olio, 1995); whereas, logistic regression can handle both continuous variables such as slope, relief, curvature etc. and categorical variables like lithology, soil type etc. as well as the ordinal variables or ranked variables. However, most of the multivariate analyses somewhat work as a black-box model and one of the main constraints of the model is that it does not consider inherent relationships between landslide and geo-factors while generating the landslide susceptibility model (Ghosh et al., 2013). A summary of pros and cons of these models have been provided in Table 1. Deterministic approaches are widely used in site-specific

engineering projects to determine the slope stability in terms of Factor of Safety calculation (Aleotti and Chowdhury, 1999).

In the Appalachian highlands, debris-slides and debris flows are very frequent events and more than 3000 slides have been recorded in this region (Pariseau and Voight, 1979). Since 1940, as many as 200 deaths have been reported in the Appalachian region as a direct effect of mass movement activities (Scott 1972, Wooten, et al., 2016).

Table 1: Comparison of different models.

Parameters	*Knowledge-driven method*	*Data-driven method*
Debris-slide inventory	Not required	Required.
Expert input	Highly required.	Only for selecting geo-factors.
Rule for selecting weightage or co-efficient of the geo-factors.	Selected by the expert.	Calculated based on statistical or mathematical relationship with occurrence of debris-slide.
Model generation process	Mostly explicit.	Most of the bi-variate models are explicit but multivariate models work as black box.
Model Validation	Difficult for qualitative models.	Mostly done using the ROC curve.
Software requirement	Can be done in GIS.	Bi-variate models can be generated in GIS but multivariate models require addition software.
Complexity involved	Flexible	Moderate to highly complicated.
Time	Model can be generated in a short amount of time.	Model generation is a rigorous and time-consuming process.

2. Objective of the study

The primary objective of the study is to compare the efficacy of four different debris-slide susceptibility models using Information Value Method (bivariate), Frequency Ratio (bivariate), Logistic Regression (multivariate) and Maximum Entropy Model (multivariate). The secondary objective is to identify the most import geo-factors for causing debris-slide in the area.

3. Background

3.1. Study area

3.1.1. Climate

The study was conducted in the Anakeesta rock formation; surrounding the Anakeesta Ridge, part of the Upper West Prong Little Pigeon River watershed in Great Smoky Mountains National Park (GRSM) (Fig. 1). Elevation of Anakeesta ridge ranges from 1105 m (3625 feet) to 2010 m (6594 feet). The Climatic pattern of the GRSM varies significantly with change in elevation and the area hosts variety of microclimates, which are mainly caused by difference in solar illumination, altitude, and orographic effects (Band and Moore, 1995). GRSM receives annual rainfall of 1397 mm (55 inches) in valleys to over 2195 mm (85 inches) on park ridges. Maximum intensity in rainfall can be observed during the summer time ranging from >1inch/hour to > 3inch/24 hours (TVA, 1937). Both intensity and amount of rainfall increases with increase in the elevation (Bogucki, 1972). Anakeesta Ridge receives the highest annual rainfall within the park, which triggers debris-slide in the area (Bogucki, 1970; Scott, 1972). Temperature varies from -2.22˚C (28 ˚F) to 31.11˚C (88˚F) at the base

and -7.2˚C (19˚F) to 18.33˚C (65˚F) at the top of ridges. The area receives average (annual) 2.45 cm (1 inch) snow at the base and nearly 60.96 (24 inches) at the top (Fig. 1).

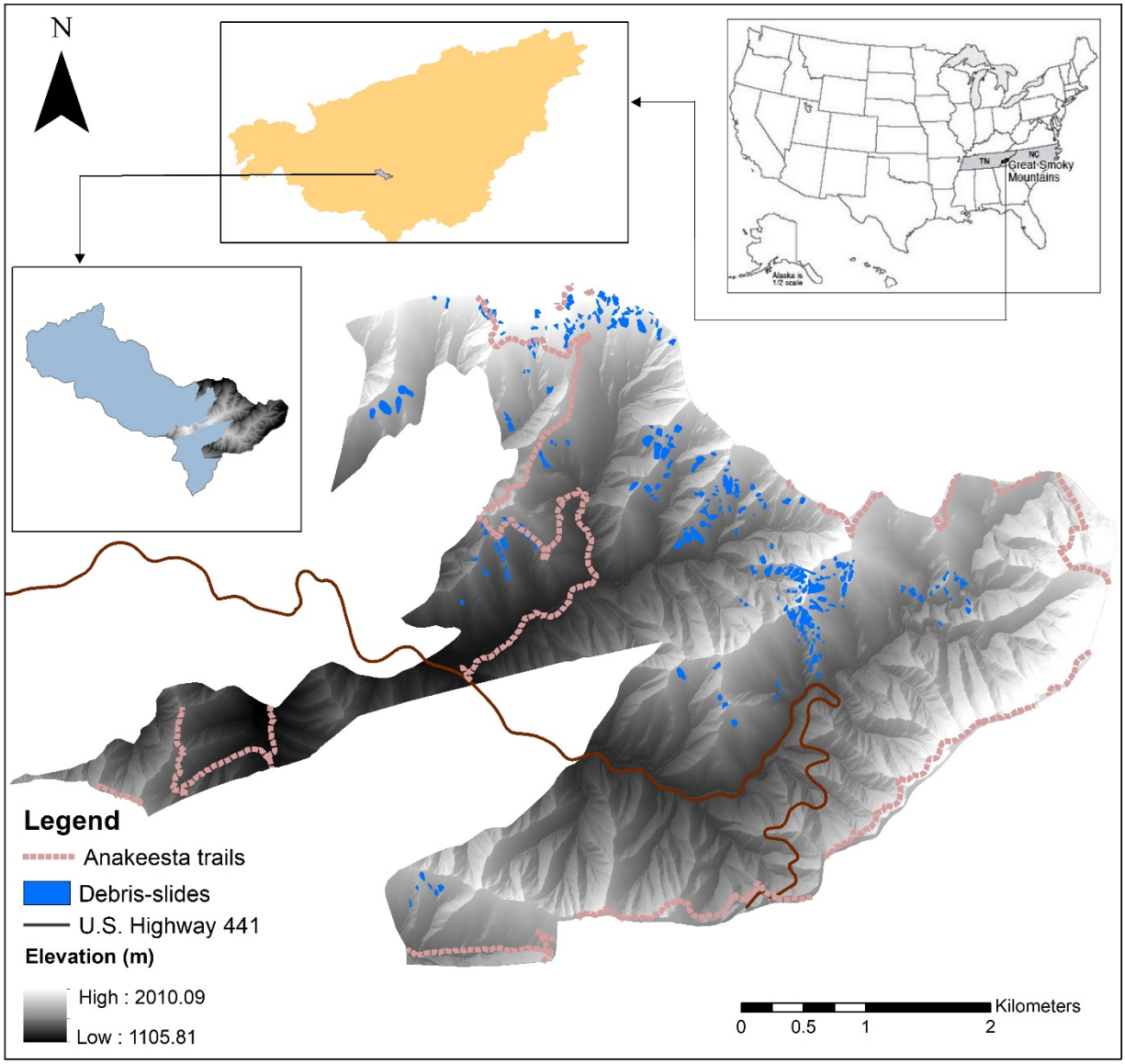

Figure 1: Digital Elevation Model of the study area with debris-slide locations in the GRSM.

3.1.2. Geological setting

Metasedimentary rocks dominate the lithology of the Great Smoky Mountains National Park with occasional occurrence of igneous rocks (Fig. 2). The rock types of the study area belong to Ocoee Supergroup, which is primarily characterized by metasedimentary rocks such as sandstone, interbedded slates, phyllites and schists. Sedimentary rocks of Ocoee series were originally deposited as unconsolidated sand, silt, clay and fine gravel at the bottom of the ocean during the Cambrian period, which eventually consolidated together into sedimentary rock layer with a thickness over 20,000 feet (King et al., 1950) (Fig.3). The formation shows the signature of varying grade of metamorphism along with complexly folded and faulted structures (King et al., 1968). The underlying basement complex is composed granite and metasedimentary gneiss of earlier Precambrian age (Moore, 1988). The Ocoee series of rocks occur beyond the Great Smoky Mountains and has a spatial extent from Asheville, North Carolina to Cartersville, Georgia, encompassing a distance of more than 225 km (175 miles) (King et al., 1968).

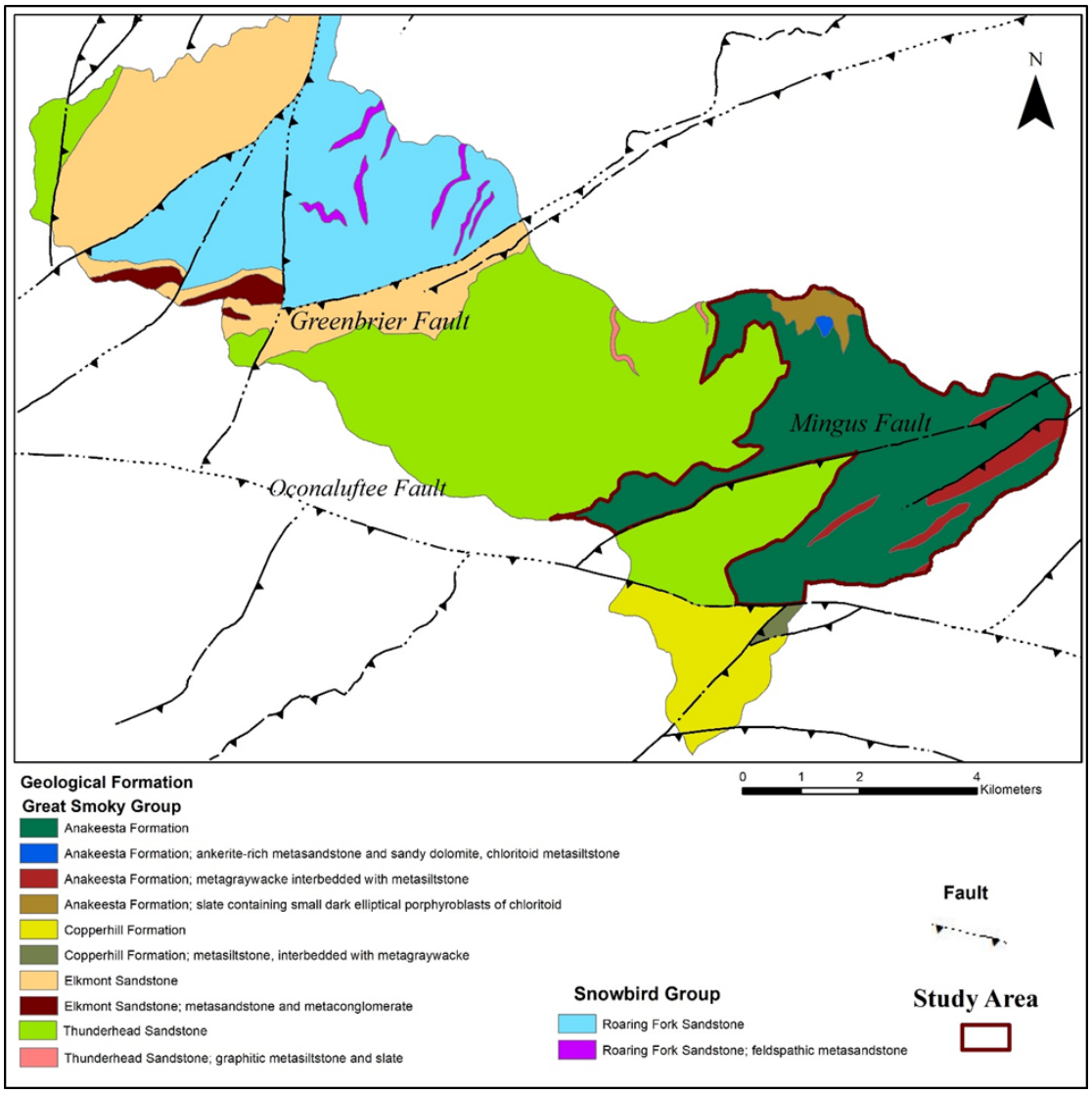

Figure 2: Geological Map of the Study Area. (Source: King, Neuman, and Hadley, 1968).

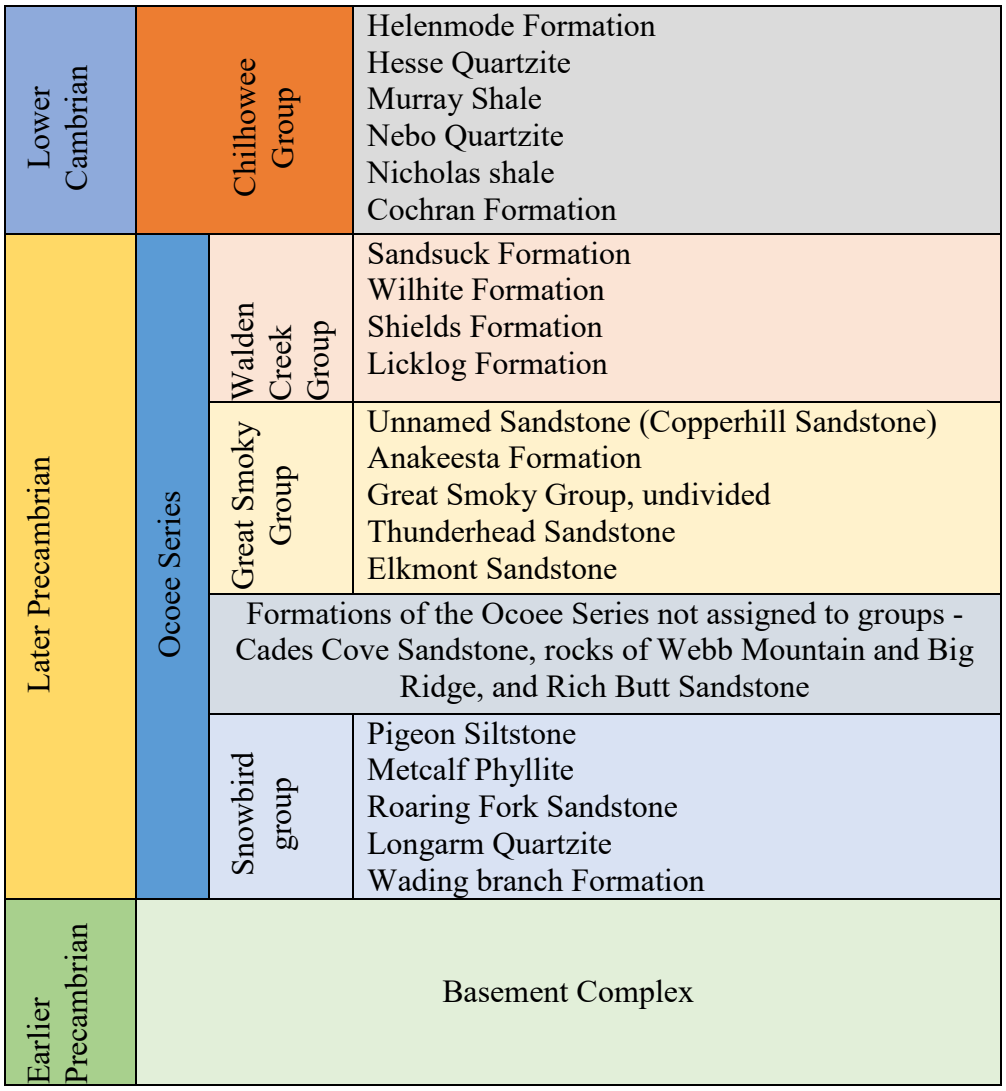

Figure 3: Stratigraphy of Great Smoky Mountain National Park and Vicinity (Source: Philip B. King et al., 1968).

The Ocoee series is divided into three groups: Snowbird, Great Smoky and Walden Creek Group, which are separated from each other by major thrust faults (King et al., 1958). The study area is part of Anakeesta Formation of Great Smoky group. Outcrops of the Anakeesta Formation are characterized by craggy pinnacle structures, having steep slope and consisting of numerous bedding, joint and cleavage planes that provides abundant discontinuity surfaces for slope failure (Delcourt and Delcourt, 1985). The Anakeesta

Formation hosts a variety of rock types and shows significant contrast in color, which varies from dark grey due to presence of graphite to rusty orange due to sulfide minerals (Fig. 2). The dominant rock type of the formation includes phyllite, chloritoidal slate, dark grey graphitic and sulfidic slate, feldspathic sandstone, laminated metasiltstone and coarse grained metagraywacke (Southworth et al., 2005).

Three major faults of the Great Smoky Mountain play a crucial role in the structural arrangement of the rocks (Moore, 1988). The Great Smoky group is separated from the underlying Snowbird group by a low angle NE-SW trending thrust fault called Greenbrier Fault, which is located north of the study area. The Oconaluftee fault is a right lateral fault located southwestern part of the study area that separates lower tongue of the Anakeesta Formation from Copperhill formation by approximately 0.8 km (Ryan, 1989). The fault trends NW-SE and dips towards southeast with an angle of 25˚ to 55˚ (Bogucki, 1970). The Mingus fault is a high angle reverse fault that trends almost east west and goes through the Anakeesta Formation (Hadley and Goldsmith, 1963). The Mingus fault has displaced the outcrop of Anakeesta Formation by approximately 1.5 km (Ryan, 1989).

3.2. Debris-slide History

Most of the debris-slides in the area are triggered by torrential rainfall associated with thunderstorms and hurricanes (Henderson, 1997). Previous research has reported a steady increase in landslide activity since 1940 (Clark, 1987; Ryan, 1989; Henderson, 1997) and along with the formation of new debris-slide scars, the older scars have

enlarged and many of these have moved retrogressively towards the crest of the mountain (Ryan, 1989). However, despite of having such a long history of debris-slide activity, no systematic documentation of past debris-slide documentation exists. A very few debris-slide events were recorded but no data about the spatial extent or volumetric loss during these events are available (Table 2).

On January 16th 2013, a massive slope failure took place on U.S highway 441 that destroyed about 200 m road segment. As per National Park Service report, the slide generated 70,000 cubic meters of material and moved nearly 243 meters downslope. The slide was caused by torrential rainfall as the area received more than 8 inches (203.2 mm) of rainfall in a 24-hour period before the sliding, which eventually saturated the soil and debris with water and triggered the disaster.

Table 2: Past Debris-slide events in the area.

Date	Type of Storm	Area
10 July 1942	Thunderstorm	Newfound Gap
1 September 1951	Cloudburst	Mt. Leconte
15 June 1971		Mt. Leconte
March 1975 – through 1983	Multiple Storm	Anakeesta Ridge
August 3,1978	Thunderstorm	Mt. Leconte
Mar / Sep 1985	Thunderstorm	Anakeesta Ridge
July 1984	Thunderstorm	Anakeesta Ridge
10 August 1984	Thunderstorm	Anakeesta Ridge
28 June , 1993	Cloudburst	Mt. Leconte
October 4-6, 1995	Hurricane Opal	Mt. Leconte / Anakeesta Ridge
16-17 September, 2004	Hurricane Ivan	Mt. Leconte / Anakeesta Ridge
August 5-6, 2012	Thunderstorm	Anakeesta Ridge
January 16, 2013	Torrential Rainfall	U.S. highway 441
Sept. 10-14, 2017	Hurricane Irma	Anakeesta Ridge

4. Methodology

The study consisted of three distinct parts. First data were collected, including mapping of debris-slide initiation zones. Second, four data-driven debris-slide susceptibility models were developed using Information Value Method (IVM), frequency ratio, logistic regression and Maximum Entropy Model (Maxent). Of the four models, IVM and frequency ratio are bi-variate models and logistic regression and Maxent are multivariate models. The models were developed in ArcGIS and SPSS, except Maxent, which was developed using the standalone version of Maxent software. Finally, the models were verified using the area under ROC curve in SPSS software.

4.1. Data

4.1.1. Debris-slide location

Debris-slide patches were mapped using satellite imageries and aerial photographs from the year 2004 to 2018, which were also verified during the field survey (Fig. 1). In total, 256 debris-slide initiation zones were identified in the study area, with a cumulative area of 307,658 m^2. The debris-slide data set was randomly divided into 75:25 ratio, where 75% of the data were used for building debris-slide initiation zone susceptibility models and 25% were kept for model validation.

4.1.2. Digital Elevation Model (DEM)

The LiDAR Digital Elevation Model having spatial resolution of 0.76 meter (2.49 feet) was used in this study. LiDAR DEM for the entire state of Tennessee is available in TNGIS website (http://www.tngis.org/). The DEM was

processed in ArcMap 10.6.1 to generate elevation (Fig. 4a) and slope curvature (Fig. 4b) maps of the study area.

4.1.3. Kinematic Index layer

The geometrical relationship between the orientations of topographical slope and aspect with geological discontinuities can play a crucial role in controlling slope stability within a rock mass. This mutual relationship is known as rock kinematic and slope instability analysis based on this relationship is termed as rock kinematic analysis. Rock kinematic analysis includes different factors like topographic slope and aspect, orientation of geological discontinuities and internal friction angle of the bedrock to calculate the stability of a slope. Depending upon topographical orientation and geological discontinuities, three different modes of failure can occur within a rock mass, (i) Planar (ii) Wedge and (iii) Topple failures (Godman and Bray, 1976, Hoek and Bray, 1981) based on the following relationships (Ghosh et al., 2010):

$$\phi \leq \beta \leq \theta \text{ (for Plane and Wedge Failure)} \quad (1)$$

$$\theta \geq [\phi + (90° - \beta)] \text{ (for Topple Failure)} \quad (2)$$

where, ϕ = Internal friction angle of the rock, β = Dip/plunge of the discontinuity and θ = Topographic slope.

In this study, the kinematic index layer for the study area was developed by using ArcGIS 10.5.1. A total of 313 geological discontinuity data points were used in the study, which were directly collected from the field mapping and a previous study (Ryan, 1989). These data were plotted in Stereonet 10 software (Allmendinger et al., 2012) to identify the different sets of discontinuities in the

study area. Internal friction of the rock was empirically derived using the Rock Mass Rating system data (Bieniawski, 1989), which were collect during the field survey. Topographic slope angle was extracted from LiDAR DEM. Subsequently, Eq. 1 & 2 were applied in ArcGIS to identify areas where slope failures are kinematically possible (Ghosh et al. 2010). The detailed description of the preparation of composite kinematic index layer is presented in a forthcoming paper (Das, et al., in preparation) and in the second chapter of the thesis. The kinematic index layer is the function of topographic slope angle, aspect, lithology, and geological discontinuity, hence, it can substitute for individual layers and act as one independent variable or geo-factor in debris-slide susceptibility modelling (Fig. 4c).

4.1.4. Other variables

Land cover, annual rainfall and soil texture (Fig.4 d, e, f) data were collected from the National Park Service's database (https://irma.nps.gov/DataStore/Search/Quick). The rainfall map was further processed and converted from a categorical variable to a continuous variable using Inverse Distance Weighted interpolation method. Whereas, land cover and soil texture maps were used as categorical variables in the analysis.

In the debris-slide susceptibility analysis, six geo-factors or independent variables were used namely, elevation, curvature, kinematic index, land cover, soil texture and annual rainfall. The details of the geo-factors are summarized in Table 3.

Table 3: Summary of the geo-factors

Geo-factor	**Source**	**Average (Range)**
Elevation	Digital Elevation Model	1526 m (1105m – 2010m)
Rainfall	National Park Services	2051mm (1854mm– 2159mm)
Soil	National Park Services	Channery loam, Channery silt loam, Loam, Slide area, Peat, Very Channery loam
Kinematical Index	Digital elevation model and Lithological map (National Park Service)	5.68 (0 - 57.95)
Landcover	National Park Services	Barren land, Deciduous forest, Developed Open space, Developed low intensity, Developed medium intensity, Evergreen Forest, Mixed Forest, Shrub
Curvature	Digital Elevation Model	-6.62 (-6839 to + 11380)

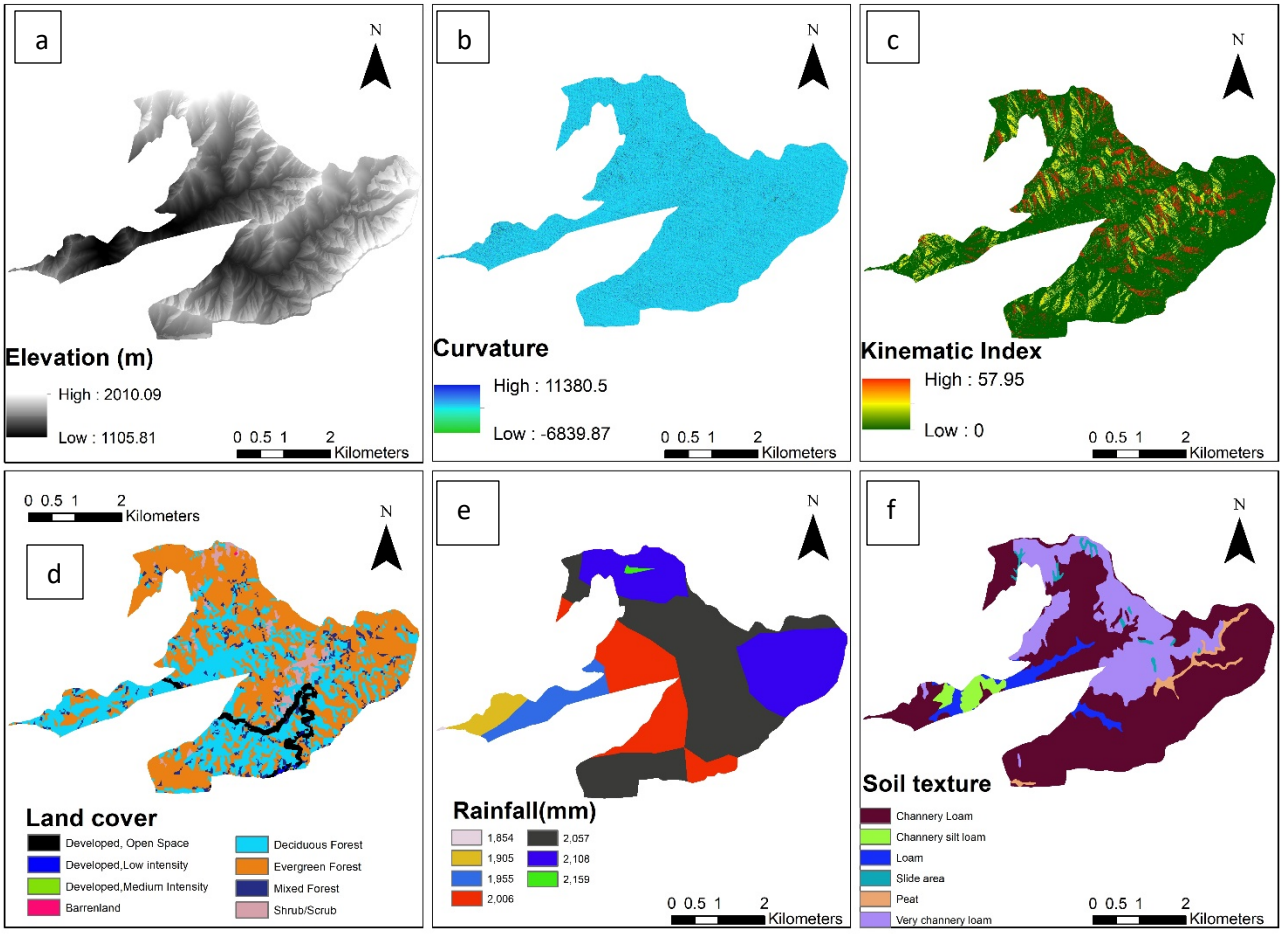

Figure 4 : Geo-factors map of the study area: (a) Elevation (b) Curvature (c) Kinematic index (d) Land cover (e) Annual rainfall (f) Soil texture.

4.2. Analyis

The analysis was performed using four different statistical methods including Information Value Method (IVM), frequency ratio, logistic regression and Maxent model.

4.2.1. Information Value Method (IVM) :

Information Value Method is a bivariate statistical method that was originally proposed by Yin and Yan (1988), while van Western slighly modified the equation (1997) and introduced it for landslide hazard zonation (Saha et al., 2005). This is one of simplest statistics that calculates the weights of individual classes of geofactor as a ratio of the density of landslide in a particular class to the landslide density of the total study area (Sarkar et al., 2013). Following is the equation for weight calculation:

$$\mathbf{W_i} = \ln \frac{\mathrm{NPix(Si)} / \mathrm{NPix(Ni)}}{\Sigma\mathrm{NPix(Si)} / \Sigma\mathrm{NPix(Ni)}} \quad (3)$$

where, Wi = Weight of a class of a geo-factor; NPix(Si) = Number of pixel of debris-slide within class i; NPix(Ni) = Number of pixel of class i; ΣNPix(Si) = Total number of debris-slide pixels within the entire study area ; ΣNPix(Ni) = Total number of pixel of the study area. Natural logarithm is used to control the large variation in the weights.

A positive weight indicates positive correlation between the individual classes of the geofactor with the occurrence of debris-slide. The higher the values, the stronger the influence of the geo-factor on debris-slide occurence. Similarly, a negative weight depicts negative correlation between the geo-factor and debris-slide occurence, which indicated that the geo-factor is not a good predictor of debris-slide.

To generate the debris-slide susceptibility map, Debris-slide Susceptibility Index (DSI) was calculated pixel-by-pixel by summing the weighted values of each geo-factor as shown below:

$$DSI_{(IVM)} = \sum_{j=1}^{M} X_j \times W_i \quad (4)$$

where, X is the geo-factor and j = 1, 2, ...M, M = Total number of geofactors. W_i = Weight of a class of a geo-factor.

The calculation was done in ArcGIS 10.6.1, where the weights of individual classes of the geofactors were calculated and the debris-slide susceptibility map was generated by adding up the weights of the geofactors. The model was validated using 25% test data in SPSS software.

4.2.2. Frequency Ratio (FR)

Frequency ratio is a bivariate statistic, which has been extensively used for landslide susceptibility modelling (Lee, S. and Sambath, 2006; Lee and Pradhan, 2007; Yilmaz, 2009). The FR model reveals the relationship between landslide causative factors and occurrence of landslide by quantifying the correlation between them. The FR is a ratio of probability of presence and absence of landslide (Lee and Pradhan, 2007). Higher the FR value is, the stronger the correlation between landslide and the individual class of the geo-factor. Following is the equation for FR value calculation:

$$FR = \frac{NPix(Si) / \Sigma NPix(Si)}{NPix(Ni) / \Sigma NPix(Ni)} \quad (5)$$

where, FR = Weight of a class of the geo-factor; Npix(Si) = Number of pixel of debris-slide within class i; NPix(Ni) = Number of pixel of class i; ΣNPix(Si) = Total number of debris-slide pixels within the entire study area ; ΣNPix(Ni) = Total number of pixel of the study area.

Debris-slide Suscepetibility Index (DSI) can be calculated by summing the values of the individual geo-factors using the following formula:

$$DSI_{(FR)} = \sum_{j=1}^{N} FR \times X_j \quad (6)$$

where, X is the geo-factor and j = 1,2,3,…N, N= total number of geo-factors. DSI is calculated for every individual pixels in the study area and the higher the DSI value the greater the probability of occurrence of debris-slide in the pixel.

DSI was calcualted for every geofactors using ArcGIS 10.6.1 and efficacy of the model was tested using rest of the 25% data in the SPSS software.

4.2.3. Logistic Regression (LR)

Logistic regression is a widely used multivariate statistical method in landslide susceptibility studies to determine the relationship between a dependent variable with several independent variables or geo-factors (Lee and Pradhan, 2007). LR predicts the outcome of an event in dichotomous form i.e., presence/absence, true/false based on the values of several independent variables. It uses a link function called logit, which transforms the non-linear model to a linear model. Some of the advantages of LR models are that it can process both categorical and continuous variables simultaneously and variables don't need to be normally distributed which is uncommon in natural environment (Lee, 2005). The logistic link function is applied when the dependent variable is binary, which calculates the probability of an event on an S-shaped logistic curve that ranges between 0 to 1. LR model uses the following formula to fit the dependent variables and calculate the probability:

$$P = 1/(1+e^{-z}) \quad (7)$$

where, P is the probability of occurrence of debris-slide and z is the linear combination of independent variables. Z can be calculated using the following formula:

$$Z= b_0 + b_1X_1 + b_2 X_2 +\ldots\ldots b_nX_n \quad (8)$$

Where, b_0 is the intercept of the model, the b_i (i = 0, 1, 2, … , n) are the regression coefficients of the logistic regression model, and the X_i (i = 0, 1, 2, … , n) are the independent variables.

IBM SPSS Statistics 25 softwarewas used to calculate the regression coefficient. Debris-slide data were classified into binary format based on presence (1) or absence (0) of debris-slide (Fig. 5). Debris-slide absence points were generated randomly using ArcGIS 10.6.1. Although SPSS is capable of processing categorical variables, however, it generates the coefficient values for n-1 numbers of classes of the categorical variable i.e., if a variable has five different classes, SPSS would

generate coefficient values for 4 classes. Therefore, to overcome this ambiguity, dummy variables were generated to calculate regression coefficients for all individual classes of the categorical variables. After calculating the regression coefficients, eq. 8 &7 were used in ArcGIS raster calculator to calculate the spatial probability of debris-slide in the study area. Values closer to 1 depict greater probability of debris-slide, whereas, values closer 0 zero indicate stability of the slope i.e., lower probability of debris-slide.

4.2.4. Maximum Entropy Model (MaxEnt)

Maxent is a widely used program for species distribution modeling which uses presence only data. MaxEnt predicts suitable habitat for occurrences of a species based on certain environmental factors or covariance. The probability of presence of the species, conditioned on environment: Pr (y = 1|z)

Where z is the covariance or factor that influences the presence or absence of a species e.g., temerarure, rainfall etc. and y= 1 is presence of a species (Elith. *et al.,* 2011).

Similar concept has been applied in this study, where suitable locations for the future debris-slide are being predicted based on the present conditions, which are causing debris-slide in the study area (Felicisimo et al., 2013). The model adapts a multivariate approach to find out suitable zones for debris-slide based on the influence of the geo-factors. Before running the model, all geo-factors or independent variables were resized into similar spatial extent and pixels size (0.76 m) was made same for all the geo-factors. Subsequently, the geo-factors were converted to ASCII format; as Maxent doesn't process any raster format expect ASCII. The entire analysis was performed using the standalone version of Maxent software (Phillips et al., 2010).

A flow chart provides the entire process of methodology in Figure. 6.

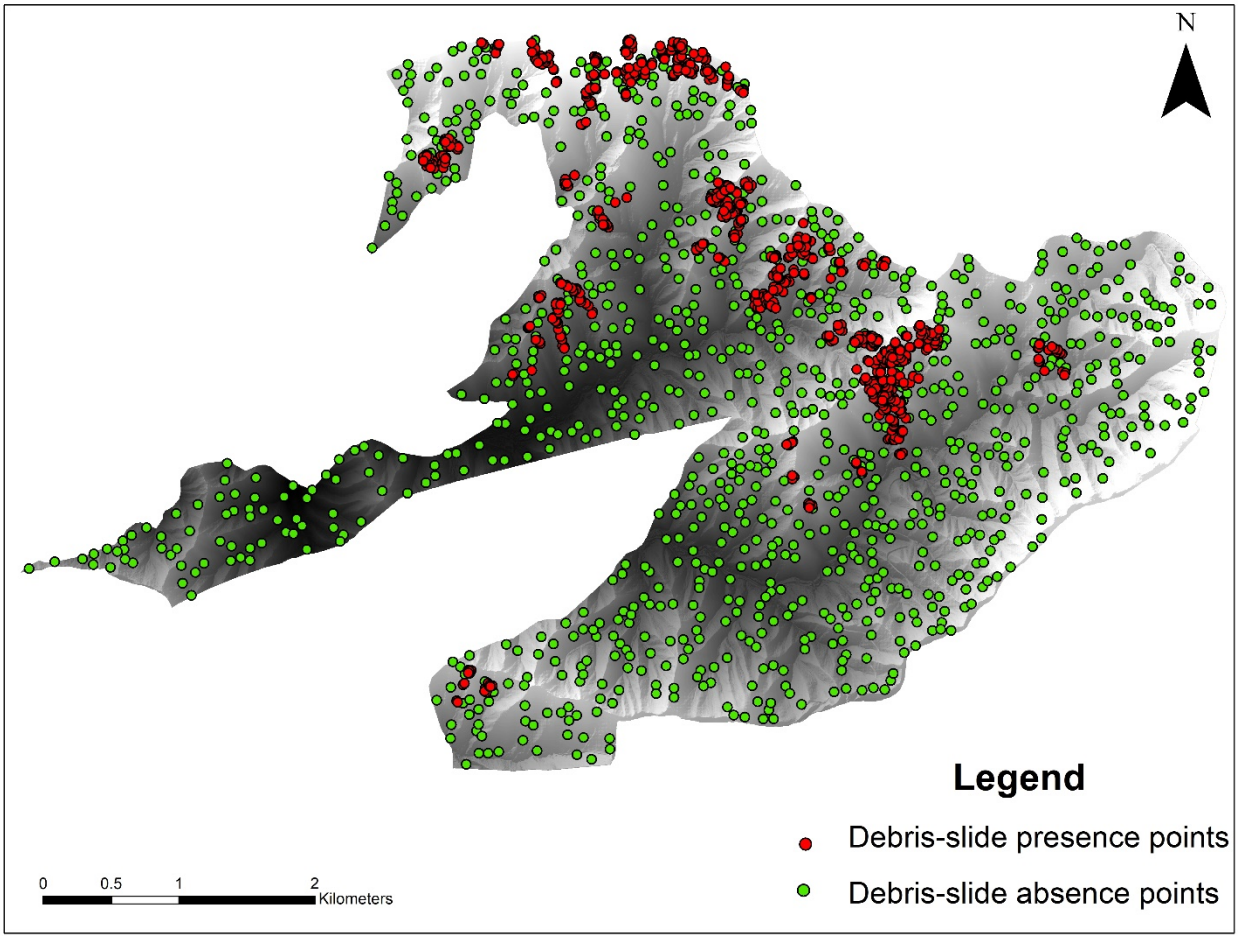

Figure 5: Presence and absence debris-slide points.

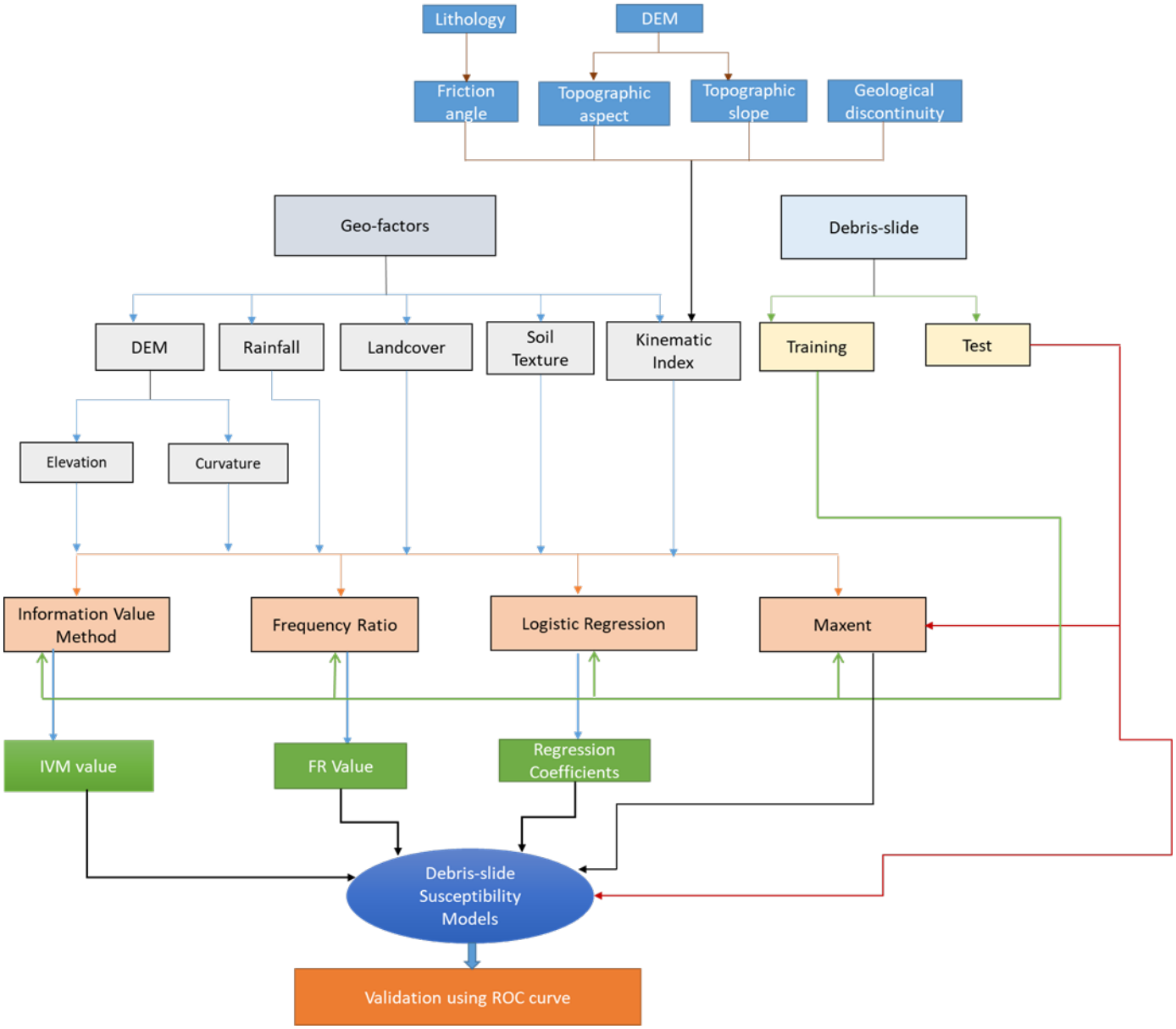

Figure 6. Flow chart of the methodology.

5. Results

5.1. Information Value Method (IVM)

A quite satisfactory result was achieved using bivariate Information Value Method (Fig. 7) in comparison with the multivariate methods. The overall IVM coefficients of the model range from -7.18 to 3.88 (Table 4). A positive value indicates more influence of the class on debris-slide and vice-versa. Barren land has the highest IVM coefficient (3.88) that signifies a high influence on debris-slide followed by shrubs/scrubs with a value of 2.17. Two soil texture classes, slide area and very channey loam, have a positive correlation while the rest of the classes are negatively correlated with debris-slide. Kinematic index has relatively high number of classes associated positively with debris-slides. Of five classes of kinematic index, four classes are positively associated with debris-slides and the IVM coefficient value increases with an increase in the kinematic index. The same correlation can be observed in the case of elevation; the IVM coefficient value steadily increases with increase in elevation and lower elevations have negative coefficient values. Large negative IVM coefficient values, such as in low elevation range (1105 m – 1339 m), low rainfall (73 mm to 77mm) were indicative of less to no debris-slide occurrence in the study area.

Curvature did not appear to influence debris-slide occurrence differently as both concave and convex curvatures had a positive IVM coefficient. Rainfall showed positive correlation with the sliding activity. The model achieved an AUC value of 0.855 or the prediction accuracy of the model is 85.5% and hence, falls under the category of ‘Good’ model (Fig. 8).

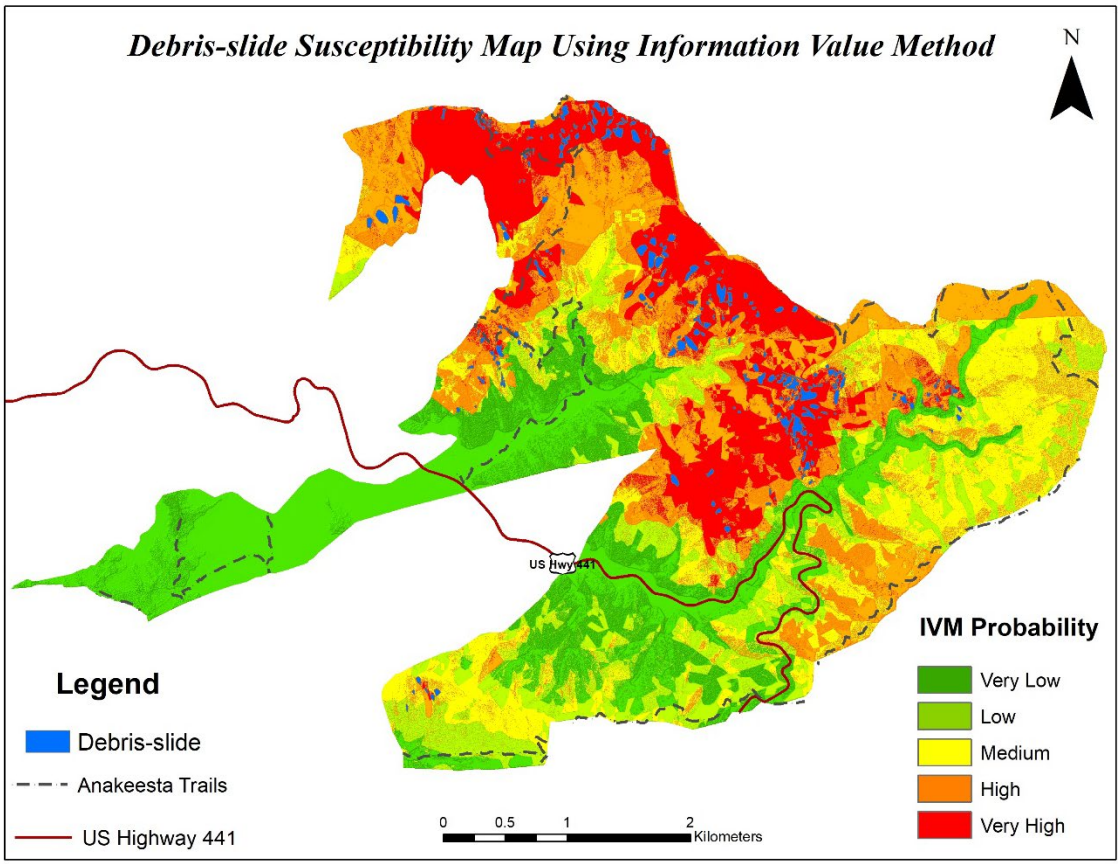

Figure 7: Debris-slide susceptibility model using IVM

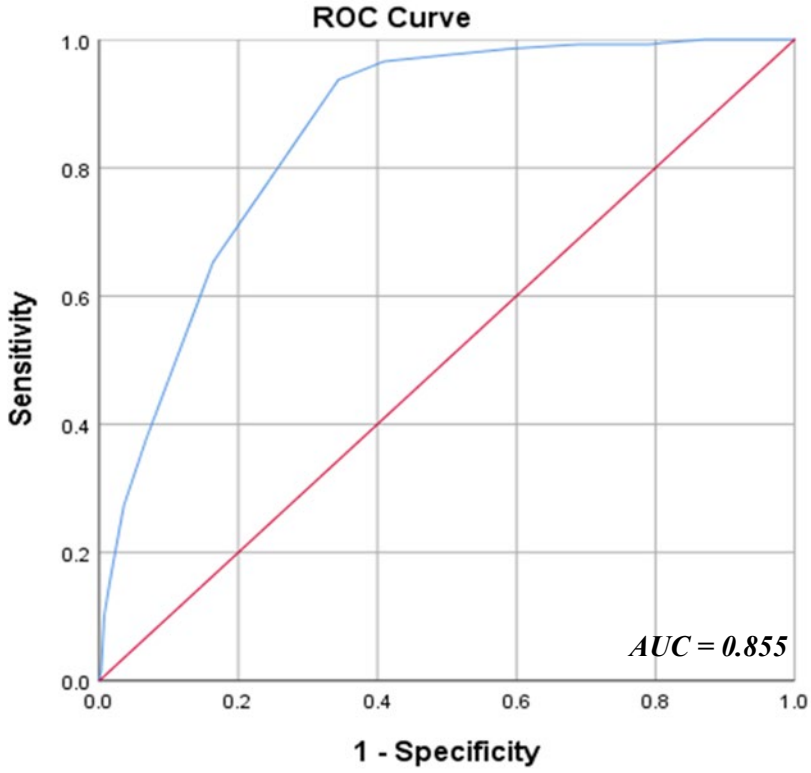

Figure 8: ROC curve of IVM model.

5.2. Frequency Ratio

Frequency Ratio yielded result very similar to the IVM (Fig. 9). The value of FR coefficients range from 0 to 48.76 (Table 4). An absolute zero value indicates total absence of debris-slide in that class. While, values less than 1 indicates a lower correlation and greater than 1 signify higher correlation between debris-slide and classes of geo-factors. Barren land is the highest contributor towards debris-slides having a coefficient of 48.76. Considering the overall contribution of the geo-factors, elevation and kinematic index have strong influence on debris-slides as individual geo-factors because most of the classes within these geo-factors show positive FR coefficient values. Curvature does not reveal any trend in controlling debris-slide as both positive and negative coefficient values occur in concave and convex curvature. The model achieved a good prediction rate with 0.863 AUC value that classify the model as a good predictor of debris-slide (Fig. 10).

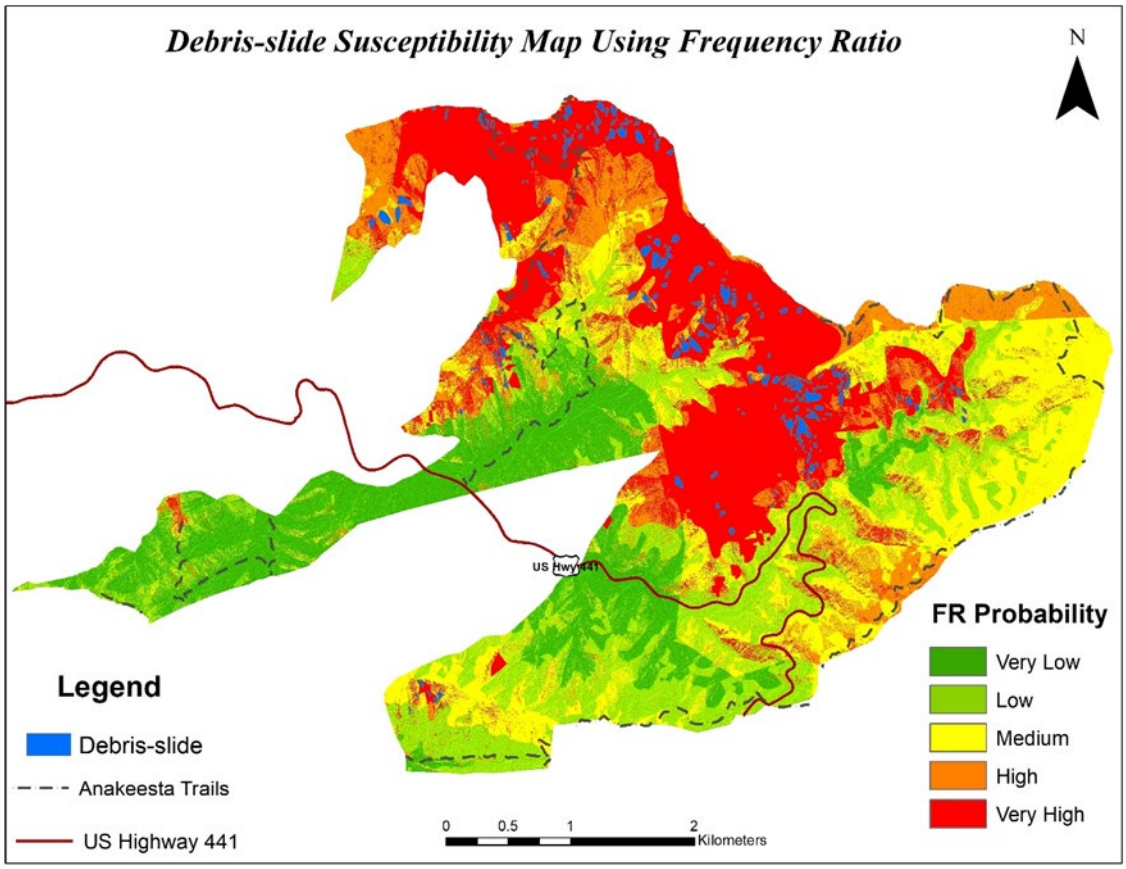

Figure 9: Debris-slide susceptibility model using FR

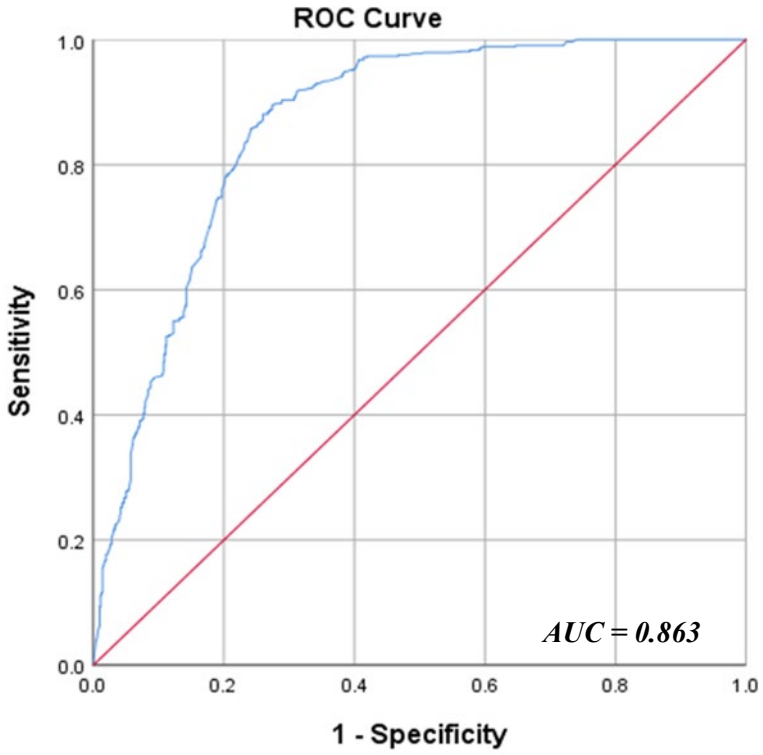

Figure 10: ROC curve of FR model.

5.3. Logistic Regression (LR)

To obtain regression coefficients for the geo-factors, logistic regression was performed using SPSS software (Table 6). The study included four continuous variables of which elevation, kinematic index, and rainfall were statistically significant, whereas, curvature was statistically insignificant and was eliminated from the final model. Categorical geo-factors were analyzed by generating dummy variables for individual categories of geo-factors. Only four classes (deciduous forest, developed area, evergreen forest and mixed forest) from the Land cover category and two classes (channery loam, old slide area) from the Soil Texture category were statistically significant. Multi-collinearity tests among the independent revealed that the values of Variation Inflation Factor (VIF) are well within prescribed limits (Table 5). VIF value greater than 3 indicates probability of multicollinearity among the independent variables and value greater than 10 indicates definite multicollinearity between variables. All the variables in the study have the VIF well below the threshold limit of 3 (Table 5). Therefore, the independent variables were not correlated with each other. A statistically significant Chi-square value was obtained in Omnibus Tests of Model coefficients, which indicates that the model performed better than the model with no predictors. The model also yielded a Narelkerke R square value of 0.541 that indicates the model is moderate to good predictor of the variables within the data set. Finally, the logistic regression model was obtained by incorporating the coefficient values in the Eq. 7 & Eq. 8 using ArcGIS as shown below (Fig. 11):

$$Z = 12.160 + Kinematic\ Index \times 0.037 + Elevation \times 0.005 + Rainfall \times (-0.227) + Deciduous \times (-1.90) + Developed\ Area \times (-2.28) + Evergreen\ forest \times (-1.61) + Mixed\ forest \times (-1.04) + Channery\ Loam \times (-1.75) + Old\ slide\ area \times (0.85).$$

Validation of the model using Receiver Operating Characteristic (ROC) to calculate the area under the Curve (AUC) showed the AUC value of .856 that suggests the model to be good to excellent one (Fig. 12).

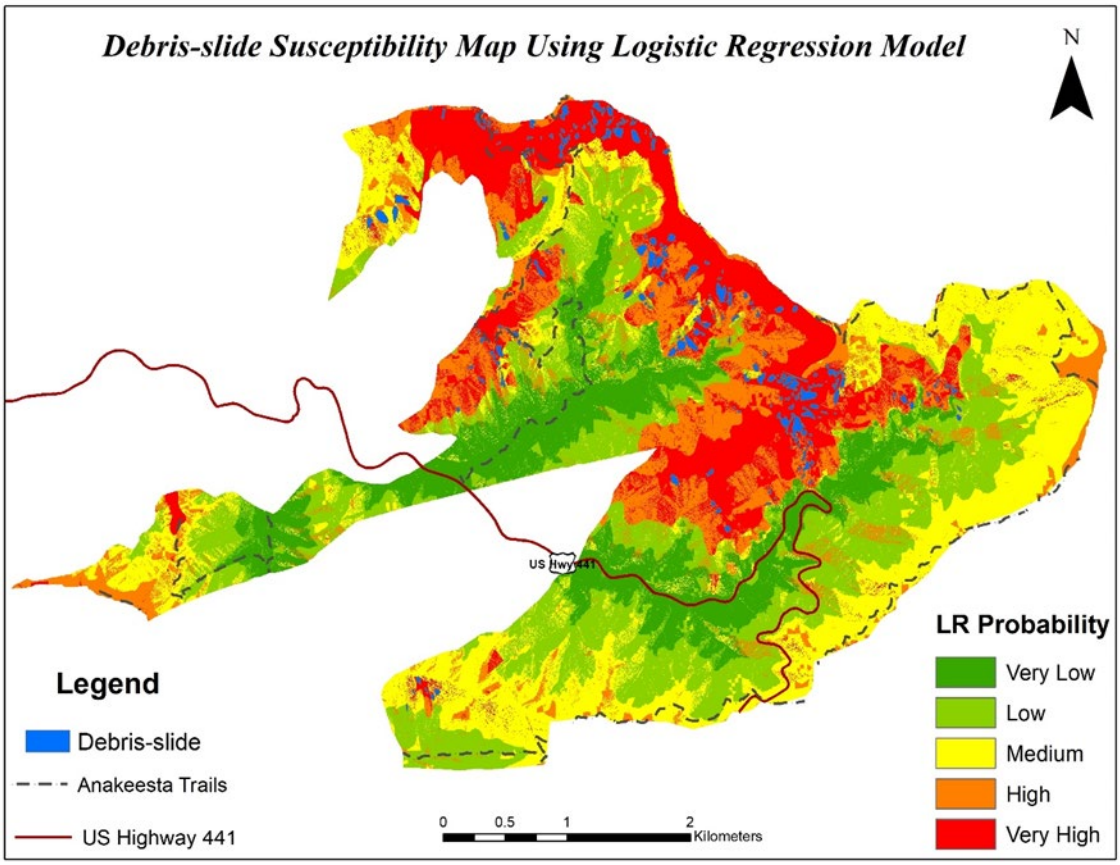

Figure 11: Debris-slide susceptibility model using LR.

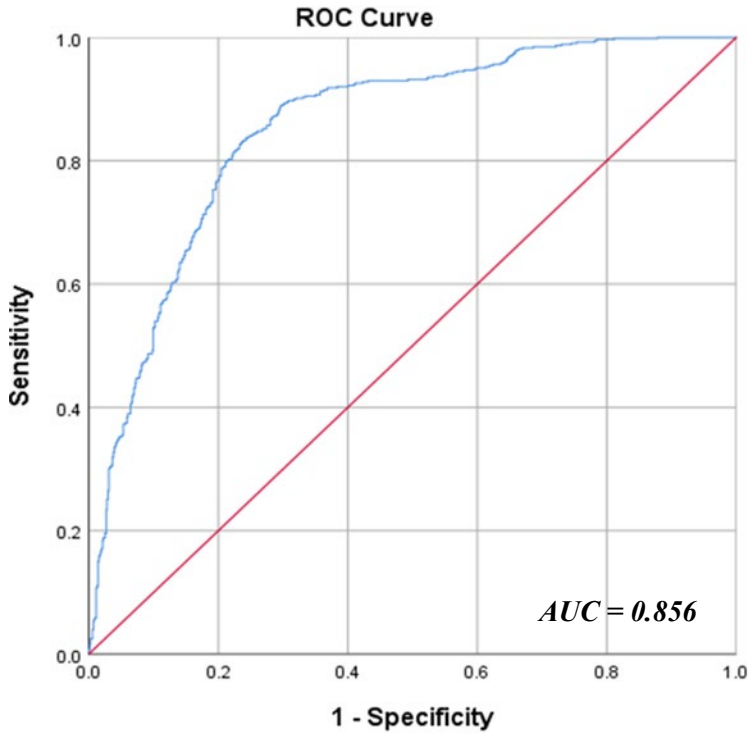

Figure 12: ROC curve of LR model.

5.4. Maxent

The Jackknife test for training data shows (Fig. 13) that the soil texture has the highest gain when used in isolation, which indicates that the soil texture has the most useful information among the geo-factors and is a good predictor of distribution of debris-slide in the area. On the other hand, the gain is lowest for curvature, which appears to have the least useful information and is not useful to predict the distribution of the debris-slide. The overall gain of the model decreases the most when rainfall is omitted, which suggests the rainfall possesses highest information among the geo-factors. The overall gain of the model increases the most if curvature is removed from the training model. In the case of test data, soil texture seems to have the most useful information as well as the highest information among the variables (Fig. 14). It is important to note, that the omission of kinematic index from the test data significantly reduces the

gain of the model. It contains the second most information among the geo-factors and has third highest useful information in the test data. However, it not possible from this model to determine the coefficient or the relative weight of importance of the geo-factors.

In the final debris-slide susceptibility map (Fig. 15) Soil has the highest percentage of contribution to the model with 35.9% followed by elevation and land cover having contribution of 22.7% and 18.4% respectively (Table 7). Whereas, curvature seems to contribute least to the debris-slide model with 0.1% of contribution. The model achieved AUC values of 0.853 for the test data, which indicates the model to be a good one for predicting debris-slide in the study area (Fig. 16).

The final debris-slide susceptibility aggregate map was prepared by adding all individual debris-slide susceptibility maps, which represents the outcome of all four susceptibility models (Fig. 17).

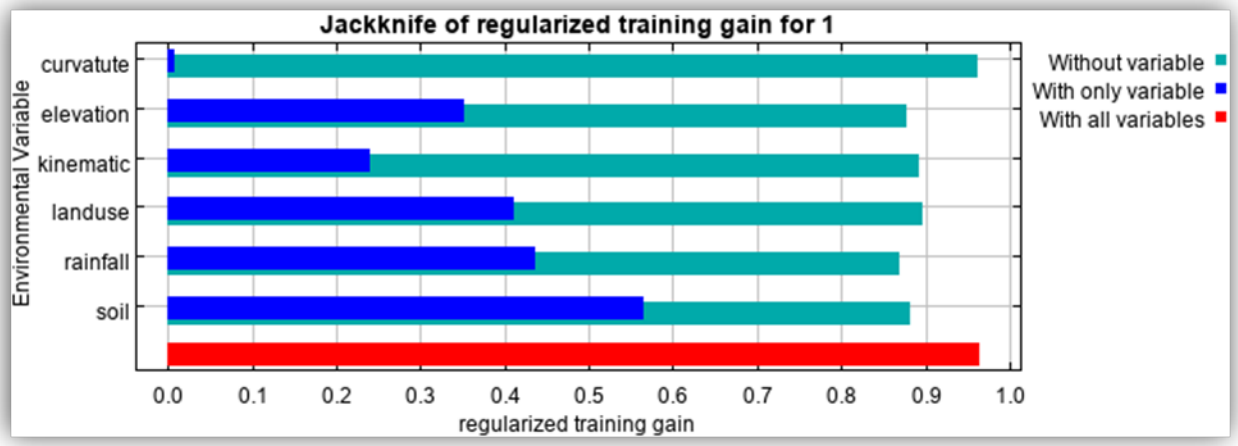

Figure 13: Result of Jackknife test of the variables for training data.

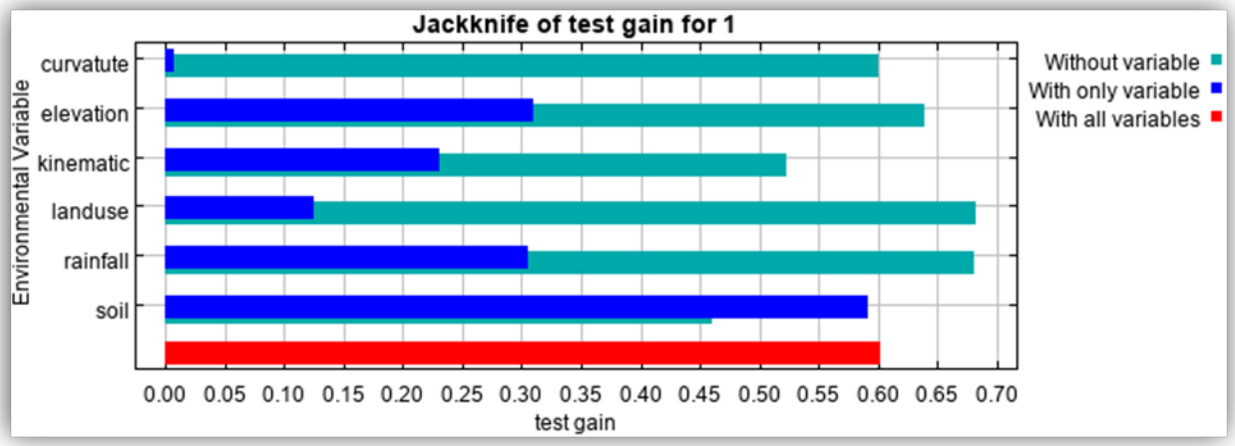

Figure 14: Result of Jackknife test of the variables for training data.

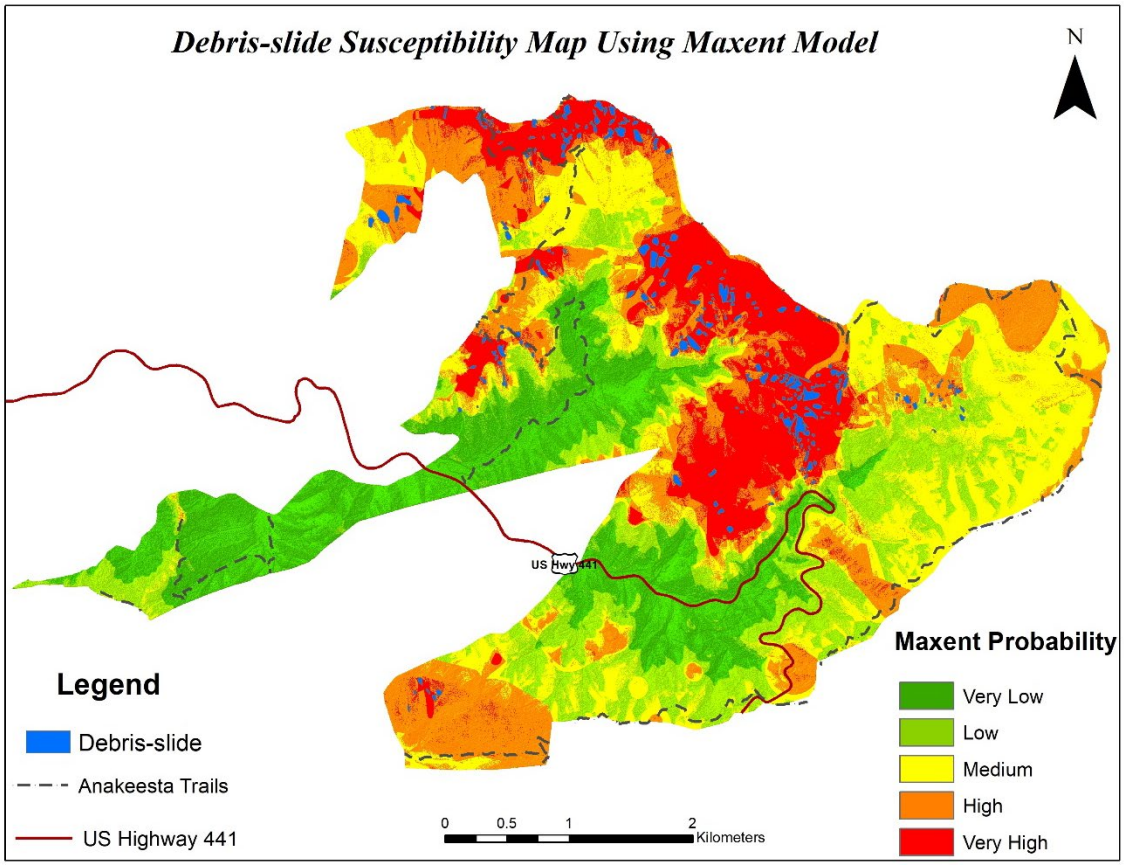

Figure 15: Debris-slide susceptibility model using Maxent

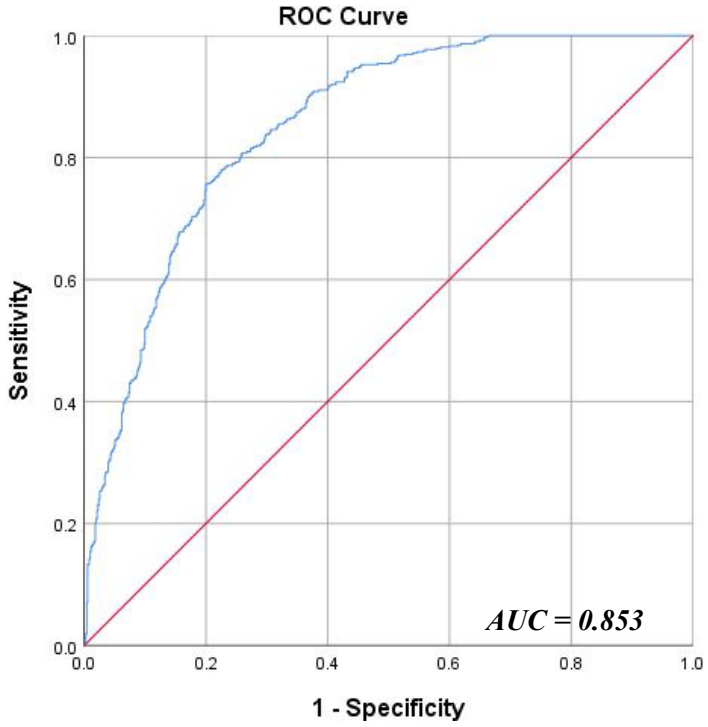

Figure 16: ROC curve of Maxent model.

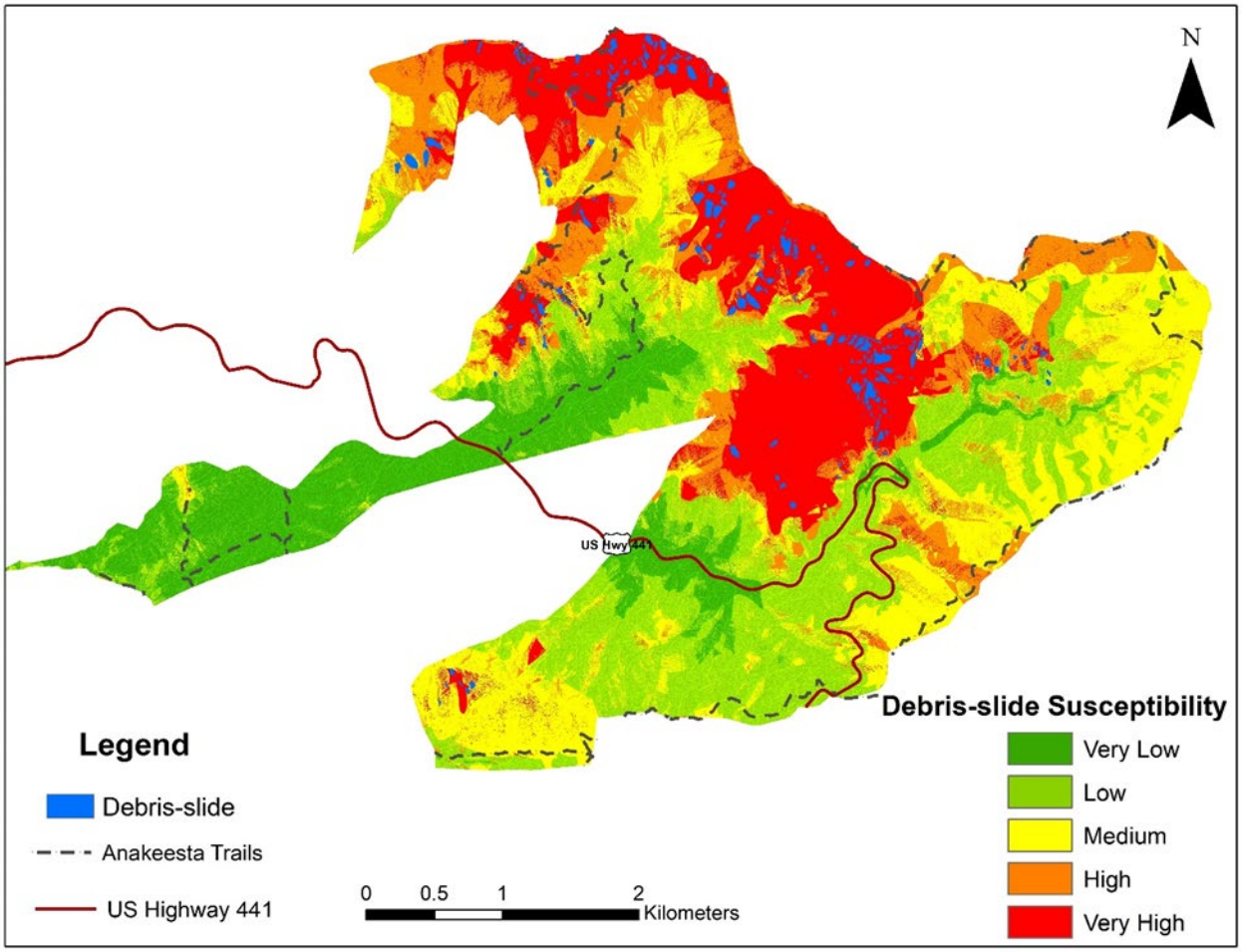

Figure 17: Debris-slide susceptibility aggregate map.

Table 4: Weights of different classes of geo-factors.

Geo-factors	*IVM Coefficient*	*FR Coefficient*
Curvature (Range)		
-6839 – -194	0.585	1.79
-194 – -51	0.77	1.08
-51 – 19	-0.12	0.88
19 – 162	-0.03	0.96
162 – 11380	0.44	1.56
Elevation (Range)		
1105 m – 1339m	-4.25	0.014
1339 m – 1478 m	-1.03	0.35
1478 m – 1602 m	0.14	1.15
1602 m – 1737 m	0.41	1.51
1737 m – 2010 m	0.78	2.19
Annual Rainfall		
73in	-7.18	0
75in	-7.18	0
77in	-7.18	0
79in	-0.99	0.36
81in	0.15	1.79
83in	0.0078	0.47
85in	1.18	3.28
Kinematic Index		
0 – 2.95	-0.45	0.63
2.95 – 11.36	0.89	2.44
11.36 – 20.68	0.36	1.43
20.68 – 27.27	1.14	3.13
27.27 – 57.95	1.28	3.62
Land cover		
Barren land	3.88	48.76
Developed Open Space	-2.47	0.08
Developed Low Intensity	-7.18	0
Developed Medium Intensity	-7.18	0
Mixed forest	-0.45	0.63
Deciduous Forest	-1.17	0.30
Shrub/Scrub	2.17	8.80
Evergreen Forest	-0.03	0.96
Soil Texture		
Channery Loam	-1.22	0.29
Very Channery Loam	1.04	2.84
Old slide area	2.14	8.57
Peat	-7.53	0.000
Channery Silt Loam	-7.18	0
Loam	-7.18	0

Table 5: Multi-collinearity test of geo-factors for logistic regression model.

Geo-factors	Tolerance	VIF
Curvature	.997	1.003
Elevation	.376	2.663
Rainfall	.426	2.349
Barren land	.910	1.099
Developed area	.910	1.099
Evergreen forest	.569	1.758
Mixed forest	.892	1.121
Shrub	.553	1.809
Channery loam	.762	1.313
Channery silt loam	.859	1.164
Loam	.809	1.236
Peat	.921	1.086
Old slide area	.903	1.107

Dependent variable: kinematic index

Table 6: Variables included in the equation for logistic regression model.

Geo-factors	Coefficient	Statistical Significance
Kinematic Index	0.037	.000
Elevation	0.005	.000
Rainfall	-0.227	.000
Deciduous	-1.908	.000
Developed Area	-2.284	.001
Evergreen Forest	-1.618	.000
Mixed Forest	-1.049	.003
Channery Loam	-1.753	.000
Channery Silt	-20.596	.998
Loam	-19.951	.997
Peat	-20.381	.998
Old slide area	0.856	.020
Intercept	12.160	.002

Table 7: Analysis of relative contributions of the geo-factors in Maxent model.

Variable	Percentage Contribution	Permutation Importance
Soil Texture	35.9	10.8
Elevation	22.7	55.1
Land Cover	18.4	4.8
Rainfall	12.9	22.6
Kinematic	10.1	6.4
Curvature	0.1	0.2

6. Discussion

Mass wasting is a complex phenomenon, highly controlled by different causing factors with varying degrees of influence. Debris-slides and debris-flows are very common in the Great Smoky Mountains National Park and different authors have addressed this problem by adopting different approaches (Bogucki, 1970; Ryan, 1989; Henderson, 1997; Nandi and Shakoor, 2017). Most of the researchers in this area agree that excessive rainfall is the main triggering factor for the gigantic slides in the area (Bogucki, 1970; Harp, 1983; Clark, 1987; Ryan, 1989). However, some minor earthquake activity was reported from this area but no major landslide or debris-slide has been reported because of earthquake induced slope failure. The Great Smoky Mountains National Park is comprised of complex geological structures, especially Anakeesta Formation, which possesses numerous failure planes due to the pattern of geological structures such as joints, bedding, fractures etc. Studies have been conducted to identify the orientation of these discontinuities and their possible role to initiate the debris-slide in the area (Ryan, 1989; Das et al., in preparation). It is evident from aerial photo, satellite imagery, and field surveys that most slope failures in the area form wedge structure due to the intersection of different discontinuities. Hence, the role of structural geology is evident in generating the debris-slide or debris-flow. Adverse orientation of topographic slope and direction with the orientation of geological discontinuity plays a very crucial role in terms of controlling the slope stability of an area (Ghosh et al., 2010). The study conducted by Das and Nandi (2018), suggests a strong control of geological discontinuities over generating debris-slide in the Anakeesta Formation.

Data-driven methods provide advantages over other models as the former can process large amount of data in a timely manner using the GIS software. Researchers in this study area

have previously applied multivariate statistics such as logistic regression (Henderson, 1997; Nandi and Shakoor, 2017) to model debris-slide susceptibility, however, did not address geological discontinuities in spatial scale. This study has also used the logistic regression statistics, however, Kinematic index map, a product of geological discontinuities with respect to topographic orientation that could cause slope failure were used to map the debris-slide susceptibility. Along with the logistic regression model, three other models namely Information Value Method (IVM), Frequency Ratio (FR) and Maximum Entropy model (Maxent) were applied to map the susceptible zone for future debris-slide in the area (Fig.11,7,9,13). Based on model validation using ROC curve, all models ranged from AUC of 0.85 to 0.86, with FR model showing a slightly better output.

All these methods have their own advantage and disadvantages. IVM and FR are some of the simple statistical models, which require meticulous calculation of the attributes of the geo-factors in order to generate the debris-slide susceptibility map. The entire bivariate analysis can be done only using ArcGIS software. Whereas, performing a more complicated multivariate analysis like logistic regression requires advanced statistical software like SPSS or SAS in addition to ArcGIS. In IVM and FR, analysis can be done either manually or the process can be automated using Python or model builder within the ArcGIS. However, the calculation in bivariate analyses are explicit and clearly depict how weights or coefficients are being assigned to the individual classes of the geo-factors. On the other hand, logistic regression is more complicated, where user has no control over the generation of coefficients and the process of generating data is implicit. Nevertheless, statistical packages provide numerous functions, which allow the user to develop a better understanding about the data and execute complicated analysis to enhance the capacity of the model. Standalone version of Maxent software is freely available, which is extensively

used in species distribution modelling. Maxent requires the input data to be processed in ASCII format and generates useful information in a very simple way, which can be comprehensible to the user easily.

The prediction accuracy of all four models is similar and each model came out with some unique information about the geo-factors. Therefore, it is very difficult to select the best model. However, it has been observed that the efficacy of Maxent model is slightly lower than the other models. Maxent model uses presence only data and does not calculate coefficients or weights for individual geo-factors, which makes it difficult to comprehend the interrelationship of geo-factors with debris-slide. However, the jackknife diagrams display some crucial information about the relative influence of geo-factors on the debris-slide and Table 7. shows the contribution of each geo-factor on the model. The model works well with continuous data but statistical information about the individual classes of categorical variable cannot be obtained from the model.

All models except LR established a positive correlation between rainfall and debris-slide. LR model suggests an increase in rainfall decreases the possibility of debris-slide, which is somewhat inconsistent with our observation and findings of previous studies. One good explanation of this ambiguity can be that LR model includes both presence and absence data while generating the model and pseudo absence points for debris-slide were generated randomly, many of which fell within the high precipitation zone and therefore, associated with non-debris-slide points. That may be responsible for creating a negative correlation between precipitation and debris-slides. The Additionally, number of debris-slide and non-debris-slide points within a class can highly influence the correlation between them. On the other hand, the rest of the models used presence only data to develop the susceptibility map and draw the correlation between individual classes of geo-factors

and debris-slide solely based on true presence of debris-slide. Kinematic index has been introduced in this study for the first time, which has reduced the number of variables in the analysis. The bivariate models showed a notable association of kinematic index with the debris-slide. Per the assumption, the higher the value of kinematic index the greater possibility of debris-slide. Both the IVM and FR models revealed that higher debris-slide density was associated with high kinematic index value (Table 4). The LR model, which showed a positive regression coefficient value for the kinematic index, has supported the same assumption i.e., increase in one unit of the kinematic index value is associated with a 0.037 unit increase in the odds (i.e., $e^{0.037}$) of debris-slide event (Table 6). In the Maxent model especially for the test data, the model lost a significant amount of gain if the kinematic index layer was removed. In soil texture, historic slide area indicated strong positive correlation with debris-slide. Old slide area was classified as a soil texture where old debris-slides have occurred, thus, some of the debris-slides mapped were exactly situated within this zone. Therefore, the density of debris-slide was very high within historic slide area, which yielded a high coefficient for IVM and FR model. While, in LR model most of the slide area was represented by the presence of debris-slide points that established a positive correlation between debris-slide and historic slide area. In summary, soil texture, kinematic index, rainfall were the most important geo-factors, whereas, curvature was the least important geo-factor in this study as debris-slides took place irrespective of surface curvature (both in concave and convex surfaces) and all four models supported the fact.

All four models used in the study have achieved a good prediction accuracy and preserved some exclusive information. Hence, it would be difficult to pick the best predictive model. However, usage of the models highly depend on the objective of the work and availability

of technical as well as financial resources of the organization. Following is the summary of advantages and disadvantages of the models.

Table 8: Comparison of the models

	Logistic Regression	Information Value Method	Frequency Ratio	Maxent
Technical skill	Strong skillset in Statistics and GIS.	Strong GIS skills. Entire work can be done only using GIS.	Strong GIS skill. Entire work can be done using GIS.	GIS and Maxent skills.
Financial aspect	Statistical softwares are costly. Hence suitable for established academic and professional industries.	Can cost money but free GIS softwares are available. Best for small relative small or new company/organization.	Can cost money but free GIS softwares are available. Best for relatively small or new company/organization.	Maxent is free.
Analysis	Involves complicated analysis that are time consuming.	Automation of the methodology can save significant amount of time.	Automation of the methodology can save significant amount of time	Data preparation is time-consuming process.
Interpretation skill	Required good statistical interpretation skill.	Explicit data set makes interpretation easier.	Explicit data set makes interpretation easier.	Results are easy to interpret.
Level of complication	High	Moderate	Moderate	Moderate to high

7. Conclusion

Preparation of a debris-slide susceptibility map is the primary step towards slope instability management and mitigation planning. Landslide susceptibility maps greatly assist in selection of areas for further infrastructure development and may act as a base map. Nowadays, GIS serves as a very powerful tool to process large data sets and complex equations for executing statistics based analysis for landslide or debris-slide hazard mapping. In this study, four debris-slide susceptibility models were developed in the Great Smoky Mountains National Park and the efficacy of the models was compared using the on the Area Under the Curve (AUC) method to evaluate prediction accuracy of each model. High and similar AUC values were achieved for all four models. Therefore, it is hard to determine the best model out of the four. However, Frequency Ratio had a slight edge over others with 86.3% prediction accuracy, which was followed by Logistic Regression, Information Value Method, and Maxent with prediction accuracies of 85.6%, 85.5%, and 85.3% respectively.

Apart from finding out the best-suited model for predicting debris-slide, it is also important to evaluate the role of the geo-factors for controlling the slides. Different model showed varying degree of influence of different geo-factors. However, elevation and kinematic index seemed to have a positive influence in all four models, hence, could be regarded as the most important factors for initiating debris-slide. Despite its negative correlation in Logistic Regression model, which was mainly due to random distribution of pseudo non-debris-slide data, rainfall can surely be considered as one of the positive influencers for debris-slide in the study area, which were confirmed by rest of the models. Distribution of non-debris-slide data can highly influence the role of geo-factors in predicting debris-slides using Logistic Regression model. This suggests high level of sensitivity of the model

associated with spatial distribution of data and should be explored in a future study. Most of the debris-slide events reordered in the area were triggered by torrential rainfall and spatial distribution of slide patches suggest a strong positive correlation between quantity of annual rainfall and number of debris-slides. Soil texture and land cover have moderate influence in terms of generating debris-slide. On the other, all four models affirmed curvature to be an insignificant geo-factor for initiating debris-slides.

Frequency Ratio and Information Value methods are simple statistical models, where large data sets can be processed in GIS environment and the process of data calculation is explicit, which helps the user to fully understand the process of generating the debris-slide susceptibility map. On the other hand, multivariate statistics such as Logistic Regression and Maxent involve conversion of data into different formats before processing them in GIS. Moreover, processing data in Logistic Regression and Maxent is a time consuming process and requires additional knowledge in statistical packages like SPSS, SAP, and/or in Maxent. Considering the time and complexity involved in Maxent and Logistic Regression models, the bivariate models seem to be less complicated, yet effective. Selection of causative factors or geo-factors can significantly affect the accuracy of the model, as there is no specific guideline for selecting geo-factors. However, it is important to note that landslide or debris-slide susceptibility mapping is a scale dependent process and for any site-specific assessment, these models might not be very useful but could serve as reference. Nevertheless, the maps certainly indicate some specific regions, which are very prone to debris-slides and such areas should be taken into consideration for detailed survey, which indeed will save time and effort for debris-slide hazard mitigation planning.

References

Aleotti, P. and Chowdhury, R.,1999, Landslide Hazard Assessment: Summary Review and New Perspectives. Bulletins of Engineering Geology and the Environment, 58, 21-44. http://dx.doi.org/10.1007/s100640050066

Allmendinger, R. W., Cardozo, N. C., and Fisher, D., 2012, Structural Geology Algorithms: Vectors & Tensors: Cambridge, England, Cambridge University Press, 289 pp.

Ayalew, L. and Yamagishi, H., 2005, The Application of GIS-Based Logistic Regression for Landslide Susceptibility Mapping in the Kakuda-Yahiko Mountains, Central Japan. Geomorphology, 65, 15-31. http://dx.doi.org/10.1016/j.geomorph.2004.06.010

Band, L.E. , and I .D. Moore., 1995, " Scale : and Geographical Information Systems ." Processes 9: 401-422 .

Bieniawski, Z.T. 1989, Engineering rock mass classifications. New York: Wiley.

Bogucki , Donald J., 1970, Debris slides and Related Damaae Associated with the September 1, 1951 Cloudburst in the Mt . Leconte-Sugarland Mountain Area, Great Smoky Mountains National Park. Doctoral Dissertation, University of Tennessee, Knoxville .

Bogucki, Donald J. 1972, " Intense Rainfall in the Great Smoky Mountains National Park . " Journal of the Tennessee Academy of Science 47 (3) : 93 -97 .

Carrara, A., Cardinali M., Guzzetti F., Reichenbach P.,1995, Gis Technology in Mapping Landslide Hazard. In: Carrara A., Guzzetti F. (eds) Geographical Information Systems in Assessing Natural Hazards. Advances in Natural and Technological Hazards Research, vol 5. Springer, Dordrecht.

Clark, G.M., 1987, Debris slide and debris flow historical events in the Appalachians south of the glacial border: Geological Society of America, Reviews in Engineering Geology, Volume VII, p. 125-137.

Clerici, A. and Dall'Olio ,N.,1995, "The realization of a Charter of the potential stability of the slopes through techniques of Multivariate Statistical Analysis and a Geographical Information System", *Technical and Environmental Geology* , no. 4, pp. 49-57.

Delcourt, H.R. & Delcourt, P.A., 1985, Quaternary palynology and vegetation history of the southeast United States. Pollen records of late-Quaternary North American sediments. 1-37.

Elith J. *et al.* 2011, A statistical explanation of MaxEnt for ecologists. *Divers. Distrib.*17: 43–57.

Felicísimo, Á.M., Cuartero, A., Remondo, J. et al., 2013, 10: 175. https://doi.org/10.1007/s10346-012-0320-1

Ghosh S, Günther A, Carranza EJM, van Westen CJ, Jetten VG.,2010, Rock slope instability assessment using spatially distributed structural orientation data in Darjeeling Himalaya (India). Earth Surf Proc Land 35(15):1773–1792

Ghosh, S., Das, R., Goswami, B., 2013, Developing GIS-based techniques for application of knowledge and data-driven methods of landslide susceptibility mapping. Indian Journal of Geosciences 67 (3-4), 249-272.

Goodman, R.E., and Bray, J.W., 1976, Toppling of rock slopes. In Rock Engineering: American Society of Civil Engineers, Geotechnical Engineering Division Conference, Boulder, Colorado, Vol. II, pp. 201–234.

Gupta, R. P . , and Joshi, B. C., 1990, " Landslide Hazard Zoning Using the GIS Approach - A Case Study from the Ramganga Catchment, Himalayas ." Engineering Geology 2 8 : 119-131.

Guzzetti, F., Carrara, A., Cardinali, M., Reichenbach, P., 1999, Landslide hazard evaluation: a review of current techniques and their application in a multi-scale study, Central Italy. Geomorphology 31, 181–216.

Hadley, J. B., and Goldsmith, R., 1963, Geology of the eastern Great Smoky Mountains, North Carolina and Tennessee: U. S. Geol. Survey 9 Prof. Paper 349-B.

Henderson, J. P., 1997, Debris slide Susceptibility Analysis in the Mt. LeConte-Newfound Gap Area of the Great Smoky Mountains, Tennessee and North Carolina. Unpublished Masters Thesis, The University of Tennessee, Knoxville.

Hoek. E., Bray J.W., 1981, Rock slope engineering. Institution of Mining and Metallurgy, London.

Jones, D.K.C., 1992, " Landslide Hazard Assessment in the Context of Development ." Pages 117-141 in McCall, G. J. H . , D. J. C. Manmade Laming, and S. C. Scott, eds . Geohazards : Natural and . Chapman and Hall , New York .

King, P.B., Neuman, R.B., Hadley, J.B., 1968, Geology of the Great Smoky Mountains National Park, Tennessee and North Carolina.. U. S. Geol. Surv. Prof. Pap. 587.

King, Philip B., and Stupka, A., 1950, "The Great Smoky Mountains - Their Geology and Natural History . " The Scientific Monthly 71 (July) : 3 1-43 .

Lee, S. and Sambath, T., 2006, Landslide Susceptibility Mapping in the Damrei Romel Area, Cambodia Using Frequency Ratio and Logistic Regression Models. Environmental Geology, 50,847-855. https://doi.org/10.1007/s00254-006-0256-7

Lee, S. & Pradhan, B., 2007, Landslide hazard mapping at Selangor, Malaysia using frequency ratio and logistic regression models. Landslides. 4. 33-41. Doi: 10.1007/s10346-006-0047-y.

Leroi, E., 1996, Landslide hazard Risk maps at different scales: objectives, tools and developments. In: Proc VII Int Symp Landslides, Trondheim, June 1996, 1:35-52

Moore, H.L.A., 1988, A Roadside Guide to the Geology of the Great Smoky Mountains National Park. University of Tennessee Press, Knoxville, TN. 178 pp.

Nandi, A., Shakoor, A., 2010, A GIS-based landslide susceptibility evaluation using bivariate and multivariate statistical analyses. Engineering Geology 110, 11–20, doi:10.1016/j.enggeo.2009.10.001.

Pariseau, W.G. and Voight, B., 1979, " Rockslides and Avalanches : Basic Principles , Perspectives in the Realm of Civil and Mining Operations ." Pages 1-92 in Barry Voight, ed . Rockslides and Avalanches. Elsevier Scientific Publishing Company, Amsterdam.

Phillips, S., Dudík, M., & Schapire, R., 2010, Maxent software. Version 3.3.3k. Available at http:// biodiversityinformatics.amnh.org/ open_source/maxent/.

Ryan, P. T., 1989, Debris slides and Flows on Anakeesta Ridge Within the Great Smoky Mountains National Park Tennessee, U.S.A. Unpublished Master's Thesis, The University of Tennessee, Knoxville

Lee, S.,2005, Application of logistic regression model and its validation for landslide susceptibility mapping using GIS and remote sensing data, International Journal of Remote Sensing, 26:7, 1477-1491, DOI: 10.1080/01431160412331331012

Saha, Ashis & P. Gupta, Ravi & Sarkar, Irene & K. Arora, Manoj & Csaplovics, Elmar., 2005, An approach for GIS-based statistical landslide susceptibility zonation—with a case study in the Himalayas. Landslides. 2. 61-69. Doi:10.1007/s10346-004-0039-8.

Sarkar, Shraban & Roy, Archana & Martha, Tapas.,2013, Landslide Susceptibility Assessment using Information Value Method in parts of the Darjeeling Himalayas. Journal of the Geological Society of India. 82. 351-362. DOI: 10.1007/s12594-013-0162-z.

Scott, R.C., 1972, The geomorphic significance of debris avalanching in the Appalachian Blue Ridge Mountains [Ph.D. thesis]: Athens, University of Georgia, 185 p.

Soeters R, Van Westen C.J., 1996, Slopeinstability recognition, analysis andzonation. In: Turner AK, Schuster RL(eds) Landslides, investigation and mit-igation. Transportation ResearchBoard, National Research Council,Special Report 247, National AcademyPress, Washington, USA, pp 129–177

Southworth, S., A. Schultz and Denenny, D., 2005, Geologic Map of the Great Smoky Mountains National Park Region, Tennessee and North Carolina. U.S. Geological Survey Open File Report 2005-1225, scale 1:100,000.

Tennessee Valley Authority . 1937, Precioitation in the Tennessee River Basin Annual 1937 . Tennessee Valley Authority, Knoxville, Tennessee .

Van Westen CJ, Rengers N, Soeters R., 2003, Use of geomorphological infor-mation in indirect landslide susceptibil-ity assessment. Nat Hazards 30(3):399–419

Van Westen, CJ., 1993, Application of Geographical Information System to landslide hazard zonation. ITC Publication no. 15, lTC, Enschede, The Netherlands, 245 pp.

Varnes, D.J., 1978, Slope movements types and processes. *In*: Landslides: Analysis and Control, R.L. Schuster and R.L. Krizek (eds.), Special Report 176. Transportation Research Board, National Academy of Sciences, Washington, D.C., 11-33 p.

Wooten, Richard M.; Witt, Anne C.; Miniat, Chelcy F.; Hales, Tristram C.; Aldred, Jennifer L., 2016, Frequency and magnitude of selected historical landslide events in the southern Appalachian Highlands of North Carolina and Virginia: relationships to rainfall, geological and ecohydrological controls, and effects. In: Greenberg, Cathryn H.; Collins, Beverly S. editors. Natural Disturbances and Historic Range of Variation. Springer International Publishing, p. 203-262, doi:10.1007/978-3-319-21527-3_9.

Yilmaz, I., 2010, Comparison of landslide susceptibility mapping methodologies for Koyulhisar, Turkey: conditional probability, logistic regression, artificial neural networks, and support vector machine. Environ Earth Sci 61:821–836

Yin K.L., and Yan T.Z., 1988, Statistical prediction model for slope instability of metamorphosed rocks. In: Proceedings of 5th Int Symp on Landslides, Lausanne, Switzerland 2:1269-1272.

CHAPTER 5

CONCLUSION

Study 1: The study successfully depicted an effective methodology for performing GIS based kinematic analysis. A kinematical susceptibility map was developed using the geological discontinuities and topographical orientation, which predicted nearly about 67% of the debris-slide locations. A higher prediction rate couldn't be achieved because debris-slide is a complex phenomenon and controlled by the influence of other factors such as rainfall, slope curvature, drainage, lands use etc. This kinematical susceptibility layer was named as "Kinematic index', which is function of topographic slope and aspect, lithology and geological discontinuities. This layer can be used as an independent geo-factor for debris-slide susceptibility mapping.

Study 2: A knowledge-driven debris-slide susceptibility map was developed using Weighted Overlay method in ArcGIS. Geo-factors used in the study were the important for predicting debris-slides in the study area. For a qualitative model validation of the model becomes difficult, however, 86% of the debris-slides were predicted by the very high and high susceptible zones. This indicates that a GIS based knowledge-driven method can be effective for debris-slide susceptibility model, if correct set of geo-factors are selected and assigned with appropriate weights. This kind of model is beneficial for rapid analysis for a region in a short amount of time.

Study 3: Four different data-driven models were generated using IVM, FR, LR and Maxent. Prediction rate of the models were very close to each other, however, FR performed slightly better than the other models having area under ROC curve value of 0.863. Therefore, considering the performance and other pros and cons of these models, we would say that bivariate models (IVM, FR) are less complicated than multivariate model (LR, Maxent) and

processing the data are much easier, less tedious, GIS friendly and cost effective in bi-variate models than multivariate models. The outcome of three different studies has been summarized in the Table 1.

Table 1: Comparison of three studies.

	Study 1	Study 2	Study 3
Purpose	Generate a debris-slide initiation susceptibility map based on geometrical relationship between orientations of topography with geological discontinuities.	Generate a knowledge guided debris-slide initiation susceptibility map based on our observation and understanding.	Generate four data-driven debris-slide initiation susceptibility map using different statistics and create a debris-slide susceptibility aggregate map using all four models.
Variables used	Geological discontinuities, lithology, topographical slope and aspect.	Elevation, annual rainfall, land cover, soil texture, curvature and kinematic index (from study 1).	Elevation, annual rainfall, land cover, soil texture, curvature and kinematic index (from study 1).
Methodology	Rock Kinematic analysis.	Weighted Overlay analysis.	Information Value Method (IVM), Frequency Ratio (FR), Logistic Regression (LR), Maximum Entropy model (Maxent)
Primary information obtained	Susceptibility zones due to kinematic property of rocks.	Susceptibility zones due to influence of different variables used in the study.	Susceptibility zones due to influence of different variables used in the study.
Implication	The final map can be used as an independent variable for debris-slide susceptibility modelling and also for obtaining rock kinematic information for geo-technical survey.	Useful for reconnaissance survey and selecting sites for detailed geo-technical investigation.	Four different debris-slide susceptibility models were combined to a single map. This highly precise map can be used for reducing areas for detailed geo-technical survey.

Future study may include a spatio-temporal analysis of debris-slide hazard, which we couldn't do this time due to absence of time-stamped debris-slide inventory. Dates of these debris-slides will help to get the information about rainfall amount and duration during these

events, which will be required to calculate the rainfall threshold value for initiating the debris-slides. Therefore, a time-stamped debris-slide inventory should be created in order to perform a debris-slide hazard analysis in the study area.

REFERENCES

1. Aleotti P, Chowdhury R. Landslide Hazard Assessment: Summary Review and New Perspectives. Bulletins of Engineering Geology and the Environment. 1999; 58:21-44. http://dx.doi.org/10.1007/s100640050066
2. Allmendinger RW, Cardozo NC, Fisher D. Structural Geology Algorithms: Vectors & Tensors: Cambridge, England. Cambridge University Press. 2012; 289.
3. Ayalew L, Yamagishi H. The Application of GIS-Based Logistic Regression for Landslide Susceptibility Mapping in the Kakuda-Yahiko Mountains, Central Japan. Geomorphology. 2005; 65:15-31. http://dx.doi.org/10.1016/j.geomorph.2004.06.010
4. Aydan Ö, Akagi T, Kawamoto T. The squeezing potential of rocks around tunnels; theory and prediction. Rock Mechanics and Rock Engineering. 1993; 26(2):137–163. DOI: 10.1007/BF01023620
5. Aydin A, Basu A. The use of Brazilian test as a quantitative measure of rock weathering. Rock Mechanics and Rock Engineering. 2006; 39(1):77–85. doi : 10.1007/s00603-005-0069-0.
6. Band LE, ID Moore. Scale : and Geographical Information Systems . Processes 1995; 9:401-422.
7. Barton NR, Choubey V. The shear strength of rock joints in theory and practice. Rock Mech. 1977; 10(1-2):1-54.
8. Bieniawski ZT. Engineering rock mass classifications. New York: Wiley.1989.
9. Bogucki DJ. Debris slides and Related Damaae Associated with the September 1, 1951 Cloudburst in the Mt . Leconte-Sugarland Mountain Area, Great Smoky Mountains National Park. Doctoral Dissertation, University of Tennessee, Knoxville. 1970.

10. Bogucki DJ. Debris slides in the Mt. Le Conte Area, Great Smoky Mountains National Park, U.S.A. Geografiska Annaler: Series A, Physical Geography. 1976; 58(3):179-191. doi:10.1080/04353676.1976.11879937.
11. Bogucki DJ. Intense Rainfall in the Great Smoky Mountains National Park. Journal of the Tennessee Academy of Science. 1972; 47(3):93 -97 .
12. Brabb EE. Innovative approaches to landslide hazard mapping. 4th International Symposium on Landslides, Toronto. 1984; 1:307-324.
13. Carrara A, Cardinali M, Guzzetti F, Reichenbach P. Gis Technology in Mapping Landslide Hazard. In: Carrara A., Guzzetti F. (eds) Geographical Information Systems in Assessing Natural Hazards. Advances in Natural and Technological Hazards Research. Springer, Dordrecht. 1995; 5.
14. Clark GM. Debris slide and debris flow historical events in the Appalachians south of the glacial border. Geological Society of America, Reviews in Engineering Geology. 1987; 7:125-137.
15. Clerici A, Dall'Olio N. The realization of a Charter of the potential stability of the slopes through techniques of Multivariate Statistical Analysis and a Geographical Information System. Technical and Environmental Geology. 1995; 4:49-57.
16. Cruden DM. Limits to common toppling. Canadian Geotechnical Journal. 1989; 26:737–742.
17. Delcourt HR, Delcourt PA. Quaternary palynology and vegetation history of the southeast United States. Pollen records of late-Quaternary North American sediments. 1985; 1-37.
18. Elith J. et al. A statistical explanation of MaxEnt for ecologists. Diversity and Distributions. 2011; 17:43–57.
19. Eschner AR, Patric JH. Debris Avalanches in Eastern Upland Forests. Journal of Forestry.1982; 80:343-347.

20. Fawcett T. An introduction to ROC analysis. Pattern Recognition Letters. 2006; 27:861-874.
21. Felicísimo ÁM, Cuartero A, Remondo J, et al. Mapping landslide susceptibility with logistic regression, multiple adaptive regression splines, classification and regression trees, and maximum entropy methods: a comparative study.2013;Landslides,10,175–189. https://doi.org/10.1007/s10346-012-0320-12013.
22. Ghosh S, Das R, Goswami B. Developing GIS-based techniques for application of knowledge and data-driven methods of landslide susceptibility mapping. Indian Journal of Geosciences. 2013, 67(3-4):249-272.
23. Ghosh S, Günther A, Carranza EJ, Westen CJ, Jetten VG. Rock slope instability assessment using spatially distributed structural orientation data in Darjeeling Himalaya (India). Earth Surface Processes and Landforms. 2010; 35(15):1773– 1792, doi:10.1002/esp.2017.
24. Gokceoglu C, Sonmez H, Ercanoglu M. Discontinuity controlled probabilistic slope failure risk maps of the Altindag (settlement) region in Turkey. Eng Geol. 2000; 55(4):277–296.
25. Goodman RE. Introduction to RockMechanics,-2nd Edn, John Wiley and Sons, Inc., New York. 1989.
26. Goodman RE, Bray JW. Toppling of rock slopes. In Rock Engineering: American Society of Civil Engineers, Geotechnical Engineering Division Conference, Boulder, Colorado. 1976; 2:201–234.
27. Günther A. SLOPEMAP: programs for automated mapping of geometrical and kinematical properties of hard rock hill slopes. Computers & Geosciences. 2003; 29(7):865–875.
28. Gupta RP, Joshi BC. Landslide Hazard Zoning Using the GIS Approach - A Case Study from the Ramganga Catchment, Himalayas. Engineering Geology. 1990; 28:119-131.

29. Guzzetti F, Carrara A, Cardinali M, Reichenbach P. Landslide hazard evaluation: a review of current techniques and their application in a multi-scale study, Central Italy. Geomorphology. 1999; 31:181–216.
30. Hadley JB, Goldsmith R. Geology of the eastern Great Smoky Mountains, North Carolina and Tennessee. U. S. Geol. Survey 9 Prof. 1963; Paper 349-B.
31. Hansen A. Landslide hazard analysis. In: Brunsden, D. & Prior, D.B. (Eds.), Slope Instability, John Wiley and Sons, New York. , 1984; 523-602.
32. Henderson JP. Debris slide Susceptibility Analysis in the Mt. LeConte-Newfound Gap Area of the Great Smoky Mountains, Tennessee and North Carolina. Unpublished Masters Thesis, The University of Tennessee, Knoxville. 1997.
33. Hoek E, Bray JW. Rock slope engineering. Institution of Mining and Metallurgy, London. 1981.
34. Hupp CR. Seedling establishment on a landslide site. Castanea. 1983;48:89-98.35.
35. Jones DKC. Landslide Hazard Assessment in the Context of Development. McCall, G. J. H . , D. J. C. Manmade Laming, and S. C. Scott, eds . Geohazards : Natural and . Chapman and Hall , New York. 1992; 117-141.
36. King PB, Neuman RB, Hadley JB. Geology of the Great Smoky Mountains National Park, Tennessee and North Carolina. U. S. Geol. Surv. Prof. 1968; 587.
37. King Philip B, Stupka A. The Great Smoky Mountains - Their Geology and Natural History . The Scientific Monthly.1950; 71(July):31-43 .
38. King PB, Jarvis BH, Robert B, Neuman WH. Stratigraphy of the Ocoee Series , Great Smoky Mountains , Tennessee and North Carolina. Geological Society of America Bulletin, 1958; 69:947-966 .

39. Lee S, Pradhan B. Landslide hazard mapping at Selangor, Malaysia using frequency ratio and logistic regression models. Landslides. 2007; 4:33-41. Doi: 10.1007/s10346-006-0047-y.
40. Lee S, Sambath T. Landslide Susceptibility Mapping in the Damrei Romel Area, Cambodia Using Frequency Ratio and Logistic Regression Models. Environmental Geology. 2006; 50:847-855. https://doi.org/10.1007/s00254-006-0256-7
41. Lee, S. Application of logistic regression model and its validation for landslide susceptibility mapping using GIS and remote sensing data. International Journal of Remote Sensing. 2005; 26(7):1477-1491. DOI: 10.1080/01431160412331331012
42. Lee S, Pradhan B. Landslide hazard mapping at Selangor, Malaysia using frequency ratio and logistic regression models. Landslides.2007; 4:33–41. doi:10.1007/s10346-006-0047-y.
43. Leroi E. Landslide hazard Risk maps at different scales: objectives, tools and developments. In: Proc VII Int Symp Landslides, Trondheim. June 1996; 1:35-52.
44. Mandal A, Nandi A. Hydrological Modeling to Estimate Runoff and Infiltration in Southeastern Appalachian Debris Flow Complex, 3rd North American Symposium on Landslides, Roanoke, Virginia, USA. 2017.
45. Markland, JT. A useful technique for estimating the stability of rock slopes when the rigid wedge sliding type of failure is expected. Imperial College Rock Mechanics, Reserach Report, no.19, Imperial College Press, London. , 1972.
46. Matheson GD. Rock Stability Assessment in Preliminary Site Investigations – Graphical Methods, Report 1039. Transport and Road Research Laboratory: Crownthorne. 1983.
47. Moore HLA. A Roadside Guide to the Geology of the Great Smoky Mountains National Park. University of Tennessee Press, Knoxville, TN. 1988; 178 pp.

48. Nandi A, Shakoor A. A GIS-based landslide susceptibility evaluation using bivariate and multivariate statistical analyses. Engineering Geology. 2010; 110:11–20. doi:10.1016/j.enggeo.2009.10.001.

49. Nandi A, Shakoor A. Predicting Debris Flow Initiation Zone Using Statistical And Rock Kinematic Analyses, A Case Study From West Prong Little Pigeon River, TN, 3rd North American Symposium on Landslides Proceedings. 2017; 912-922.

50. Palmstrom A. The volumetric joint count - A useful and simple measure of the degree of rock mass jointing. IAEG Congress, New Delhi. 1982;221–228.

51. Pariseau WG, Voight B. Rockslides and Avalanches : Basic Principles , Perspectives in the Realm of Civil and Mining Operations. Barry Voight, ed . Rockslides and Avalanches. Elsevier Scientific Publishing Company, Amsterdam. 1979; 1-92.

52. Park HJ, Lee JH, Kim KM, Um, JG. Assessment of rock slope stability using GIS-based probabilistic kinematic analysis. Eng Geol. 2016; 203:56–69.

53. Philip B. King, Robert B. Neuman, Jarvis B. Hadley, Geology of the Great Smoky Mountains National Park, Tennessee and North Carolina, Geological Survey Professional Paper 587 (Washington: Government Printing Office, 1968).

54. Phillips S, Dudík M, Schapire R. 2010. Maxent software. Version 3.3.3k. Available at http:// biodiversityinformatics.amnh.org/ open_source/maxent/.

55. Pradhan, B. Use of GIS-based fuzzy logic relations and its cross application to produce landslide susceptibility maps in three test areas in Malaysia. Environmental Earth Sciences. 2011; 63(2):329–349.

56. Rapp A, Stromquist L. Slope Erosion Due to Extreme Rainfall in the Scandinavian Mountains, Geografiska Annaler: Series A, Physical Geography. 1976; 58(3):193-200. doi:10.1080/04353676.1976.11879938.

57. Roy S, Mandal N. Modes of hill-slope failure under overburden loads: insights from physical and numerical models. Tectonophysics. 2009; 473:324–340.

58. Ryan PT. Debris slides and Flows on Anakeesta Ridge Within the Great Smoky Mountains National Park Tennessee, U.S.A. Unpublished Master's Thesis, The University of Tennessee, Knoxville. 1989.

59. Saha AK, Gupta RP, Sarkar I. et al. An approach for GIS-based statistical landslide susceptibility zonation—with a case study in the Himalayas. Landslides. 2005; 2. 61-69. Doi:10.1007/s10346-004-0039-8.

60. Sarkar S, Roy A, Martha T. Landslide Susceptibility Assessment using Information Value Method in parts of the Darjeeling Himalayas. Journal of the Geological Society of India. 2013; 82:351-362. DOI: 10.1007/s12594-013-0162-z.

61. Scott RC. The geomorphic significance of debris avalanching in the Appalachian Blue Ridge Mountains [Ph.D. thesis]: Athens, University of Georgia. 1972; 185p.

62. Serafim JL, Pereira JP. Considerations of the geomechanical classification of Bieniawski. Proceeding on International Symposium on Engineering Geology in Underground Construction. A.A. Balkema, Boston. 1983;33-43.

63. Simonett DS. The role of landslides in slope development in the high rainfall tropics: Final report, Office of Naval Research, Geography Branch. 1970; 583(11), NR 389–133, 24 p.

64. Soeters R, Van Westen CJ. Slopeinstability recognition, analysis andzonation. In: Turner AK, Schuster RL(eds) Landslides, investigation and mit-igation. Transportation ResearchBoard, National Research Council,Special Report 247, National Academy Press, Washington, USA. 1996; 129–177.

65. Southworth S, A Schultz, Denenny D. Geologic Map of the Great Smoky Mountains National Park Region, Tennessee and North Carolina. U.S. Geological Survey Open File Report. 2005; 1225.

66. Southworth S, Schultz A, Aleinikoff JN, Merschat AJ. Geologic map of the Great Smoky Mountains National Park region, Tennessee and North Carolina: U.S. Geological Survey Scientific Investigations Map 2997, one sheet, scale 1:100,000, and 54-p. pamphlet. (Supersedes USGS Open-File Reports 03–381, 2004–1410, and 2005–1225.) 2012.

67. Tennessee Valley Authority . Precioitation in the Tennessee River Basin Annual 1937 . Tennessee Valley Authority, Knoxville, Tennessee . 1937.

68. Van Westen CJ, Rengers N, Soeters R. Use of geomorphological infor-mation in indirect landslide susceptibil-ity assessment. Nat Hazards. 2003; 30(3):399–419.

69. Van Westen, CJ. Application of Geographical Information System to landslide hazard zonation. ITC Publication no. 15, lTC, Enschede, The Netherlands. 1993; 245.

70. Varnes DJ. Slope movements types and processes. In: Landslides: Analysis and Control, R.L. Schuster and R.L. Krizek (eds.), Special Report 176. Transportation Research Board, National Academy of Sciences, Washington, D.C. , 1978; 11-33.

71. Varnes DJ. IAEG Commission on Landslides and other Mass-Movements, Landslide Hazard Zonation: a review of principles and practice. UNESCO Press, Darantiere, Paris. 1984; 61.

72. West TR, Shakkor A. GEOLOGY APPLIED To ENGINEERING. Long Grove, Illinois: Waveland Press, Inc. 2018.

73. Wieczorek GF, Morgan BA, Campbell, R.H. Debris-flow hazards in the Blue Ridge of central Virginia: Environmental and Engineering Geoscience. 2000; 6(1):3- 23.

74. Wooten RM, Witt AC, Miniat CF, Hales TC, Aldred JL. Frequency and Magnitude of Selected Historical Landslide Events in the Southern Appalachian Highlands of North

Carolina and Virginia: Relationships to Rainfall, Geological and Ecohydrological Controls, and Effects. Managing Forest Ecosystems. 2016; Vol 32. Springer, Cham.

75. Yilmaz I. Comparison of landslide susceptibility mapping methodologies for Koyulhisar, Turkey: conditional probability, logistic regression, artificial neural networks, and support vector machine. Environ Earth Sci 2010; 61:821–836.
76. Yin KL,Yan TZ. Statistical prediction model for slope instability of metamorphosed rocks. In: Proceedings of 5th Int Symp on Landslides, Lausanne, Switzerland. 1988; 2:1269-1272.
77. Yoon WS, Jeong UJ, Kim JH. Kinematic analysis for sliding failure of multi-faced rock slopes. Eng Geol. 2002; 67:51–61.

VITA

RAJA DAS

Education:	B.Sc. Geology, University of Calcutta, India, 2011.
	M.Sc. Applied Geology, University of Calcutta, 2013.
	M.S. Geospatial Analysis, East Tennessee State University, Johnson City, 2019.
Professional Experience:	Assistant Geologist, Adhunik Group, India, 2014-2017.
	Graduate Assistant, East Tennessee State University, Department of Geosciences, 2017-2019.
	Geoscience Instructor, Upward Bound program, ETSU, 2018 & 2019.
	GIS research Intern, NETREP, Johnson City, 2019 – Present.
	Geospatial Image Analyst and Drone operator, City of Johnson City, 2019- Present.
Publication:	Raja Das. (2013). Developing GIS-based techniques for application of knowledge and data-driven methods of landslide susceptibility mapping. Indian Journal of Geosciences 2013 67 (3-4), 249-272.
	Raja Das. (2019). Assessment of Debris-slides Using Kinematic Analysis in GIS Platform - A Case Study in Great Smoky Mountains National Park, TN - International Debris Flow Hazards Mitigation Conference (DFHM), 2019. (Conference Proceedings)
	Raja Das. (2019). Application of GIS based knowledge-driven and data-driven methods for debris-slide susceptibility mapping. International Journal of Applied Geospatial Research. (Submitted).
	Raja Das. (2019). Debris-slide assessment using spatial distribution of structural orientation data and kinematic properties of rock, Great Smoky Mountains National Park, TN. Engineering Geology. (Submitted).

Honors and Awards: Best Graduate Student in Geospatial Analysis, 2017-2019, East Tennessee State University.